SARGENT & LUNDY
ENGINEERS
CHICAGO

NUCLEAR SAFETY-RELATED

THERMAL STRATIFICATION AND FATIGUE ANALYSIS OF THE PRESSURIZER SURGE LINE

ZION STATION UNITS 1 AND 2

PREPARED FOR COMMONWEALTH EDISON COMPANY

PROJECT NO.:	8747-44
ACCESSION NO.	EMD-066614
REVISION NO.:	01
ISSUED:	12-20-90

SARGENT & LUNDY ENGINEERS

ENGINEERING MECHANICS DIVISION

EXECUTIVE SUMMARY

In December, 1988, NRC Bulletin No. 88-11, "Pressurizer Surge Line Thermal Stratification" was issued. This bulletin, in addition to visual inspections, required licensees to update their surge line stress and fatigue analyses to ensure compliance with applicable code requirements when the effects of fluid thermal stratification and thermal striping are included in the design basis. This report documents the results of the updated stress and fatigue analyses for the Zion Station Unit 1 and 2 surge lines.

The installed piping and support configurations for Units 1 and 2 were reviewed and the Unit 1 routing and support design were judged to be more rigid. The analytical model used on this evaluation, therefore, was based on the Unit 1 installed routing and support configuration.

The thermal stratification evaluation was performed by Sargent & Lundy using the axial stratification profile developed for Zion Station by the Westinghouse Owners Group (WOG) on the Pressurizer Surge Line Thermal Stratification. Using the stratification interface levels of the axial profile, a non-linear temperature distribution was used to define the piping circumferential temperature. Zion Station hot leg and pressurizer operating parameters were recorded for several heatup and cooldown cycles. This data was reviewed with station operating procedures and technical specification requirements to define the thermal stratification modes used in this evaluation. This included a review of Zion Station LERs to determine the maximum pressurizer to hot leg temperature differential. This evaluation assumed the maximum fluid ΔT to be 330°F. The thermal stratification analyses calculated the global structural effects and the hoop and axial localized effects associated with the non-linear temperature distributions. Based on surge line thermal monitoring data, these effects were calculated assuming the piping top to bottom temperature difference was 90% of the pressurizer to hot leg fluid temperature

R

difference. Westinghouse SSDC 1.3 was used to define the pressure and temperature transients of the other design basis events, and the pressurizer to hot leg fluid temperature differential used to calculate the thermal stratification effects of these events. Based on the thermal monitoring data, it was conservatively assumed that for each surge the stratified state changes to a uniform hot/cold thermal expansion state defined by the pressurizer or hot leg fluid temperature. The fatigue analysis combined the global and local thermal stratification effects, the pressure and temperature transient effects and seismic OBE effects.

The results of this evaluation demonstrate that the surge line piping met the Code stress and usage factor criteria. The evaluation demonstrates that the existing restraint hardware is adequate when considering the thermal stratification piping loads and movement.

ISSUE SUMMARY

ACCESSION NO.	REVISION NO.	DESCRIPTION
EMD-066631	00	ORIGINAL ISSUE

PREPARED BY: C. Sirichotiratana DATE: 12-11-90
C. Sirichotiratana

REVIEWED BY: David W. Mason DATE: 12-14-90
D. W. Mason

APPROVED BY: Gary H. DeBoo DATE: 12/14/90
G. H. DeBoo

ACCESSION NO.	REVISION NO.	DATE	DESCRIPTION
EMD-066614	01	12-20-90	Clerical Corrections. This Revision Supersedes Revision 00 in its Entirety.

PREPARED BY: C. Sirichotiratana DATE: 12-20-90
C. Sirichotiratana

REVIEWED BY: David W. Mason DATE: 12-20-90
D. W. Mason

APPROVED BY: T. D. Gerke DATE: 12-20-90
T. D. Gerke

TABLE OF CONTENTS

TABLES

FIGURES

1.0 INTRODUCTION

In May 1988 Portland General Electric Company's Trojan Station issued a preliminary notification of an unusual occurrence related to unexpected displacements of the pressurizer surge line piping. Investigations indicated the cause to be stratified flow (which resulted in thermal bowing of the piping) and the presence of stresses not considered in the original design. Concerns regarding this event were expressed as far back as 1982, and a monitoring program was initiated at Trojan in 1986. Additional industry review resulted in the issuance of INPO SER 25-87, "Surge Line Stratification," NRC Information Notice 88-80, "Unexpected Piping Movement Attributed to Thermal Stratification," and NRC Bulletin No. 88-11, "Pressurizer Surge Line Thermal Stratification," which brought this issue to the attention of all Pressurized Water Reactor owners. In addition to the effects of non-uniform circumferential thermal expansions, the oscillating, wavelike motion of the fluid thermal interface along the piping inside surface was identified. This phenomenon termed "thermal striping" affects the cumulative fatigue life of the surge line.

NRCB 88-11 required for stress integrity and fatigue life of the surge line to be reevaluated, including the effects of thermal stratification and thermal striping.

2.0 SCOPE

The scope of this evaluation is to demonstrate that the stress and fatigue life requirements of the ASME Section III Code, Reference 6.1, are acceptable for the pressurizer surge line piping at Zion Station Units 1 and 2 when the effects of thermal stratification and thermal striping are included in the design basis.

The piping analytical model has been developed from the installed piping and support configurations for units 1 and 2. The thermal stratification effects on the piping have been calculated as global structural and local stress effects. The global structural effects are the overall piping system responses, such as movement, piping moments and forces, and nozzle and restraint loading. The local stress effects are the piping stresses resulting from the differential thermal expansion about the piping circumference and along the pipe axis. These localized effects introduce additional hoop and axial stresses which are added to the global structural effects and included in the stress and fatigue evaluation.

The thermal striping effects are localized and exist in conjunction with stratified conditions. The localized thermal striping stress has been calculated and included in the fatigue evaluation. In addition to the thermal stratification and thermal striping effects, the design basis loads as required by the Zion UFSAR, Reference 6.2, have been included in this evaluation.

The piping thermal stratification motion has been calculated and used to demonstrate the existence of adequate design clearance for the piping and the functionality of the piping supports. This evaluation also provided the pressurizer and hot leg nozzle loads for qualification and the piping support loads required to qualify the structural steel. R

3.0 METHODOLOGY

3.1 ANALYTICAL MODEL

The pressurizer surge line analytical model was developed from the installed piping and support configurations for Zion Station

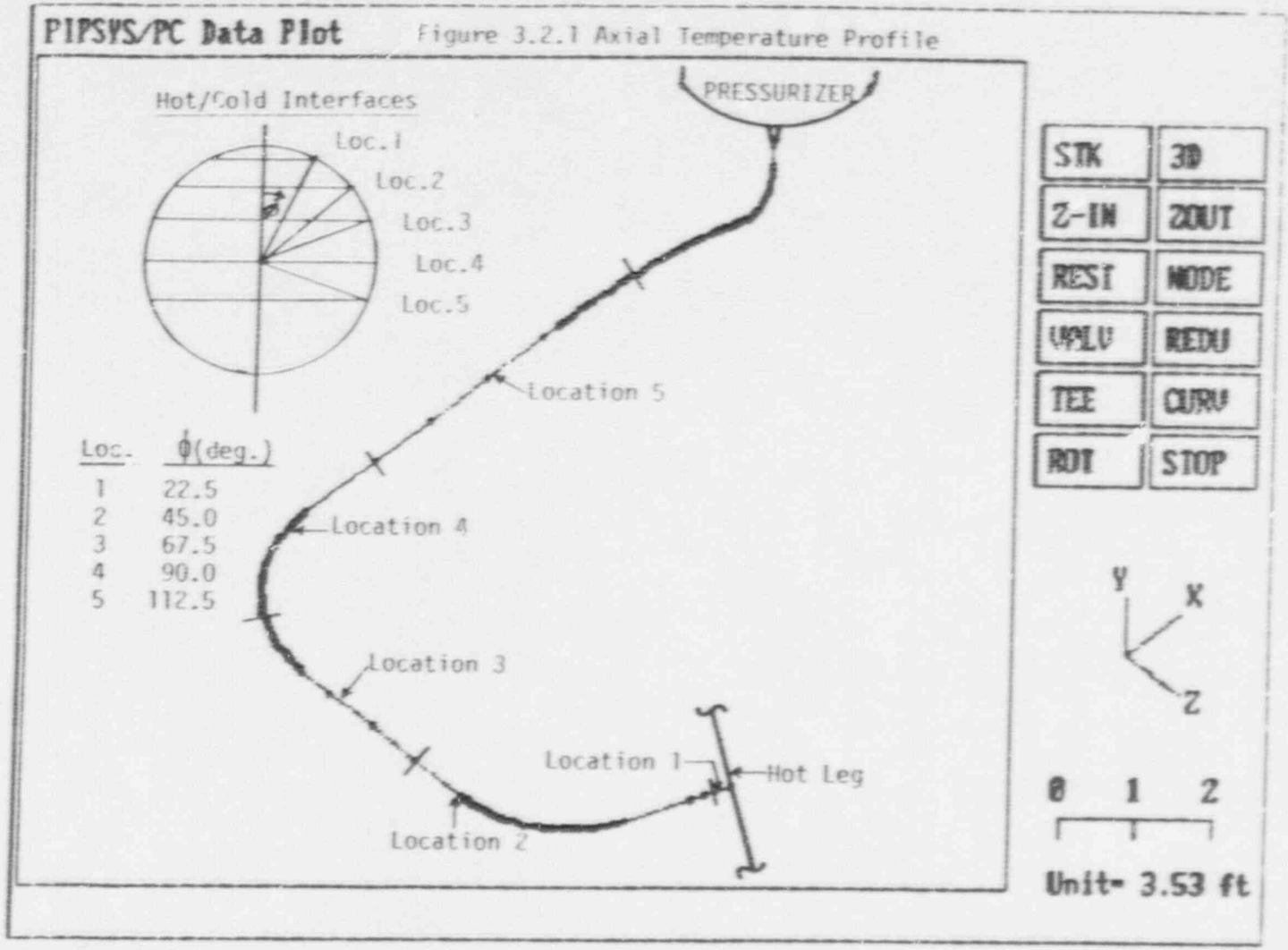

FIGURE 3.2.1
AXIAL TEMPERATURE PROFILE

FIGURE 3.2.2
CIRCUMFERENTIAL TEMPERATURE DISTRIBUTION

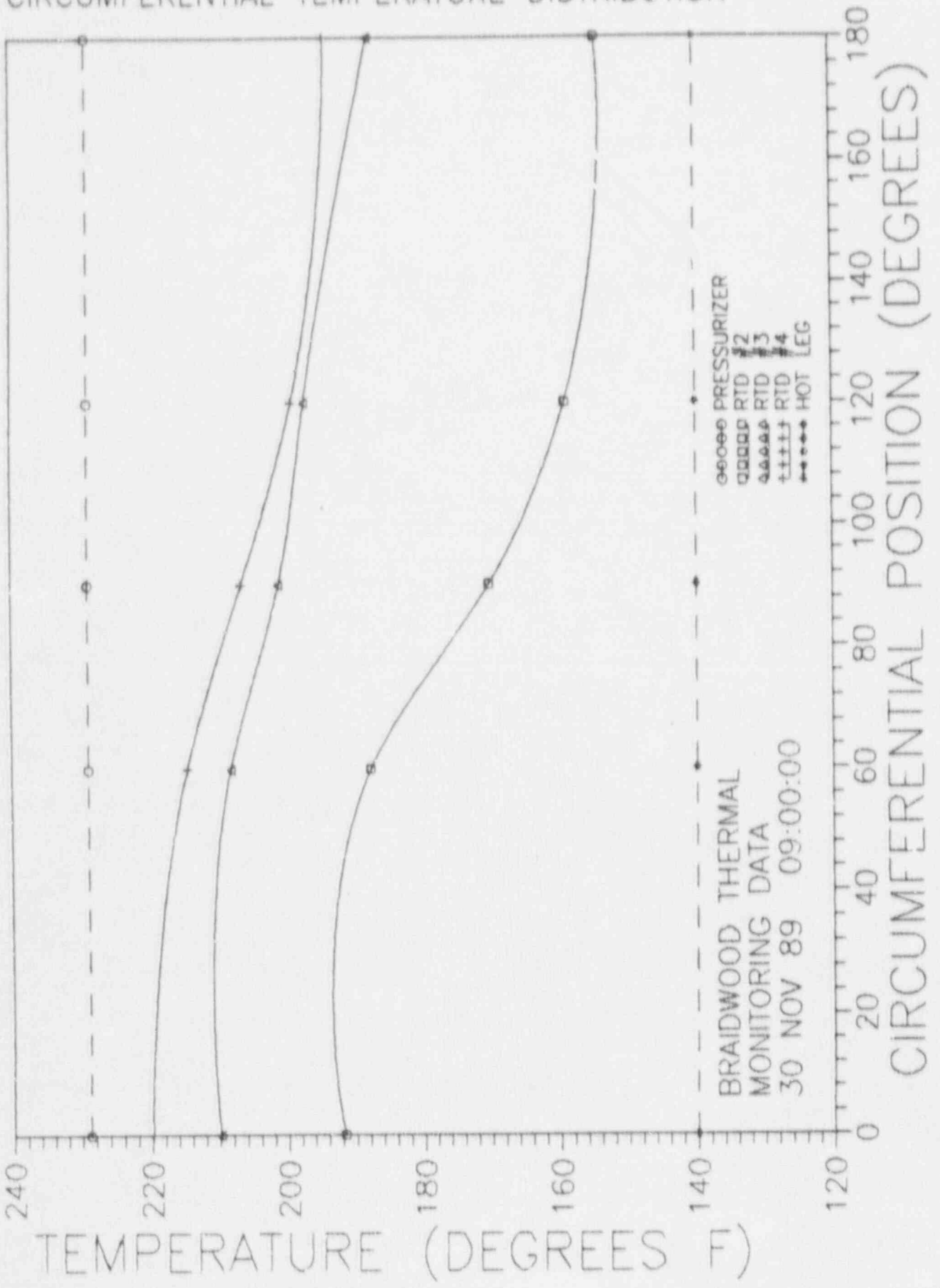

FIGURE 3.2.3
CIRCUMFERENTIAL TEMPERATURE DISTRIBUTION

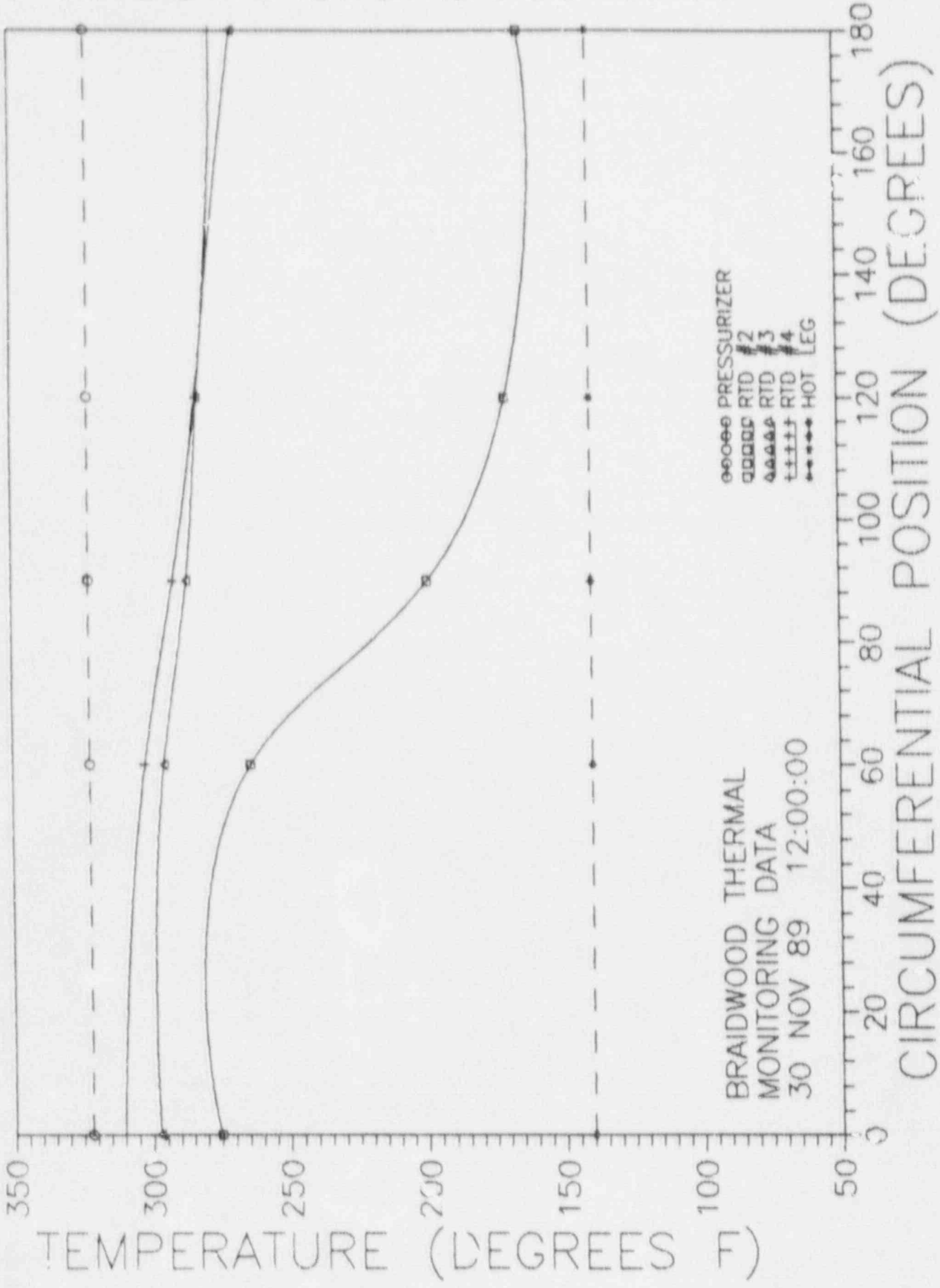

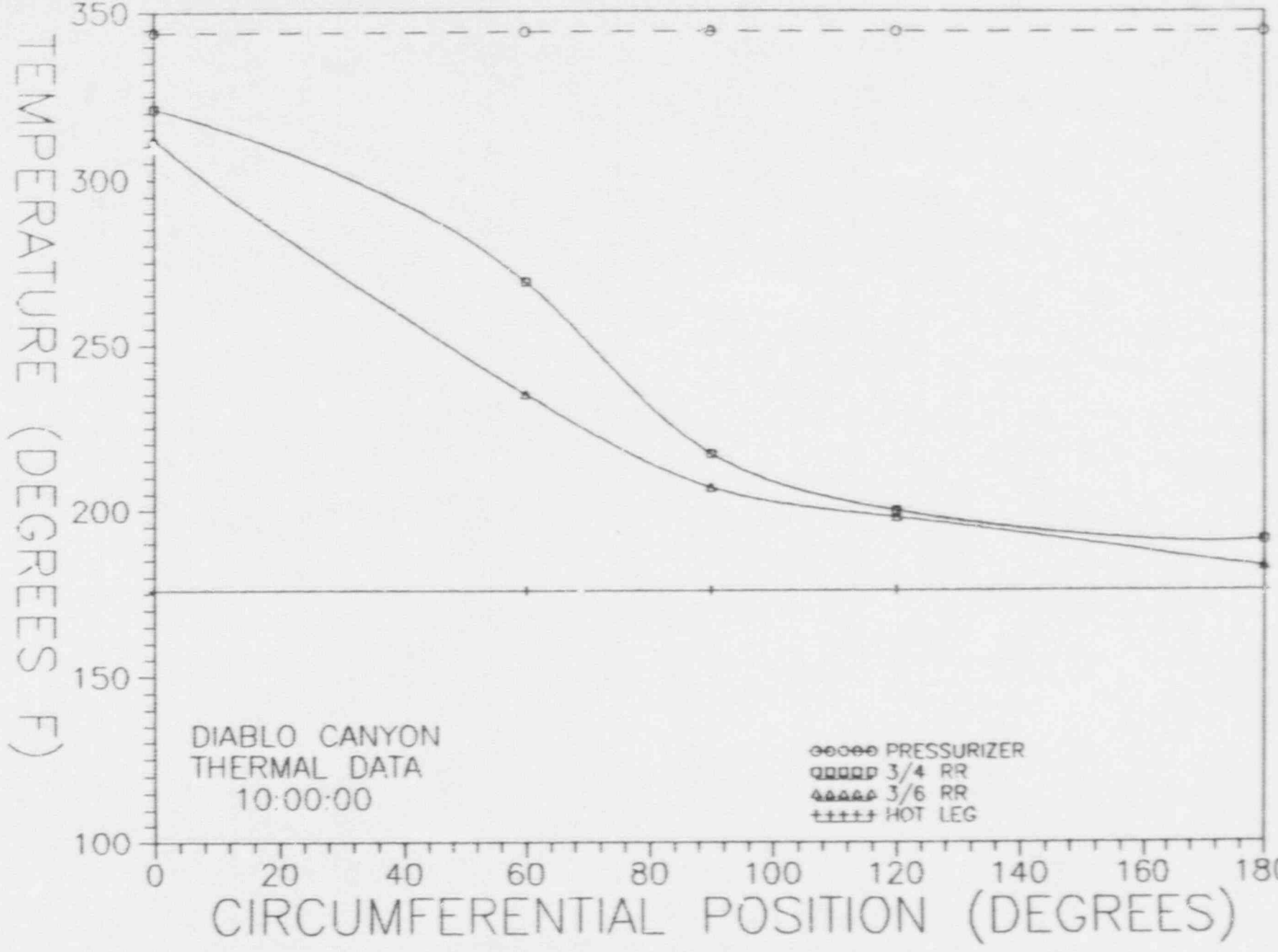

FIGURE 3.2.4
CIRCUMFERENTIAL TEMPERATURE DISTRIBUTION

FIGURE 3.2.5
CIRCUMFERENTIAL TEMPERATURE DISTRIBUTION

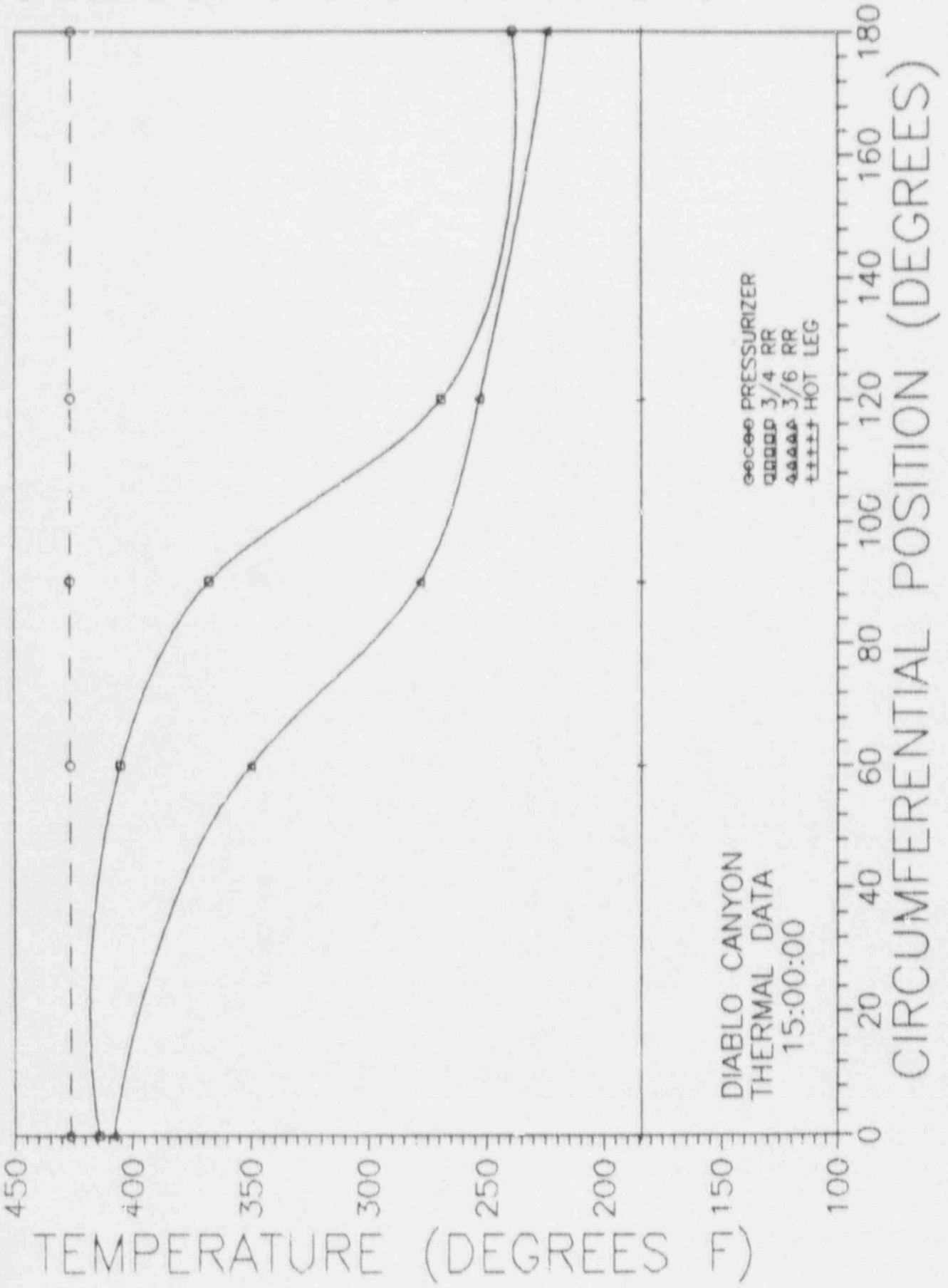

The piping circumferential temperature distribution plotted from the Diablo Canyon and Braidwood monitoring data is presented in Figures 3.2.2 through 3.2.5. Since the line size, wall thickness and material of the surge line piping is identical, using this monitoring data to represent the conductive heat transfer characteristics of the Zion surge line is justified. These figures demonstrate that a nonlinear circumferential temperature distribution exists as a result of stratified flow. Using the axial temperature profile hot-cold interface locations, the nonlinear circumferential temperature distribution was defined as the S-shape distribution seen in Figures 3.2.2 through 3.2.5, Reference 6.5.

3.3 MODES OF OPERATION

To define the modes of operation for the surge line, the UFSAR, Reference 6.2, and the Westinghouse Standard System Design Criteria 1.3, Reference 6.6 were used. This information was supplemented by the Zion Station operating records which contained hot leg temperature, prossurizer temperature, pressurizer water level, spray demand, charging and letdown flow rates, etc. The heatup and cooldown procedures, References 6.7 and 6.8, were used with the station operating records to develop representative hot leg and pressurizer temperature time-histories during heatup and cooldown, Figures 3.3.1 and 3.3.2.

To develop the design basis stratified thermal modes, the hot fluid in the surge line was assumed to be at the pressurizer fluid temperature and the cold fluid was assumed to be at the hot leg fluid temperature. Using these assumptions with the previous information, Table 3.3.1 was developed. It lists the design basis operating modes, the pressurizer and hot leg temperatures

FIGURE 3.3.1
ZION HEATUP TEMPERATURE HISTORY

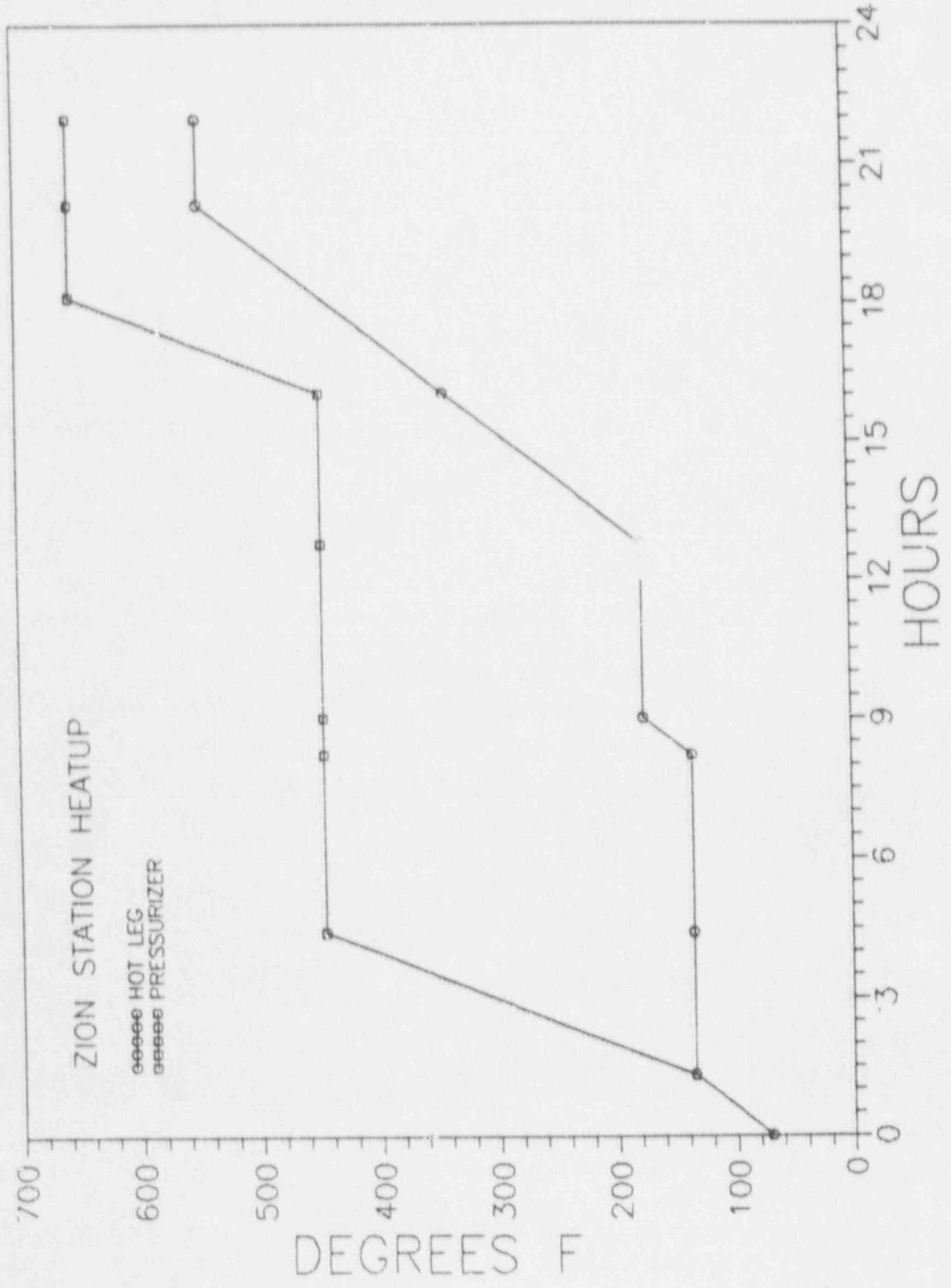

FIGURE 3.3.2
ZION COOLDOWN TEMPERATURE HISTORY

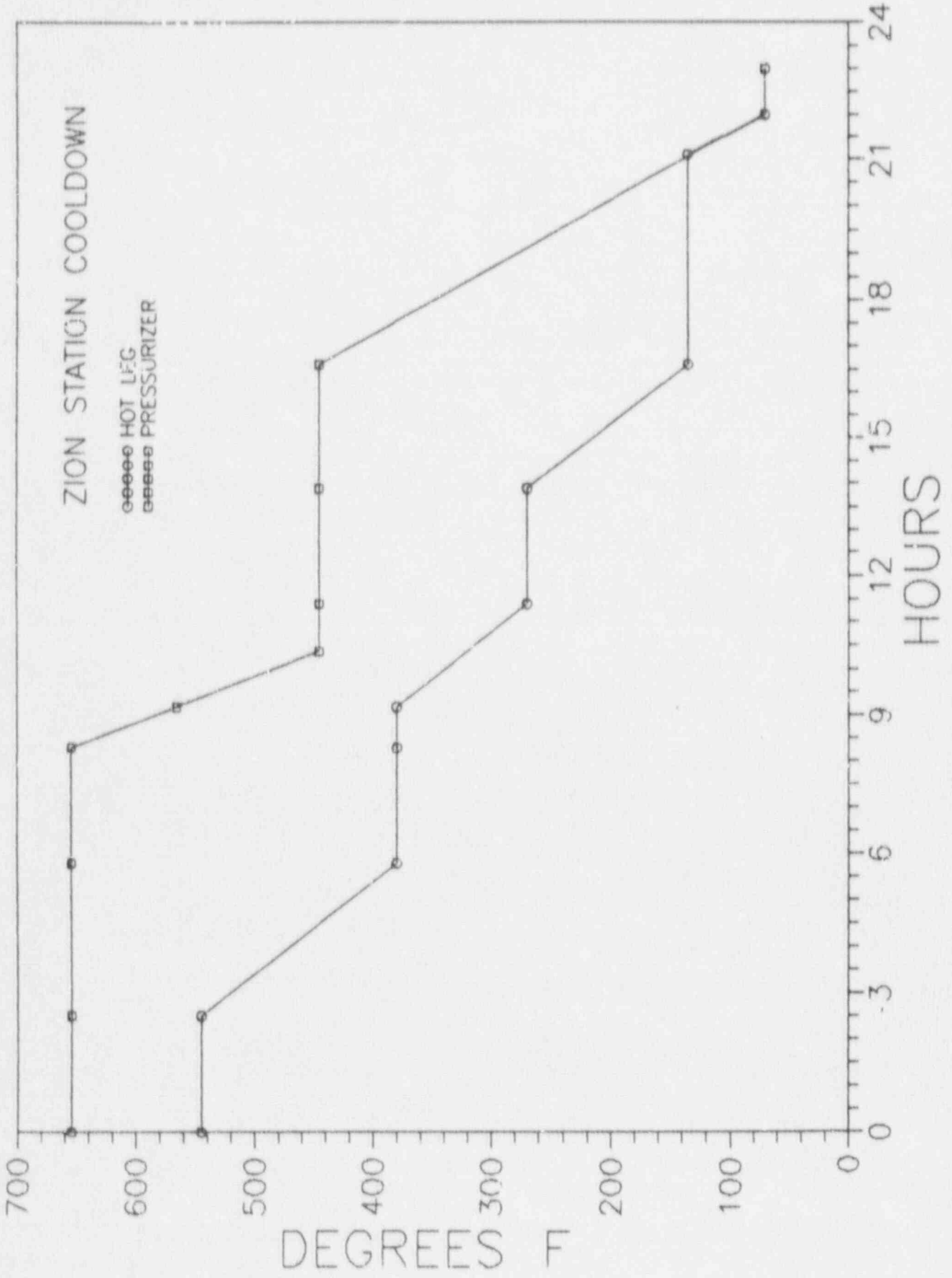

TABLE 3.3.1

THERMAL LOAD CASES

EVENT	NUMBER OF OCCURRENCES	PRESSURIZER TEMP. (°F)	HOT LEG TEMP. (°F)	ΔT (°F)
Bubble Formation	200(1)	450	120	330
Heatup	200(1)	445	175	270
Heatup	200(1)	654	545	109
Cooldown	200(1)	654	380	274
Cooldown	200(1)	445	270	175
Bubble collapse	200(1)	450	120	330
Unit loading 5%/min.	13,200	653	565	88
Unit unloading 5%/min.	13,200	653	565	88
Step load increase	2,000	653	565	88
Step load decrease	2,000	653	565	88
Large step load decrease with steam dump	200	653	547	106
Feedwater cycling at hot-shutdown	2,000	653	533	120
Steady state fluctuation				
Case A - Initial	150,000	653	588	65
Case B - Random	3,000,000	653	588	65
Boron concentration Equalization	26,400	653	588	65
Loss of load	80	653	566	87
Loss of power	40	653	564	89
Partial loss of flow	80	653	544	109
Reactor trip from full power				
Case A - no cooldown	230	653	560	93
Case B - cooldown with no SI	160	653	526	127
Case C - cooldown with SI	10	653	454	199
Inadvertent RCS depressurization	20	653	433	220
Control rod drop	80	653	555	98
Inadvertent SI actuation	60	653	544	109
Turbine roll test	20	653	450	203

Note (1) Six surges per occurrence yields 1200 cycles.

and the fluid temperature difference for stratification. Since the maximum hot to cold fluid temperature differences occur during heatup/cooldown, these events were defined as five different thermal load cases. Bubble formation and collapse determine the most extreme temperature difference and four intermediate thermal cases associated with the thermal plateaus which occur during the heatup/cooldown processes, Figures 3.3.1 and 3.3.2. Zion Station Technical Specification 3.3.2.D requires the pressurizer spray fluid and the pressurizer steam temperature difference not to exceed 320°F. Station Licensee Event Reports (LERs) were reviewed for excursion to this requirement. This review yielded a single excursion in September 1986 at unit 1 and reported a temperature difference of 323°F, Reference 6.9. Based on this event, the maximum fluid temperature difference used to define the heatup/cooldown event was defined as 330°F.

The postulated number of occurrences for each event was taken from Reference 6.6 and are listed in Table 3.3.1. However, for the heatup/cooldown events, six significant surges were assumed to occur during each event as assumed in Reference 6.6.

3.4 THERMAL STRATIFICATION ANALYSIS

Stratified conditions were assumed to exist for [illegible] of the design basis events tabulated in Table 3.3.1. Enveloping these stratified load cases, ten enveloped thermal stratification cases, listed in Table 3.4.1, were analyzed. The thermal stratification analysis calculated the surge line global response to the stratified conditions using the previously defined analytical model. This loading is defined by imposing the piping elemental bending moments necessary to simulate the piping

elemental strain deformation when the element is subjected to the non-linear circumferential temperature profile of each piping element in the model. By comparing the piping top to bottom temperature difference with the pressurizer to hot leg temperature difference in Figures 4, 6, 9 and 10 of Reference 6.3 and the Braidwood Unit 1 surge line thermal monitoring data, e.g., Figure 3.4.1, the piping temperature difference is always less than the pressurizer to hot leg fluid temperature difference. Reference 6.3 reports the ratio of the piping temperature difference to fluid temperature difference to 0.87 and less. This ratio is even smaller for the Braidwood data. Based on the conductive heat transfer similarities of surge lines at these stations to the Zion surge lines, a conservative factor of 0.9 times the fluid temperature difference was used to determine the piping hot and cold temperatures. For conservatism, the piping hot temperature was assumed to be equal to the pressurizer fluid temperature and the piping cold temperature equal to the pressurizer fluid temperature minus the 0.9 times the fluid temperature difference.

In addition to the global structural effects, the localized effects were also calculated. The localized axial and hoop membrane and hoop bending stresses resulting from the enveloped thermal stratification cases were calculated, Reference 6.5, and added to the global responses in the stress and fatigue analysis. Table 3.4.2 lists the localized stress intensities used in this evaluation.

TABLE 3.4.1

THERMAL STRATIFICATION CASES

CASE	$T_{pressurizer}$ (°F)	$T_{hot\ leg}$ (°F)	ΔT (°F)	R
1	450	120	330	
2	445	175	270	
3	445	270	175	
4	654	380	274	
5	654	545	109	
6	653	433	220	
7	653	454	199	
8	653	526	127	
9	653	555	98	
10	653	588	65	

FIGURE 3.4.1
BRAIDWOOD UNIT 1 SURGE LINE THERMAL DATA

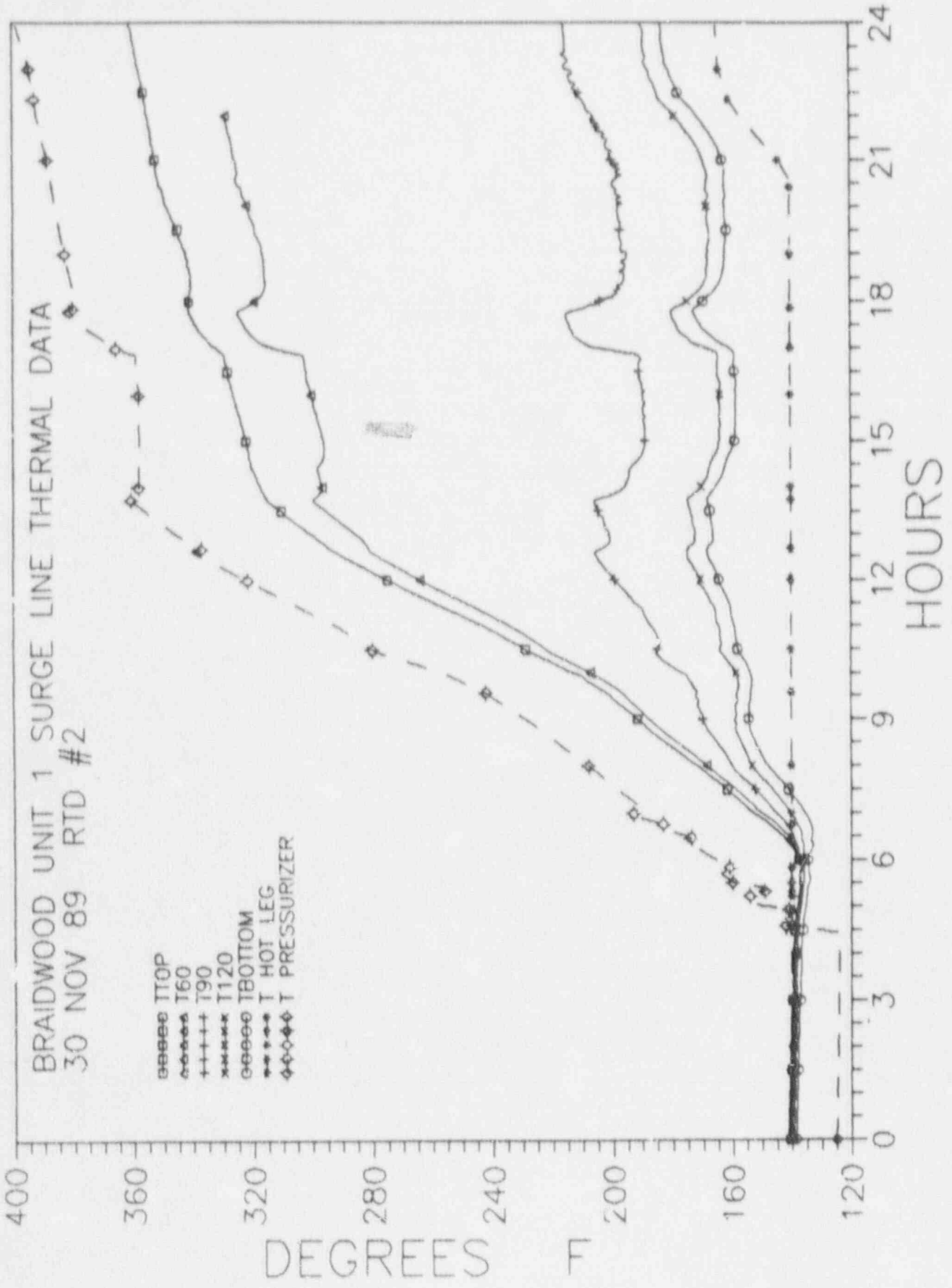

TABLE 3.4.2

THERMAL STRATIFICATION LOCALIZED
STRESS INTENSITIES

CASE	T_{top} (°F)	T_{bottom} (°F)	Axial (psi)	Hoop Bending (psi)	Hoop Membrane (psi)	R
1	450	153	12,987	10,835	1,269	
2	445	202	10,556	8,847	1,036	
3	445	287	6,910	5,761	675	
4	654	407	10,818	9,002	1,054	
5	654	556	4,361	3,550	415	
6	653	455	8,674	7,217	845	
7	653	474	7,840	6,523	764	
8	653	539	4,980	4,151	486	
9	653	565	3,860	3,210	376	
10	653	591	2,573	2,155	252	

3.5 THERMAL TRANSIENT ANALYSIS

The surge line is subjected to combined pressure-temperature transients of the pressurizer and the hot leg as a result of fluid transfers (surges) from the hot leg and the pressurizer. An outsurge is defined as a surge from the pressurizer to the hot leg and generates a significant thermal shock in the cooler hot leg nozzle. An insurge is defined as a surge from the hot leg to the pressurizer and generates a significant thermal shock at the hotter pressurizer nozzle. Since the change in temperature associated with the thermal shocks at the hot leg nozzle and the pressurizer nozzle are equal, and the pipe global structural effects are significantly larger at the hot leg nozzle, the thermal transient code stress terms ΔT_1, ΔT_2, and T_A-T_B are calculated at the hot leg nozzle and used to conservatively represent those stress terms in the remainder of the system piping. The pressure, temperature and flow time histories for the events listed in Table 3.3.1 were conservatively enveloped to reduce the number of thermal transient events to be analyzed. Using the enveloped thermal transient events, an axisymmetric finite element analysis, Reference 6.5, was performed on the hot leg nozzle mesh depicted in Figure 3.5.1 using Sargent & Lundy NOHEAT program, Reference 6.10. The code thermal transient stress terms are tabulated in Table 3.7.1.

3.6 THERMAL STRIPING ANALYSIS

Thermal striping, occurring together with the thermally stratified flow, creates additional thermal transient stress terms similar to the previously discussed thermal transient stress terms. The code ΔT_1, ΔT_2, and T_A-T_B stresses resulting from

FIGURE 3.5.1 HOT LEG SURGE LINE NOZZLE

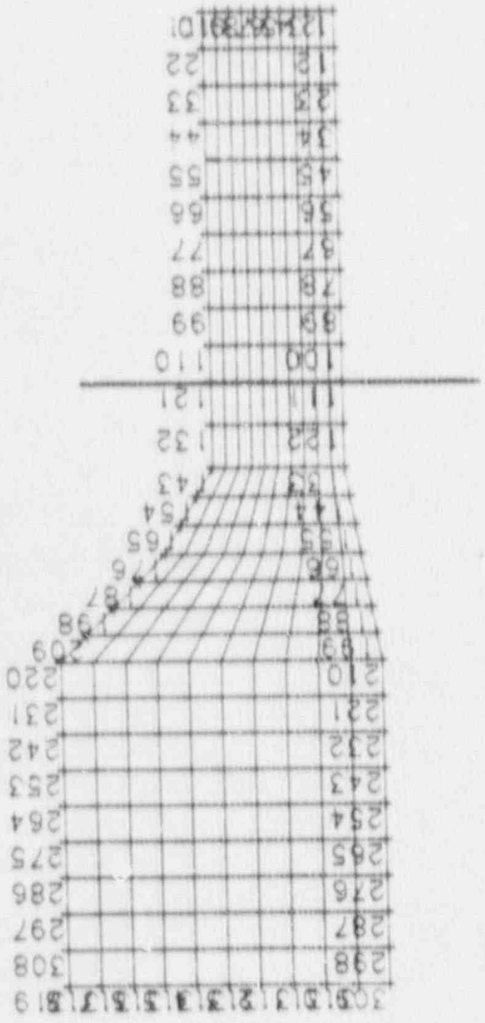

striping are based on a conservative temperature difference of 320°F and a hot fluid velocity of 2.5 ft/sec.

The code stress terms for the hot leg nozzle are
ΔT_1 = 6,477 psi,
ΔT_2 = 18,418 psi,
and $(T_A - T_B)$ = 1034 psi. Based on the calculated cyclic frequency of 4.68 cycles/min., these striping stresses occur 90,000,000 times assuming constant existence during operation and the plant operates 90% of its design life of 40 years, Reference 6.5.

3.7 PIPING ANALYSIS

The piping analysis was performed in accordance with the requirements of the Reference 6.1, Subsection NB. The analysis included the design basis weight and seismic loads, as required in Reference 6.2, as well as the thermal stratification effects previously defined. It was performed using Sargent & Lundy PIPSYS program, Reference 6.11.

It can be seen from the thermal monitoring data, e.g., Figure 3.7.1 and Figures 4, 6, 9 and 10 of Reference 6.3, that for each surge event, the piping temperature profile, both axially and circumferentially, will change to a uniform high temperature when there is an outsurge, and a uniform low temperature when the surge is an insurge. The magnitude of the surge flow rate and volume of fluid moved determines whether or not these extremes are established. It is, however; conservative to assume that for each surge the stratified state is changed to a uniform thermal expansion state defined by the pressurizer or hot leg fluid temperatures, since this will produce the greatest stress range.

FIGURE 3.7.1
PIPING TEMPERATURE RESPONSE TO SURGE

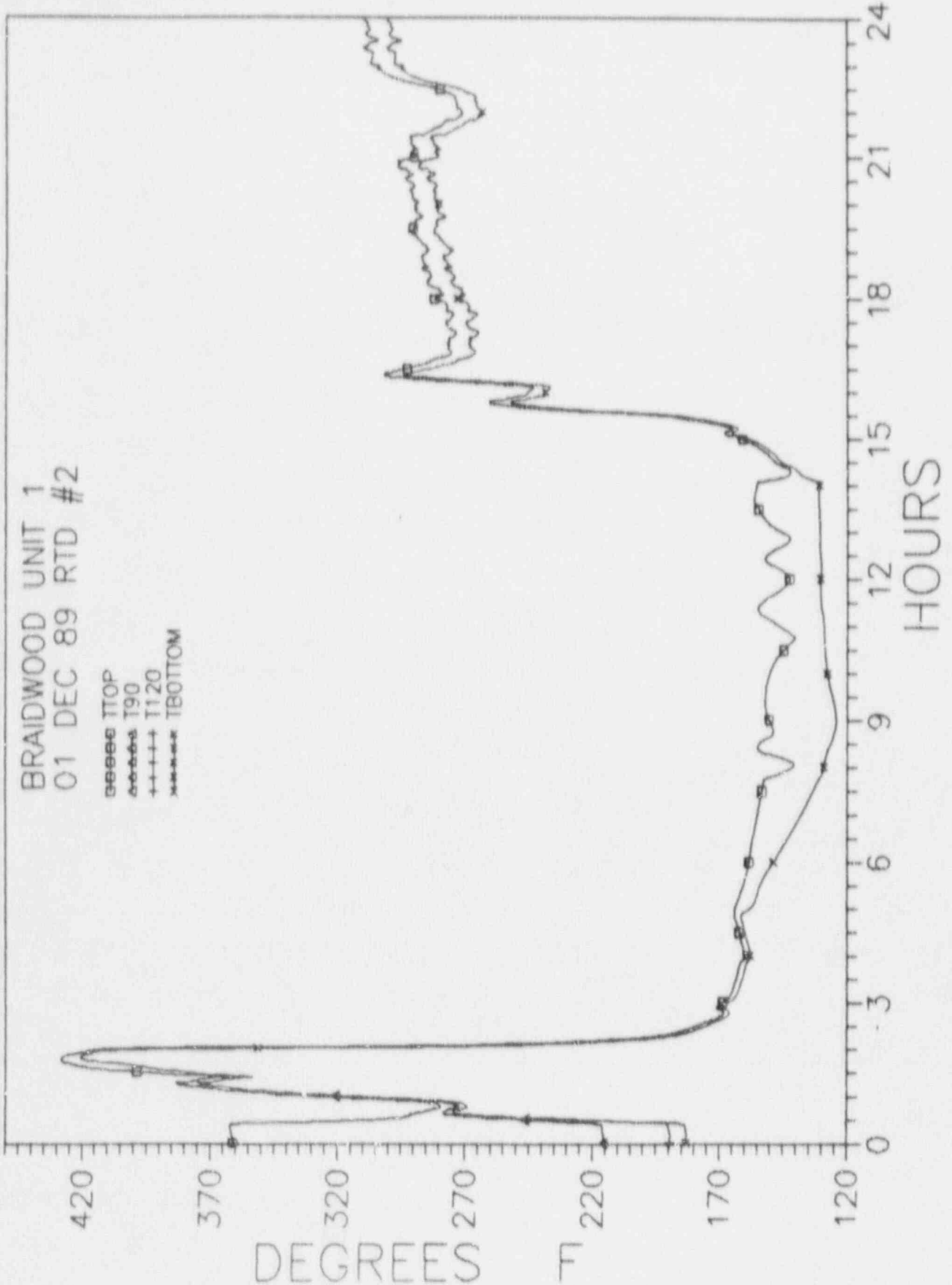

TABLE 3.7.1

EVENT	CYCLES	TEMP. (F) TPRZ	THL	TYPE	UNIFORM TEMP.(F)	DELTA T MAX	THERMAL T MIN	TRANSIENT DELTA T2 MAX	STRESS (PSI) T2 MIN	TA -TB MAX	TA -TB MIN
BUBBLE FORMATION	1200	450	120	UNIFORM	450	0	-14147	4647	0	0	-7806
BUBBLE FORMATION	1200	450	120	UNIFORM	120	16246	0	0	-12535	4908	0
BUBBLE FORMATION	1200	450	120	STRATIFIED	-	0	0	25091	25091	0	0
HEATUP/COOLDOWN	1200	445	175	UNIFORM	445	0	-17995	14350	0	0	-5690
HEATUP/COOLDOWN	1200	445	175	UNIFORM	175	0	0	0	0	0	0
HEATUP/COOLDOWN	1200	445	175	STRATIFIED	-	0	0	20439	20439	0	0
HEATUP/COOLDOWN	1200	654	380	UNIFORM	654	0	-32199	11502	0	0	-10895
HEATUP/COOLDOWN	1200	654	380	UNIFORM	380	5123	0	0	0	354	0
HEATUP/COOLDOWN	1200	654	380	STRATIFIED	-	0	0	20874	20874	0	0
HEATUP/COOLDOWN	1200	654	545	UNIFORM	654	0	-12883	9297	0	0	-4334
HEATUP/COOLDOWN	1200	654	545	UNIFORM	545	2038	0	0	-1461	141	0
HEATUP/COOLDOWN	1200	654	545	STRATIFIED	-	0	0	8326	8326	0	0
HEATUP/COOLDOWN	1200	445	270	UNIFORM	445	0	-23324	18598	0	0	-7575
HEATUP/COOLDOWN	1200	445	270	UNIFORM	270	3873	0	0	-2973	78	0
HEATUP/COOLDOWN	1200	445	270	STRATIFIED	-	0	0	13346	13346	0	0
BUBBLE COLLAPSE	1200	450	120	UNIFORM	450	0	-19994	15947	0	0	-6322
BUBBLE COLLAPSE	1200	450	120	UNIFORM	120	3382	0	0	-4354	528	0
BUBBLE COLLAPSE	1200	450	120	STRATIFIED	-	0	0	25091	25091	0	0
STEP LOAD INCREASE/STEP LOAD DECREASE	4000	653	565	UNIFORM	653	0	-9010	5286	0	0	-8124
STEP LOAD INCREASE/STEP LOAD DECREASE	4000	653	565	UNIFORM	565	0	0	0	0	0	0
STEP LOAD INCREASE/STEP LOAD DECREASE	4000	653	565	STRATIFIED	-	0	0	7446	7446	0	0
LARGE STEP LOAD-DECREASE	200	653	547	UNIFORM	653	0	-9010	5286	0	0	-8124
LARGE STEP LOAD-DECREASE	200	653	547	UNIFORM	547	0	0	0	0	0	0
LARGE STEP LOAD-DECREASE	200	653	547	STRATIFIED	-	0	0	8326	8326	0	0
FEEDWATER CYCLING/TURBINE ROLL TEST	2020	653	533	UNIFORM	653	0	-9745	5767	0	0	-8860
FEEDWATER CYCLING/TURBINE ROLL TEST	2020	653	533	UNIFORM	533	11356	0	0	-8128	7089	0
FEEDWATER CYCLING/TURBINE ROLL TEST	2020	653	450	STRATIFIED	-	0	0	15127	15127	0	0
LOSS OF LOAD/LOSS OF POWER/REACTOR TRIP CASE A	350	653	566	UNIFORM	653	0	-3861	7220	0	0	-781
LOSS OF LOAD/LOSS OF POWER/REACTOR TRIP CASE A	350	653	564	UNIFORM	560	12297	0	0	-15134	7541	0
LOSS OF LOAD/LOSS OF POWER/REACTOR TRIP CASE A	350	653	560	STRATIFIED	-	0	0	7446	7446	0	0
REACTOR TRIP CASE B	160	653	526	UNIFORM	653	0	-3861	7220	0	0	-781
REACTOR TRIP CASE B	160	653	526	UNIFORM	526	12297	0	0	-15134	7541	0
REACTOR TRIP CASE B	160	653	526	STRATIFIED	-	0	0	9617	9617	0	0
REACTOR TRIP CASE C	10	653	454	UNIFORM	653	0	-3861	7220	0	0	-781
REACTOR TRIP CASE C	10	653	454	UNIFORM	454	12297	0	0	-15134	7541	0
REACTOR TRIP CASE C	10	653	454	STRATIFIED	-	0	0	15127	15127	0	0
PARTIAL LOSS OF FLOW	80	653	544	UNIFORM	653	0	-3861	7220	0	0	-781
PARTIAL LOSS OF FLOW	80	653	544	UNIFORM	544	12297	0	0	-15134	7541	0
PARTIAL LOSS OF FLOW	80	653	544	STRATIFIED	-	0	0	8326	8326	0	0
INADVERTENT RCS DEPRESSURIZATION	20	653	433	UNIFORM	653	0	-8282	10756	0	0	-2891
INADVERTENT RCS DEPRESSURIZATION	20	653	433	UNIFORM	433	12742	0	0	-20166	10908	0
INADVERTENT RCS DEPRESSURIZATION	20	653	433	STRATIFIED	-	0	0	16736	16736	0	0
CONTROL ROD DROP	80	653	555	UNIFORM	653	0	-8282	10756	0	0	-2891
CONTROL ROD DROP	80	653	555	UNIFORM	555	12742	0	0	-20166	10908	0
CONTROL ROD DROP	80	653	555	STRATIFIED	-	0	0	7446	7446	0	0

TABLE 3.7.1
FATIGUE ANALYSIS LOAD SETS

ACC. NO.: EMD-066614
Page No. 20

TABLE 3.7.1

EVENT	CYCLES	TEMP. (F) TPRZ	TRL	TYPE	UNIFORM TEMP.(F)	DELTA TT MAX	THERMAL MIN	TRANSIENT DELTA TZ MAX	STRESS MIN	(PSI) TA -TB MAX	MIN
INADVERTENT SI-ACTUATION	60	653	544	UNIFORM	653	0	-8282	10756	0	0	-2891
INADVERTENT SI-ACTUATION	60	653	544	UNIFORM	544	12742	0	0	-20166	10908	0
INADVERTENT SI-ACTUATION	60	653	544	STRATIFIED	-	0	0	8326	8326	0	0
PRIMARY SIDE LEAK TEST	200	250	250	UNIFORM	250	0	0	0	0	0	0
SECONDARY SIDE LEAK TEST	80	250	250	UNIFORM	250	0	0	0	0	0	0
TUBE LEAK TEST	800	70	70	UNIFORM	70	0	0	0	0	0	0
UNIT LOADING/UNIT UNLOADING	26400	653	565	UNIFORM	653	0	-9010	5286	0	0	-8142
UNIT LOADING/UNIT UNLOADING	26400	653	565	UNIFORM	565	0	0	0	0	0	0
UNIT LOADING/UNIT UNLOADING	26400	653	565	STRATIFIED	-	0	0	7446	7446	0	0
STEADY STATE FLUCTUATION-INITIAL	150000	653	588	UNIFORM	653	0	-6744	4183	0	0	1910
STEADY STATE FLUCTUATION-INITIAL	150000	653	588	UNIFORM	588	1016	0	0	-1388	171	0
STEADY STATE FLUCTUATION-INITIAL	150000	653	588	STRATIFIED	-	0	0	4980	4980	0	0
STEADY STATE FLUCTUATION-RANDOM	3000000	653	588	UNIFORM	653	0	-5028	2307	0	0	-3355
STEADY STATE FLUCTUATION-RANDOM	3000000	653	588	UNIFORM	588	1757	0	0	-1734	456	0
STEADY STATE FLUCTUATION-RANDOM	3000000	653	588	STRATIFIED	-	0	0	4980	4980	0	0
BORON CONCENTRATION EQUAL	26400	653	588	UNIFORM	653	0	-7039	3909	0	0	-5035
BORON CONCENTRATION EQUAL	26400	653	588	UNIFORM	588	0	0	0	0	0	0
BORON CONCENTRATION EQUAL	26400	653	588	STRATIFIED	-	0	0	4980	4980	0	0

TABLE 3.7.1/CONT'D

FATIGUE ANALYSIS LOAD SETS

Table 3.7.1 presents the load set definitions used in the stress and fatigue analyses. The localized hoop stress intensities were increased by the code K_1 C_2 factors and added to the localized axial stress to produce a total localized stress. This total localized stress is listed as a DELTA T2 stress associated with the stratified modes in Table 3.7.1. The fatigue analysis was performed with the bubble formation and bubble collapse ranging 200 times each with the zero load set. The remaining occurrences and the other heatup/cooldown load sets were allowed to range freely with each other to produce the maximum stress ranges. The other operating loadsets were also allowed to range freely with each other producing the maximum stress ranges. R

4.0 ANALYZED RESULTS

Table 4.1 presents the code stress intensities and usage factors for the most highly stressed piping components. These results demonstrate that code stress criteria have been met, and that the predicted fatigue life is adequate.

TABLE 4.1
STRESS SUMMARY

	Eqn 10 (psi)	Eqn 12 (psi)	Eqn 13 (psi)	Usage Factor
Hot leg Nozzle	67,600	46,300	19,500	0.45
Pipe Bend	55,300	45,700	10,300	0.13
Code Stress Limit	50,100	50,100	50,100	1.00

Reference 6.5 indicates that pipe break is postulated at the nozzles and every fitting in the surge line. No additional pipe breaks are postulated as a result of this evaluation.

For spring hangers RCH-1(2)001 and RCH-1(2)003, the load settings remain unchanged, load variability is acceptable, and adequate clearance is available for the stratified thermal movements.

For the two snubbers on this system, RCRS-1(2)007 and RCRS-1(2)009, the design loads are not changed by this evaluation. The snubber stroke and cold settings have been evaluated for the stratified thermal movement and found to be adequate.

Significant load increases were calculated for rigid restraint RCRS-1(2)008 and these are listed in Table 4.2.

TABLE 4.2
RESTRAINT LOADING RCRS-1(2)008

Service Level	Load (lbs)
A	21412/-1466
B	24578/-4632
C	27176/-7230

Restraint hardware has been evaluated for these load increases and found to be acceptable, Reference 6.5.

Piping loads at the hot leg and pressurizer nozzles have increased significantly as a result of the thermal stratification effects. These loads are presented in Table 4.3 and 4.4 respectively.

The predicted piping thermal movement at the flailing restraint locations during stratified conditions has been compared to the Zion

ANCHOR OUTPUT

ID: REACTOR COOLANT

ANCHOR ID: LOCATION: NP 5 TYPE: HOT LEG NOZZLE LOOP-4

SUB-SYSTEM NO: RC-1 ANALYTICAL DWG NO: RC-1 LOCAL AXIS

SUMMARY OF INDIVIDUAL LOADS (FT-LBS)

LOAD TITLE	LOAD ID	FA	FB	FC	MA	MB	MC
DEAD WEIGHT	WGHT	1032.	230.	533.	2836.	1537.	6695.
THERMAL 1	TH01	8452.	11717.	-3575.	-338575.	95589.	99063.
THERMAL 2	TH02	7377.	9097.	-4072.	-272359.	90384.	75021.
THERMAL 3	TH03	5733.	4839.	-5023.	-166308.	83824.	35317.
THERMAL 4	TH04	9125.	7635.	-8083.	-263927.	134117.	55853.
THERMAL 5	TH05	6243.	-65.	-9906.	-72345.	123638.	-16541.
THERMAL 6	TH06	8470.	5122.	-8646.	-201147.	130424.	32429.
THERMAL 7	TH07	7641.	4135.	-8884.	-176734.	129086.	23107.
THERMAL 8	TH08	6541.	772.	-9689.	-93164.	124565.	-8507.
THERMAL 9	TH09	6030.	-579.	-10013.	-59512.	122697.	-21162.
THERMAL 10	TH10	5475.	-2097.	-10387.	-21838.	120845.	-35499.
THERMAL 11	TH11	4295.	-5157.	-11068.	54733.	116037.	-64204.
OBE SPEC X DIR	OBEX	1510.	946.	1736.	1728.	3530.	5598.
OBE SPEC Y DIR	OBEY	654.	1015.	668.	1013.	1184.	3613.
OBE SPEC Z DIR	OBEZ	724.	485.	926.	696.	2018.	3180.
SSE SPEC X DIR	SSEX	2726.	1704.	3133.	3057.	6431.	10189.
SSE SPEC Y DIR	SSEY	1150.	1763.	1166.	1757.	2063.	6277.
SSE SPEC Z DIR	SSEZ	1409.	899.	1732.	1274.	3727.	5870.

TABLE 4.4.2
HOT LEG NOZZLE LOADS

ID: REACTOR COOLANT ANCHOR OUTPUT

ANCHOR ID LOCATION: NP 345 TYPE: PRESSURIZER NOZZLE

SUB-SYSTEM NO: RC-1 ANALYTICAL DWG NO: RC-1 GLOBAL AXIS

SUMMARY OF INDIVIDUAL LOADS (FT-LBS)

LOAD TITLE	LOAD ID	FX	FY	FZ	MX	MY	MZ
DEAD WEIGHT	WGHT	1709.	1278.	163.	-3550.	-6562.	10825.
THERMAL 1	TH01	-484.	-2005.	3821.	86204.	23096.	157935.
THERMAL 2	TH02	-1568.	-1632.	3883.	65905.	32464.	116913.
THERMAL 3	TH03	-3462.	-1055.	4086.	32693.	49240.	50487.
THERMAL 4	TH04	-5623.	-1617.	6551.	52440.	79511.	76705.
THERMAL 5	TH05	-9113.	-664.	7005.	-9050.	110990.	-41670.
THERMAL 6	TH06	-6741.	-1299.	6672.	32507.	89364.	38177.
THERMAL 7	TH07	-7192.	-1172.	6734.	24720.	93468.	23014.
THERMAL 8	TH08	-8727.	-741.	6937.	-2046.	107326.	-28783.
THERMAL 9	TH09	-9342.	-570.	7020.	-12910.	112927.	-49550.
THERMAL 10	TH10	-10046.	-380.	7119.	-25071.	119284.	-72829.
THERMAL 11	TH11	-11390.	5.	7270.	-49643.	131342.	-119372.
OBE SPEC X DIR	OBEX	2236.	1836.	2055.	6131.	5315.	13990.
OBE SPEC Y DIR	OBEY	867.	1014.	1006.	3074.	2086.	4252.
OBE SPEC Z DIR	OBEZ	824.	851.	833.	1704.	1949.	7125.
SSE SPEC X DIR	SSEX	3935.	3280.	3630.	10656.	9346.	25172.
SSE SPEC Y DIR	SSEY	1511.	1789.	1748.	5331.	3613.	7431.
SSE SPEC Z DIR	SSEZ	1553.	1575.	1529.	3108.	3544.	13268.

TABLE 4.4
PRESSURIZER NOZZLE LOADS

Station visual inspection results documented in Reference 6.12 and 6.13. This comparison demonstrates that adequate clearance between the piping and the flailing restraints exists.

5.0 CONCLUSIONS

The thermal stratifications and fatigue evaluation of the Zion Station surge lines, Units 1 and 2, was performed and resulted in the following conclusions.

- Piping Code stress criteria are met.
- Cumulative usage factors are less than 1.0.
- There are no new postulated pipe breaks.
- The spring hangers and snubbers are adequate. |R
- The rigid restraint is adequate. |R
- The flailing restraint clearances are adequate. |R

6.0 REFERENCES

6.1 ASME B&PV Code Section III 1986 Edition.

6.2 Zion Stations Updated Final Safety Analysis Report, Volume 2, Section 4.

6.3 Measurement of Stratification in the Pressurizer Surge Line," by P. Hirshberg and G. A. Antaki; Design and Analysis of Piping Components, PVP Volume 169, 1989.

6.4 Commonwealth Edison letter from P. R. Donavin to G. T. Kitz, CHRON #144562, dated 07-27-90, Zion Station Units 1 and 2 Thermal Stratification Evaluation of Pressurizer Surge Lines.

6.5 "Thermal Stratification and Fatigue Analysis of Pressurizer Surge Lines," Zion Station Units 1 and 2, EMD-066548.

6.6 Westinghouse Standard System Design Criteria 1.3, Revision 2, 04-15-74. R

6.7 Zion Nuclear Station GOP-1, Plant Heatup, 05-30-90.

6.8 Zion Nuclear Station GOP-4, Plant Shutdown and Cooldown, 03-19-90.

6.9 Zion Station Licensee Event Report (LER) No. 86-033-00, 10-10-86.

6.10 Sargent & Lundy Computer Program NOHEAT, NOHØ950754.0.

6.11 Sargent & Lundy Computer Program, PIPSYS, PIPØ950650.0.

6.12 Letter from R. J. Wulf to H. E. Bliss, Subject: Visual Inspection of the Pressurizer Surge Line for Zion Station Unit 1, 02-20-89.

6.13 Letter from R. J. Wulf to R. E. Lane, Subject: Visual Examination of Zion Station Unit 2 Pressurizer Surge Line Piping Supports, 01-24-89.

WCAP-12740

TECHNICAL JUSTIFICATION FOR ELIMINATING PRESSURIZER SURGE LINE RUPTURE AS THE STRUCTURAL DESIGN BASIS FOR BYRON UNITS 1 and 2 BRAIDWOOD UNITS 1 and 2

November 1990

D. C. Bhowmick

Westinghouse Energy Systems

WCAP-12740

TECHNICAL JUSTIFICATION FOR ELIMINATING PRESSURIZER SURGE LINE RUPTURE AS THE STRUCTURAL DESIGN BASIS FOR BYRON UNITS 1 and 2 BRAIDWOOD UNITS 1 and 2

November 1990

D. C. Bhowmick

Westinghouse Energy Systems

Westinghouse Class 3

WCAP-12740

TECHNICAL JUSTIFICATION FOR ELIMINATING PRESSURIZER SURGE LINE RUPTURE AS THE STRUCTURAL DESIGN BASIS FOR BYRON UNITS 1 and 2 BRAIDWOOD UNITS 1 and 2

November 1990

D. C. Bhowmick
S. A. Swamy
Y. S. Lee
K. R. Hsu
J. F. Petsche

Verified:
J. C. Schmertz
Structural Mechanics Technology

Approved:
S. S. Palusamy, Manager
Diagnostics and Monitoring Technology

Work performed under Shop Order BZSP-950C

WESTINGHOUSE ELECTRIC CORPORATION
Nuclear and Advanced Technology Division
P.O. Box 2728
Pittsburgh, Pennsylvania 15230-2728

TABLE OF CONTENTS

TABLE OF CONTENTS (cont.)

LIST OF TABLES

LIST OF TABLES (cont.)

LIST OF TABLES (cont.)

LIST OF FIGURES

LIST OF FIGURES (cont.)

LIST OF FIGURES (cont.)

LIST OF FIGURES (cont.)

SECTION 1.0
INTRODUCTION

1.1 Background

The current structural design basis for the pressurizer surge line requires postulating non-mechanistic circumferential and longitudinal pipe breaks. This results in additional plant hardware (e.g. pipe whip restraints and jet shields) which would mitigate the dynamic consequences of the pipe breaks. It is, therefore, highly desirable to be realistic in the postulation of pipe breaks for the surge line. Presented in this report are the descriptions of a mechanistic pipe break evaluation method and the analytical results that can be used for establishing that a circumferential type break will not occur within the pressurizer surge line. The evaluations considering circumferentially oriented flaws cover longitudinal cases. The pressurizer surge line is known to be subjected to thermal stratification and the effects of thermal stratification for Byron & Braidwood surge lines have been evaluated and documented in WCAP-12743. The results of the stratification evaluation as described in WCAP-12743, have been used in the leak-before-break evaluation presented in this report.

1.2 Scope and Objective

The general purpose of this investigation is to demonstrate leak-before-break for the pressurizer surge line. The scope of this work covers the entire pressurizer surge line from the primary loop nozzle junction to the pressurizer nozzle junction. A schematic drawing of the piping system is shown in Section 3.0. The recommendations and criteria proposed in NUREG 1061 Volume 3 (1-1) are used in this evaluation. The criteria and the resulting steps of the evaluation procedure can be briefly summarized as follows:

1) Calculate the applied loads. Identify the location at which the highest stress occurs.

2) Identify the materials and the associated material properties.

3) Postulate a surface flaw at the governing location. Determine fatigue crack growth. Show that a through-wall crack will not result.

4) Postulate a through-wall flaw at the governing location. The size of the flaw should be large enough so that the leakage is assured of detection with margin using the installed leak detection equipment when the pipe is subjected to normal operating loads. A margin of 10 is demonstrated between the calculated leak rate and the leak detection capability.

5) Using maximum faulted loads, demonstrate that there is a margin of at least 2 between the leakage size flaw and the critical size flaw.

6) Review the operating history to ascertain that operating experience has indicated no particular susceptibility to failure from the effects of corrosion, water hammer or low and high cycle fatigue.

7) For the base and weld metals actually in the plant provide the material properties including toughness and tensile test data. Justify that the properties used in the evaluation are representative of the plant specific material. Evaluate long term effects such as thermal aging where applicable.

8) Demonstrate margin on applied load.

The flaw stability analyses is performed using the methodology described in SRP 3.6.3 (1-2).

The leak rate is calculated for the normal operating condition. The leak rate prediction model used in this evaluation is an [----------
---
---]^{a,c,e} The crack opening area required for calculating the leak rates is obtained by subjecting the postulated through-wall flaw to normal operating loads (1-3). Surface roughness is accounted for in determining the leak rate through the postulated flaw.

1.3 References

1-1 Report of the U.S. Nuclear Regulatory Commission Piping Review Committee - Evaluation of Potential for Pipe Breaks, NUREG 1061, Volume 3, November 1984.

1-2 Standard Review Plan; public comments solicited; 3.6.3 Leak-Before-Break Evaluation Procedures; Federal Register/Vol. 52, No. 167/Friday, August 28, 1987/Notices, pp. 32626-32633.

1-3 NUREG/CR-3464, 1983, "The Application of Fracture Proof Design Methods Using Tearing Instability Theory to Nuclear Piping Postulated Circumferential Through Wall Cracks."

SECTION 2.0

OPERATION AND STABILITY OF THE PRESSURIZER SURGE LINE AND THE REACTOR COOLANT SYSTEM

2.1 Stress Corrosion Cracking

The Westinghouse reactor coolant system primary loop and connecting Class 1 lines have an operating history that demonstrates the inherent operating stability characteristics of the design. This includes a low susceptibility to cracking failure from the effects of corrosion (e.g., intergranular stress corrosion cracking). This operating history totals over 400 reactor-years, including five plants each having over 15 years of operation and 15 other plants each with over 10 years of operation.

In 1978, the United States Nuclear Regulatory Commission (USNRC) formed the second Pipe Crack Study Group. (The first Pipe Crack Study Group established in 1975 addressed cracking in boiling water reactors only.) One of the objectives of the second Pipe Crack Study Group (PCSG) was to include a review of the potential for stress corrosion cracking in Pressurized Water Reactors (PWR's). The results of the study performed by the PCSG were presented in NUREG-0531 (Reference 2-1) entitled "Investigation and Evaluation of Stress Corrosion Cracking in Piping of Light Water Reactor Plants." In that report the PCSG stated:

> "The PCSG has determined that the potential for stress-corrosion cracking in PWR primary system piping is extremely low because the ingredients that produce IGSCC are not all present. The use of hydrazine additives and a hydrogen overpressure limit the oxygen in the coolant to very low levels. Other impurities that might cause stress-corrosion cracking, such as halides or caustic, are also rigidly controlled. Only for brief periods during reactor shutdown when the coolant is exposed to the air and during the subsequent startup are conditions even marginally capable of producing stress-corrosion cracking in the primary systems of PWRs.

Operating experience in PWRs supports this determination. To date, no stress-corrosion cracking has been reported in the primary piping or safe ends of any PWR."

During 1979, several instances of cracking in PWR feedwater piping led to the establishment of the third PCSG. The investigations of the PCSG reported in NUREG-0691 (Reference 2-2) further confirmed that no occurrences of IGSCC have been reported for PWR primary coolant systems.

As stated above, for the Westinghouse plants there is no history of cracking failure in the reactor coolant system loop or connecting Class 1 piping. The discussion below further qualifies the PCSG's findings.

For stress corrosion cracking (SCC) to occur in piping, the following three conditions must exist simultaneously: high tensile stresses, susceptible material, and a corrosive environment. Since some residual stresses and some degree of material susceptibility exist in any stainless steel piping, the potential for stress corrosion is minimized by properly selecting a material immune to SCC as well as preventing the occurrence of a corrosive environment. The material specifications consider compatibility with the system's operating environment (both internal and external) as well as other material in the system, applicable ASME Code rules, fracture toughness, welding, fabrication, and processing.

The elements of a water environment known to increase the susceptibility of austenitic stainless steel to stress corrosion are: oxygen, fluorides, chlorides, hydroxides, hydrogen peroxide, and reduced forms of sulfur (e.g., sulfides, sulfites, and thionates). Strict pipe cleaning standards prior to operation and careful control of water chemistry during plant operation are used to prevent the occurrence of a corrosive environment. Prior to being put into service, the piping is cleaned internally and externally. During flushes and preoperational testing, water chemistry is controlled in accordance with written specifications. Requirements on chlorides, fluorides, conductivity, and pH are included in the acceptance criteria for the piping.

During plant operation, the reactor coolant water chemistry is monitored and maintained within very specific limits. Contaminant concentrations are kept below the thresholds known to be conducive to stress corrosion cracking with the major water chemistry control standards being included in the plant operating procedures as a condition for plant operation. For example, during normal power operation, oxygen concentration in the RCS and connecting Class 1 lines is expected to be in the ppb range by controlling charging flow chemistry and maintaining hydrogen in the reactor coolant at specified concentrations. Halogen concentrations are also stringently controlled by maintaining concentrations of chlorides and fluorides within the specified limits. This is assured by controlling charging flow chemistry. Thus during plant operation, the likelihood of stress corrosion cracking is minimized.

2.2 Water Hammer

Overall, there is a low potential for water hammer in the RCS and connecting surge lines since they are designed and operated to preclude the voiding condition in normally filled lines. The RCS and connecting surge line including piping and components, are designed for normal, upset, emergency, and faulted condition transients. The design requirements are conservative relative to both the number of transients and their severity. Relief valve actuation and the associated hydraulic transients following valve opening are considered in the system design. Other valve and pump actuations are relatively slow transients with no significant effect on the system dynamic loads. To ensure dynamic system stability, reactor coolant parameters are stringently controlled. Temperature during normal operation is maintained within a narrow range by control rod position; pressure is controlled by pressurizer heaters and pressurizer spray also within a narrow range for steady-state conditions. The flow characteristics of the system remain constant during a fuel cycle because the only governing parameters, namely system resistance and the reactor coolant pump characteristics are controlled in the design process. Additionally, Westinghouse has instrumented typical reactor coolant systems to verify the flow and vibration characteristics of the system and connecting surge lines. Preoperational testing and operating experience have verified the Westinghouse approach. The operating transients

of the RCS primary piping and connected surge lines are such that no significant water hammer can occur.

2.3 Low Cycle and High Cycle Fatigue

Low cycle fatigue considerations are accounted for in the design of the piping system through the fatigue usage factor evaluation to show compliance with the rules of Section III of the ASME Code. A further evaluation of the low cycle fatigue loading is discussed in Section 6.0 as part of this study in the form of a fatigue crack growth analysis.

Pump vibrations during operation would result in high cycle fatigue loads in the piping system. During operation, an alarm signals the exceedance of the RC pump shaft vibration limits. Field measurements have been made on the reactor coolant loop piping of a number of plants during hot functional testing. Stresses in the elbow below the RC pump have been found to be very small, between 2 and 3 ksi at the highest. Recent field measurements on typical PWR plants indicate vibration amplitudes less than 1 ksi. When translated to the connecting surge line, these stresses would be even lower, well below the fatigue endurance limit for the surge line material and would result in an applied stress intensity factor below the threshold for fatigue crack growth.

2.4 Summary Evaluation of Surge Line for Potential Degradation During Service

There has never been any service cracking or wall thinning identified in the pressurizer surge lines of Westinghouse PWR design. Sources of such degradation are mitigated by the design, construction, inspection, and operation of the pressurizer surge piping.

There is no mechanism for water hammer in the pressurizer/surge system. The pressurizer safety and relief piping system which is connected to the top of the pressurizer could have loading from water hammer events. However, these loads are effectively mitigated by the pressurizer and have a negligible effect on the surge line.

Wall thinning by erosion and erosion-corrosion effects will not occur in the surge line due to the low velocity, typically less than 1.0 ft/sec and the material, austenitic stainless steel, which is highly resistant to these degradation mechanisms. Per NUREG-0691, a study of pipe cracking in PWR piping, only two incidents of wall thinning in stainless steel pipe were reported and these were not in the surge line. Although it is not clear from the report, the cause of the wall thinning was related to the high water velocity and is therefore clearly not a mechanism which would affect the surge line.

It is well known that the pressurizer surge lines are subjected to thermal stratification and the effects of stratification are particularly significant during certain modes of heatup and cooldown operation. The effects of stratification have been evaluated for the Byron and Braidwood plant surge lines and the loads, accounting for the stratification effects have been derived in WCAP-12743. These loads are used in the leak-before-break evaluation described in this report.

The Byron and Braidwood Units 1 & 2 surge line piping and associated fittings are forged product forms (see Section 3) which are not susceptible to toughness degradation due to thermal aging.

Finally, the maximum operating temperature of the pressurizer surge piping, which is about 650°F, is well below the temperature which would cause any creep damage in stainless steel piping.

2.5 References

2-1 Investigation and Evaluation of Stress-Corrosion Cracking in Piping of Light Water Reactor Plants, NUREG-0531, U.S. Nuclear Regulatory Commission, February 1979.

2-2 Investigation and Evaluation of Cracking Incidents in Piping in Pressurized Water Reactors, NUREG-0691, U.S. Nuclear Regulatory Commission, September 1980.

SECTION 3.0
MATERIAL CHARACTERIZATION

3.1 Pipe and Weld Materials

The pipe materials of the pressurizer surge line for the Byron Units 1 and 2 are SA376/TP316 and SA376/TP304. The pipe material of the pressurizer surge line for the Braidwood Units 1 and 2 is SA376/TP316. These are a wrought product form of the type used for the primary loop piping of several PWR plants. The surge line is connected to the primary loop nozzle at one end and the other end of the surge line is connected to the pressurizer nozzle. The surge line system does not include any cast pipe or cast fitting. The welding processes used are shielded metal arc (SMAW) and submerged arc (SAW). Weld locations are identified in Figures 3-1, 3-2, 3-3 and 3-4.

In the following section the tensile properties of the materials are presented for use in the leak-before-break analyses.

3.2 Material Properties

The room temperature mechanical properties of the Byron Units 1, 2 and Braidwood Units 1, 2 surge line materials were obtained from the Certified Materials Test Reports and are given in Table 3-1, 3-2, 3-3, and 3-4. The room temperature ASME Code minimum properties are given in Table 3-5. It is seen that the measured properties well exceed those of the Code. The representative minimum and average tensile properties were established from the Certified Material Test Report. The material properties at temperatures (135°F, 205°F, 455°F and 653°F) are required for the leak rate and stability analyses discussed later. The minimum and average tensile properties were calculated by using the ratio of the ASME Section III properties at the temperatures of interest stated above. Tables 3-6, 3-7, 3-8 and 3-9 show the tensile properties at various temperatures for the Byron Units 1 & 2 and the Braidwood Units 1 & 2. The modulus of elasticity values were established at various temperatures from the ASME Section III (Table 3-10). In the

leak-before-break evaluation, the representative minimum properties at temperature are used for the flaw stability evaluations and the representative average properties are used for the leak rate predictions. The minimum ultimate stresses are used for stability analyses. These properties are summarized in Tables 3-5 through 3-9.

3.3 References

3-1 ASME Boiler and Pressure Vessel Code Section III, Division 1, Appendices July 1, 1989.

TABLE 3-1

Room Temperature Mechanical Properties of the Pressurizer Surge Line Materials and Welds of the Byron Unit 1

ID	HEAT NO./SERIAL NO.	MATERIAL	ULTIMATE STRENGTH psi	YIELD STRENGTH psi	ELONG. (%)	R/A (%)
A	L1284/13816	SA376/TP304	84,100	42,400	53.7	62.3
B	L1284/13816	SA376/TP304	84,900	42,400	54.0	57.0
C	L1281/13803	SA376/TP304	84,600	42,200	55.7	67.7
D	L1283/13812	SA376/TP304	87,900	44,900	53.7	68.2
E	J3536/9083	SA376/TP316	83,100	44,900	55.0	70.4
F	55009/9071	SA376/TP316	78,900	38,700	55.7	72.3
G	L1283/13812	SA376/TP304	87,900	44,900	53.7	68.2
H	L1283/13812	SA376/TP304	88,600	45,200	50.5	65.2
SW1	E7444 (GTAW)	SFA5.9/ER308	N/A	N/A	N/A	N/A
	34839 (SMAW)	SFA5.4/E308	85,700	59,000	40.0	64.9
SW2	E7444 (GTAW)	SFA5.9/ER308	N/A	N/A	N/A	N/A
	E7444 (SAW)	SFA5.9/ER308	N/A	N/A	N/A	N/A
SW3	E7444 (GTAW)	SFA5.9/ER308	N/A	N/A	N/A	N/A
	346839 (SMAW)	SFA5.4/E308	85,700	59,000	40.0	64.9
	536768 (SMAW)	SFA5.4/E308	84,900	57,400	40.0	64.7
SW4	E7444 (GTAW)	SFA5.9/ER308	N/A	N/A	N/A	N/A
	E7444 (SAW)	SFA5.9/ER308	N/A	N/A	N/A	N/A
SW5	E7444 (GTAW)	SFA5.9/ER308	N/A	N/A	N/A	N/A
	346839 (SMAW)	SFA5.4/E308	84,900	57,400	40.0	64.7
FW1	SMAW AND GTAW	N/A	N/A	N/A	N/A	N/A
FW2	SMAW AND GTAW	N/A	N/A	N/A	N/A	N/A
FW3	SMAW AND GTAW	N/A	N/A	N/A	N/A	N/A
FW4	SMAW AND GTAW	N/A	N/A	N/A	N/A	N/A
FW5	SMAW AND GTAW	N/A	N/A	N/A	N/A	N/A

N/A = Not Available

TABLE 3-2

Room Temperature Mechanical Properties of the Pressurizer Surge Line Materials and Welds of the Byron Unit 2

ID	HEAT NO./SERIAL NO.	MATERIAL	ULTIMATE STRENGTH psi	YIELD STRENGTH psi	ELONG. (%)	R/A (%)
A	L1284/13816	SA376/TP304	84,100	42,400	53.7	62.3
B	L1284/13816	SA376/TP304	84,900	42,400	54.0	57.0
C	L1284/13808	SA376/TP304	85,900	42,900	56.6	64.2
D	L1281/13807	SA376/TP304	84,900	43,400	57.9	73.0
E	J3536/9083	SA376/TP316	83,100	44,900	55.0	70.4
F	L1283/13808	SA376/TP304	85,900	43,900	57.0	65.9
G	L1283/13807	SA376/TP304	87,400	43,700	57.1	71.0
H	L1281/13807	SA376/TP304	87,400	43,700	57.1	71.0
SW1	E7444/GTAW	SFA5.9/ER308	N/A	N/A	N/A	N/A
	346839/SMAW	SFA5.4/E308	85,700	59,000	40.0	64.9
	536768/SMAW	SFA5.4/E308	84,900	57,400	40.0	64.7
SW2	E7444/GTAW	SF5.9/ER308	N/A	N/A	N/A	N/A
	E7444/SAW	SFA5.9/ER308	N/A	N/A	N/A	N/A
SW3	E7444/GTAW	SFA5.9/ER308	N/A	N/A	N/A	N/A
	346839/SMAW	SFA5.4/E308	85,700	59,000	40.0	64.9
SW4	E7444/GTAW	SFA5.9/ER308	N/A	N/A	N/A	
	E7444/SAW	SFA5.9/ER308				
SW5	E7444/GTAW	SFA5.9/ER308				
	346839/SMAW	SFA5.4/E308				
FW1	SMAW AND GTAW	N/A	N/A	N/A	N/A	N/A
FW2	SMAW AND GTAW	N/A	N/A	N/A	N/A	N/A
FW3	SMAW AND GTAW	N/A	N/A	N/A	N/A	N/A
FW4	SMAW AND GTAW	N/A	N/A	N/A	N/A	N/A
FW5	SMAW AND GTAW	N/A	N/A	N/A	N/A	N/A

N/A = Not Available

TABLE 3-3

Room Temperature Mechanical Properties of the Pressurizer Surge Line Materials and Welds of the Braidwood Unit 1

ID	HEAT NO./SERIAL NO.	MATERIAL	ULTIMATE STRENGTH psi	YIELD STRENGTH psi	ELONG. (%)	R/A (%)
A	J6569/28427Z	SA376/TP316	89,900	43,700	51.2	69.3
B	J6569/28427Z	SA376/TP316	89,900	43,700	51.2	69.3
C	J6569/28426	SA376/TP316	88,200	46,100	50.3	66.4
D	J6569/28426	SA376/TP316	88,200	46,100	50.3	66.4
E	J6568/28422Y	SA376/TP316	87,400	44,100	51.8	70.0
F	J6569/28427Z	SA376/TP316	89,900	43,700	51.2	69.3
SW1	16654C/GTAW	SFA5.9/ER308	92,500	N/A	41	N/A
	6D38010/SMAW	SFA5.4/E308	85,000	64,000	45	54
	6D38011/SMAW	SFA5.4/E308	82,820	58,900	45	50
	742059A/SMAW	SFA5.4/E308	82,700	58,900	45	50
SW2	16654C/GTAW	SFA5.9/ER308	92,500	N/A	41	N/A
	6D38010/SMAW	SFA5.4/E308	85,000	64,000	45	54
	6D38011/SMAW	SFA5.4/E308	82,820	58,900	45	50
	7H2059A/SMAW	SFA5.4/E308	82,700	58,900	45	50
SW3	16654C/GTAW	SFA5.9/ER308	92,500	N/A	41	N/A
	6D38011/SMAW	SFA5.4/E308	82,700	58,900	45	50
	7H2059A/SMAW	SFA5.4/E308	82,700	58,900	45	50
FW1	SMAW AND GTAW	N/A	N/A	N/A	N/A	N/A
FW2	SMAW AND GTAW	N/A	N/A	N/A	N/A	N/A
FW3	SMAW AND GTAW	N/A	N/A	N/A	N/A	N/A
FW4	SMAW AND GTAW	N/A	N/A	N/A	N/A	N/A
FW5	SMAW AND GTAW	N/A	N/A	N/A	N/A	N/A

N/A = Not Available

TABLE 3-4

Room Temperature Mechanical Properties of the Pressurizer Surge Line Materials and Welds of the Braidwood Unit 2

ID	HEAT NO./SERIAL NO.	MATERIAL	ULTIMATE STRENGTH psi	YIELD STRENGTH psi	ELONG. (%)	R/A (%)
A	J6568/28416	SA376/TP316	87,800	45,700	52.6	66.9
B	J6570/28428	SA376/TP316	87,600	46,400	50.6	68.6
C	J6570/28428	SA376/TP316	87,600	46,400	50.6	68.6
D	J6568/28416	SA376/TP316	87,800	45,700	52.6	66.9
E	J6570/28429	SA387/TP316	90,600	47,600	50.0	66.7
F	J6568/28416	SA376/TP316	87,800	45,700	52.6	66.9
SW1	16654C/GTAW	SFA5.9/ER308	92,500	N/A	41	N/A
	14975C/SMAW	SFA5.4/E308	92,900	N/A	36	N/A
	04756/SMAW	SFA5.4/E308	94,000	N/A	44	N/A
SW2	16654C/GTAW	SFA5.9/ER308	92,500	N/A	41	N/A
	6D38010/SMAW	SFA5.4/E308	85,000	64,000	45	54
	14975C/SMAW	SFA5.4/E308	92,900	N/A	36	N/A
	04756/SMAW	SFA5.4/E308	94,000	N/A	44	N/A
SW3	16654C/GTAW	SFA5.9/ER308	92,500	N/A	41	N/A
	6D38010/SMAW	SFA5.4/E308	85,000	64,000	45	54
	6D38011/SMAW	SFA5.4/E308	82,820	60,240	50	57
	04756/SMAW	SFA5.4/E308	94,000	N/A	44	N/A
FW1	SMAW AND GTAW	N/A	N/A	N/A	N/A	N/A
FW2	SMAW AND GTAW	N/A	N/A	N/A	N/A	N/A
FW3	SMAW AND GTAW	N/A	N/A	N/A	N/A	N/A
FW4	SMAW AND GTAW	N/A	N/A	N/A	N/A	N/A
FW5	SMAW AND GTAW	N/A	N/A	N/A	N/A	N/A

N/A = Not Available

TABLE 3-5

Room Temperature ASME Code Minimum Properties

Material	Yield Stress (psi)	Ultimate Stress (psi)
SA376/TP304	30,000	75,000
SA376/TP316	30,000	75,000

TABLE 3-6

Representative Tensile Properties for Byron Unit 1

Material	Temperature (°F)	Minimum Yield (psi)	Average Yield (psi)	Minimum Ultimate (psi)
SA376/TP304	100	42,200	43,670	84,100
	135	39,740	41,120	82,530
	205	34,990	36,210	79,330
	455	28,110	29,090	71,660
	653	25,160	26,040	71,200
SA376/TP316	100	38,700	41,800	78,900
	135	36,800	39,750	78,900
	205	33,130	35,780	78,800
	455	26,540	28,670	75,530
	653	23,840	25,750	75,530

TABLE 3-7

Representative Tensile Properties for Byron Unit 2

Material	Temperature (°F)	Minimum Yield (psi)	Average Yield (psi)	Minimum Ultimate (psi)
SA376/TP304	100	42,400	43,200	84,100
	135	39,920	40,680	82,530
	205	35,150	35,820	79,330
	455	28,240	28,780	71,660
	653	25,280	25,760	71,200
SA376/TP316	100	44,900	44,900	83,100
	135	42,700	42,700	83,100
	205	38,430	38,430	83,000
	455	30,790	30,790	79,550
	653	27,660	27,660	79,550

TABLE 3-8

Representative Tensile Properties for Braidwood Unit 1

Material	Temperature (°F)	Minimum Yield (psi)	Average Yield (psi)	Minimum Ultimate (psi)
SA376/TP316	100	43,700	44,570	87,400
	135	41,150	42,380	85,770
	205	36,230	38,160	82,450
	455	29,110	30,560	74,470
	653	26,060	27,450	73,990

TABLE 3-9

Representative Tensile Properties for Braidwood Unit 2

Material	Temperature (°F)	Minimum Yield (psi)	Average Yield (psi)	Minimum Ultimate (psi)
SA376/TP316	100	45,700	46,250	87,600
	135	43,030	43,980	85,960
	205	37,890	39,590	82,630
	455	30,440	31,720	74,640
	653	27,250	28,490	74,170

TABLE 3-10

Modulus of Elasticity (E)

Temperature (°F)	E (ksi)
100	28,138
135	27,950
205	27,600
455	26,115
653	25,035

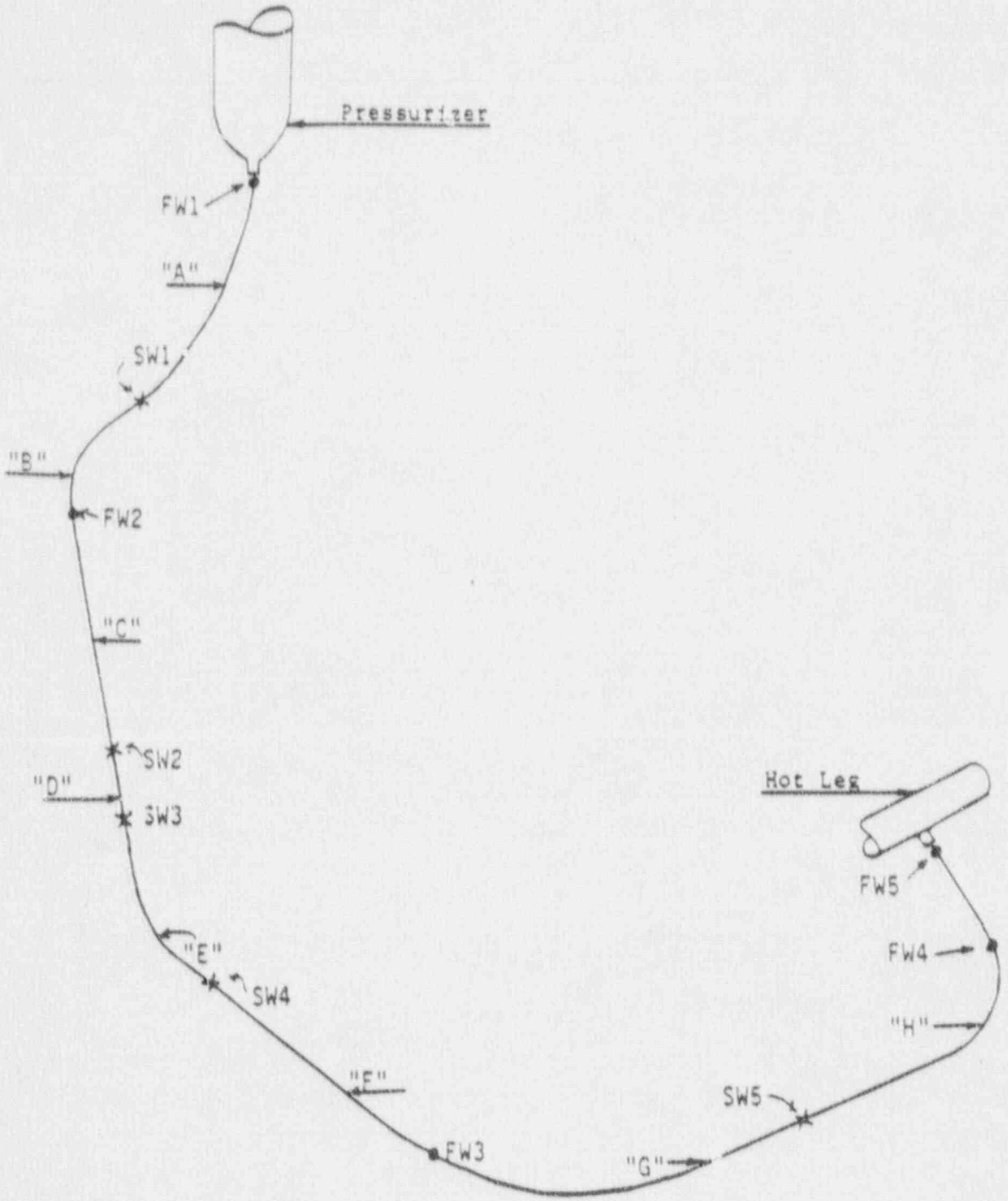

NOTE:
FW1 to FW5 - Field Weld
SW1 to SW5 - Shop Weld

Figure 3-1 Byron Unit 1 Surge Line Layout

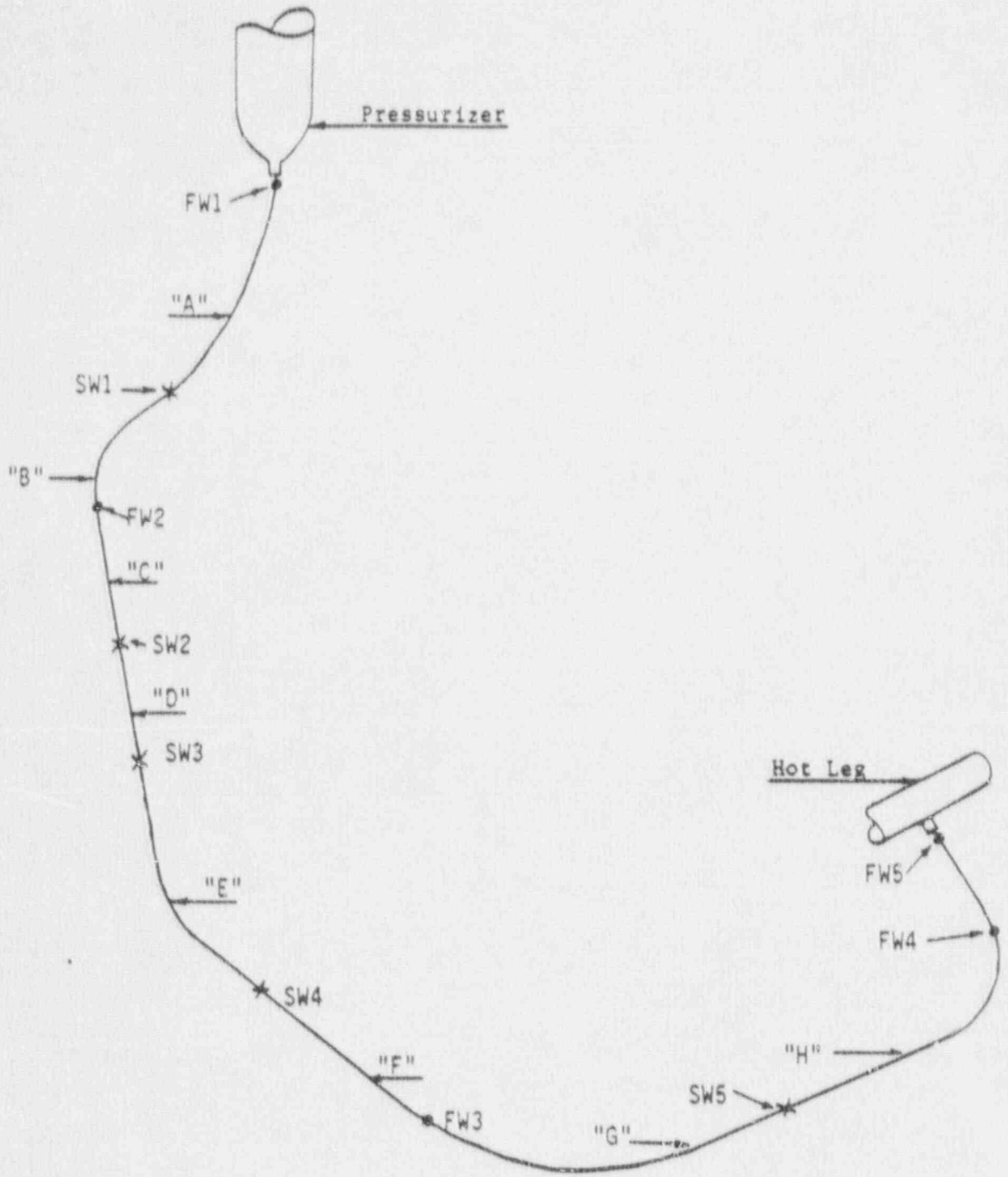

Note:
FW1 to FW5 - Field Weld
SW1 to SW5 - Shop Weld

Figure 3-2 Byron Unit 2 Surge Line Layout

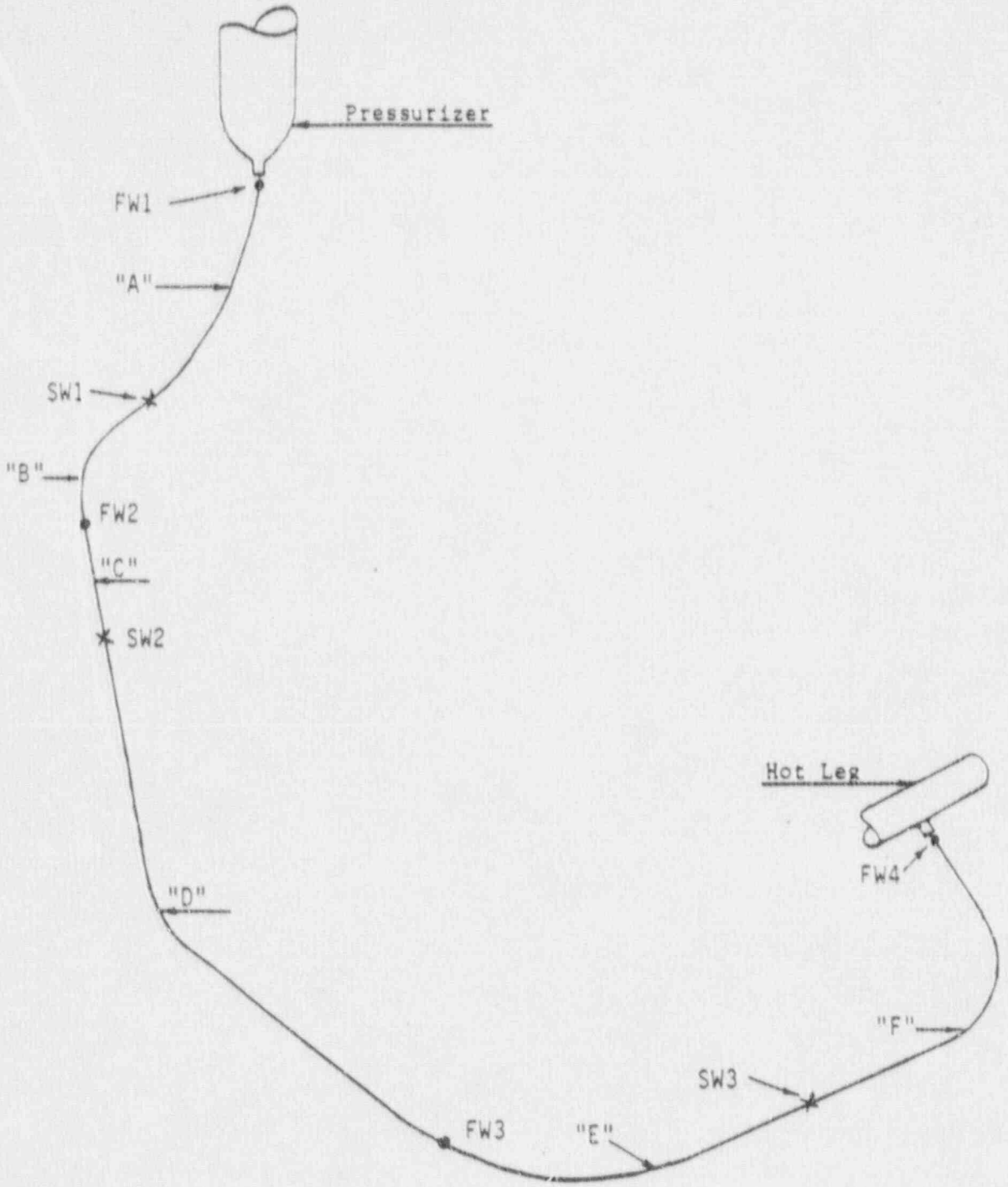

Note:
FW1 to FW4 - Field Weld
SW1 to SW3 - Shop Weld

Figure 3-3 Braidwood Unit 1 Surge Line Layout

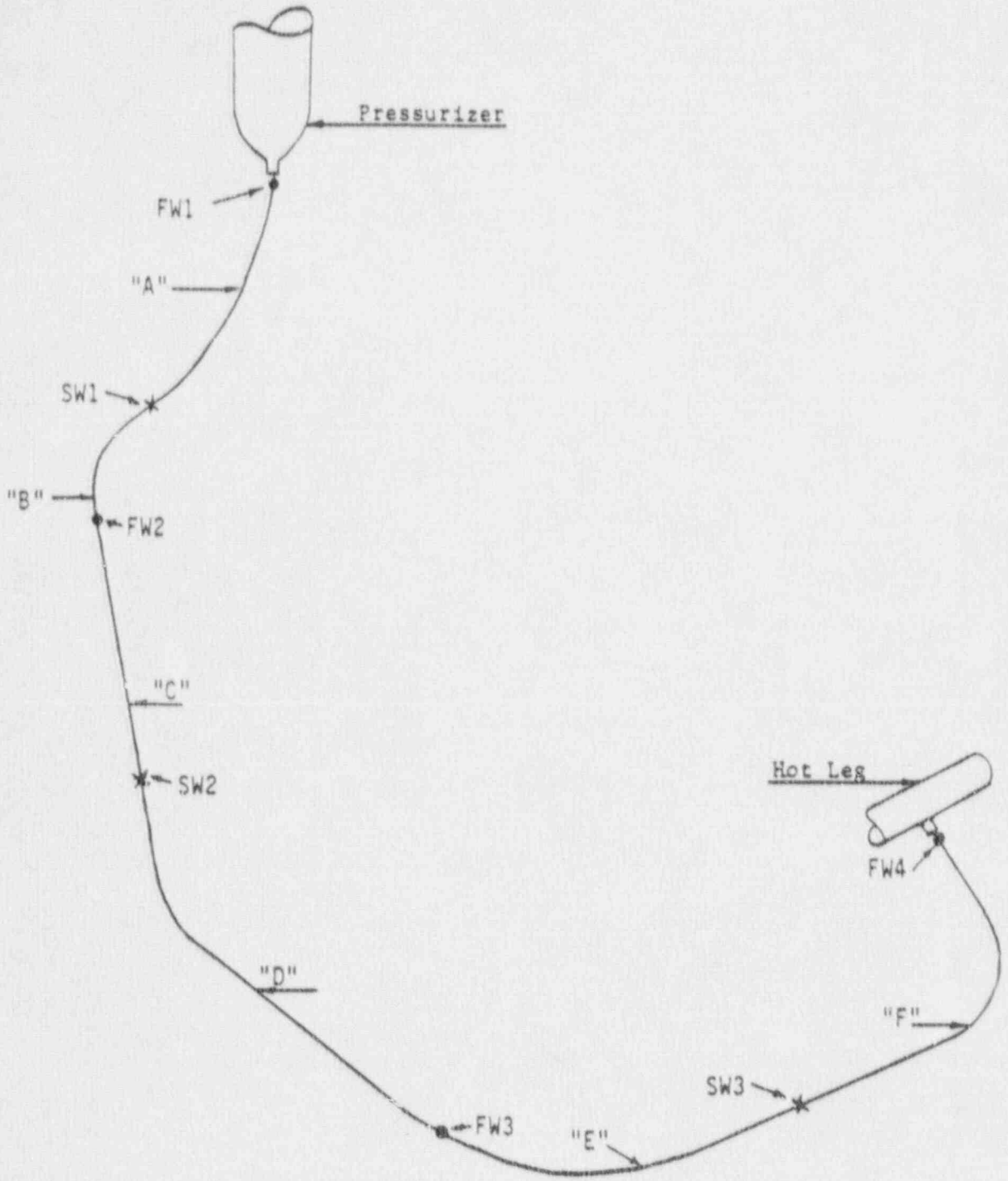

Note:
FW1 to FW4 - Field Weld
SW1 to SW3 - Shop Weld

Figure 3-4 Braidwood Unit 2 Surge Line Layout

SECTION 4.0

LOADS FOR FRACTURE MECHANICS ANALYSIS

Figures 3-1 through 3-4 show schematic layouts of the surge lines for Byron Units 1 & 2 and Braidwood Units 1 & 2 and identify the weld locations.

The stresses due to axial loads and bending moments were calculated by the following equation:

$$\sigma = \frac{F}{A} + \frac{M}{Z} \qquad (4\text{-}1)$$

where,

σ	=	stress
F	=	axial load
M	=	bending moment
A	=	metal cross-sectional area
Z	=	section modulus

The bending moments for the desired loading combinations were calculated by the following equation:

$$M_B = (M_Y^2 + M_Z^2)^{0.5} \qquad (4\text{-}2)$$

where,

M_B	=	bending moment for required loading
M_Y	=	Y component of bending moment
M_Z	=	Z component of bending moment

The axial load and bending moments for crack stability analysis and leak rate predictions are computed by the methods to be explained in Sections 4.1 and 4.2 which follow.

4.1 Loads for Crack Stability Analysis

The faulted loads for the crack stability analysis were calculated by the following equations:

$$F = |F_{DW}| + |F_{TH}| + |F_p| + |F_{SSE}| \quad (4\text{-}3)$$

$$M_Y = |(M_Y)_{DW}| + |M_{Y\ TH}| + |M_{Y\ SSE}| \quad (4\text{-}4)$$

$$M_Z = |(M_Z)_{DW}| + |M_{Z\ TH}| + |M_{Z\ SSE}| \quad (4\text{-}5)$$

DW = Deadweight
TH = Applicable thermal load
P = Load due to internal pressure
SSE = SSE loading including seismic anchor motion

4.2 Loads for Leak Rate Evaluation

The normal operating loads for leak rate predictions were calculated by the following general equations:

$$F = F_{DW} + F_{TH} + F_p \quad (4\text{-}6)$$

$$M_Y = (M_Y)_{DW} + (M_Y)_{TH} \quad (4\text{-}7)$$

$$M_Z = (M_Z)_{DW} + (M_Z)_{TH} \quad (4\text{-}8)$$

The parameters and subscripts are the same as those explained in Section 4.1.

4.3 Loading Conditions

Because thermal stratification can cause large stresses at heatup and cooldown temperatures in the range of 455°F, a review of stresses was used to identify the worst situations for LBB applications. The loading states so identified are given in Table 4-1.

Seven loading cases were identified for LBB evaluation as given in Table 4-2. Cases A, B, C are cases for leak rate calculations with the remaining cases being the corresponding faulted situations for stability evaluations.

The cases postulated for leak-before-break are summarized in Table 4-3. The cases of primary interest are the postulation of a detectable leak at normal power conditions [----------
---

---]a,c,e

The combination [----------

---]a,c,e

The more realistic cases [----------

----------]^{a,c,e}

[----------

----------]^{a,c,e} The logic for this ΔT [-------]^{a,c,e} is based on the following:

Actual practice, based on plant experience with this type of situation, indicates that the plant operators complete the cooldown as quickly as possible once a leak in the primary system is detected. Technical Specifications may require cold shutdown within 36 hours but actual practice is that the plant depressurizes the system as soon as possible once a primary system leak is detected. Therefore, the hot leg is generally on the warmer side of the limits (~200°F) when the pressurizer bubble is quenched. Once the bubble is quenched, the pressurizer is cooled down fairly quickly reducing the ΔT in the system.

4.4 Summary of Loads and Geometry

The load combinations were evaluated at the various weld locations. Normal loads were determined using the algebraic sum method whereas faulted loads were combined using the absolute sum method.

4.5 Governing Locations

All the welds at Braidwood Units 1 and 2 surgelines are fabricated using the SMAW procedure. In Byron Units 1 and 2 surge lines both SMAW and SAW procedures were used. The following governing locations were established for each type of weld.

SMAW Weld

Node 1030 (hot leg nozzle junction) for Byron 1 & 2 and Braidwood 1 & 2.

SAW Weld

Node 1350 for Byron Units 1 and 2.

The loads and stresses at these critical locations for all the loading combinations are shown in Tables 4-4 through 4-7.

TABLE 4-1

Types of Loadings

Pressure (P)
Dead Weight (DW)
Normal Operating Thermal Expansion (TH)
Safe Shutdown Earthquake and Seismic Anchor Motion (SSE)[a]
[redacted] a,c,e

[a] SSE is used to refer to the absolute sum of these loadings.

TABLE 4-2

Normal and Faulted Loading Cases for Leak-Before-Break Evaluations

CASE A: This is the normal operating case at 653°F consisting of the algebraic sum of the loading components due to P, DW and TH.

a,c,e

CASE B: [redacted]

CASE C: [redacted]

CASE D: This is the faulted operating case at 653°F consisting of the absolute sum (every component load is taken as positive) of P, DW, TH and SSE.

a,c,e

CASE E: [redacted]

CASE F: [redacted]

CASE G: [redacted]

TABLE 4-3

Associated Load Cases for Analyses

A/D This is here-to-fore standard leak-before-break evaluation.

a,c,e

A/F	[redacted]
B/E	[redacted]
B/F	[redacted]
B/G[a]	[redacted]
C/G[a]	[redacted]

[a] These are judged to be low probability events.

TABLE 4-4

Summary of LBB Loads and Stresses by Case for Byron Unit 1

Node	Case	F_X(lbs)	S_X(psi)	M_B(in-lb)	S_B(psi)	S_T(psi)	
1030	A	228508	4561	1025567	6986	11547	
1030	B	------	----	-------	-----	-----	a,c,e
1030	C	------	----	-------	-----	-----	
1030	D	246488	4920	3053650	20801	25721	a,c,e
1030	E	------	----	-------	-----	-----	
1030	F	------	----	-------	-----	-----	
1030	G	------	----	-------	-----	-----	
1350	A	239393	4778	758895	5170	9948	
1350	B	------	----	-------	-----	-----	a,c,e
1350	C	------	----	-------	-----	-----	
1350	D	245579	4902	1610046	10968	15869	a,c,e
1350	E	------	----	-------	-----	-----	
1350	F	------	----	--------	-----	-----	
1350	G	------	----	-------	-----	-----	

TABLE 4-5

Summary of LBB Loads and Stresses by Case for Byron Unit 2

Node	Case	F_X(lbs)	S_X(psi)	M_B(in-lb)	S_B(psi)	S_T(psi)	
1030	A	228678	4564	1031829	7029	11593	
1030	B	------	----	-------	-----	-----	a,c,e
1030	C	------	----	-------	-----	-----	
1030	D	254903	5088	3157781	21511	26599	
1030	E	------	----	-------	-----	------	a,c,e
1030	F	------	----	-------	-----	-----	
1030	G	------	----	-------	-----	-----	
1350	A	239363	4778	766365	5220	9998	
1350	B	------	----	-------	-----	-----	a,c,e
1350	C	------	----	-------	-----	-----	
1350	D	256460	5119	1452482	9894	15013	
1350	E	------	----	-------	-----	-----	a,c,e
1350	F	------	----	-------	-----	-----	
1350	G	------	----	-------	-----	-----	

TABLE 4-6

Summary of LBB Loads and Stresses by Case for Braidwood Unit 1

Node	Case	F_X(lbs)	S_X(psi)	M_B(in-lb)	S_B(psi)	S_T(psi)	
1030	A	228508	4561	1025567	6985	11547	
1030	B	------	----	-------	-----	-----	a,c,e
1030	C	------	----	-------	-----	-----	
1030	D	246488	4920	3053650	20801	25721	
1030	E	------	----	-------	-----	-----	a,c,e
1030	F	------	----	-------	-----	-----	
1030	G	------	----	-------	-----	-----	

TABLE 4-7

Summary of LBB Loads and Stresses by Case
for P-aidwood Unit 2

Node	Case	F_X(lbs)	S_X(psi)	M_B(in-lb)	S_B(psi)	S_T(psi)	
1030	A	228508	4561	1025567	6986	11547	
1030	B	------	----	-------	-----	-----	a,c,e
1030	C	------	----	-------	-----	-----	
1030	D	254733	5084	3003583	20460	25545	
1030	E	------	----	-------	-----	-----	a,c,e
1030	F	------	----	-------	-----	-----	
1030	G	------	----	-------	-----	-----	

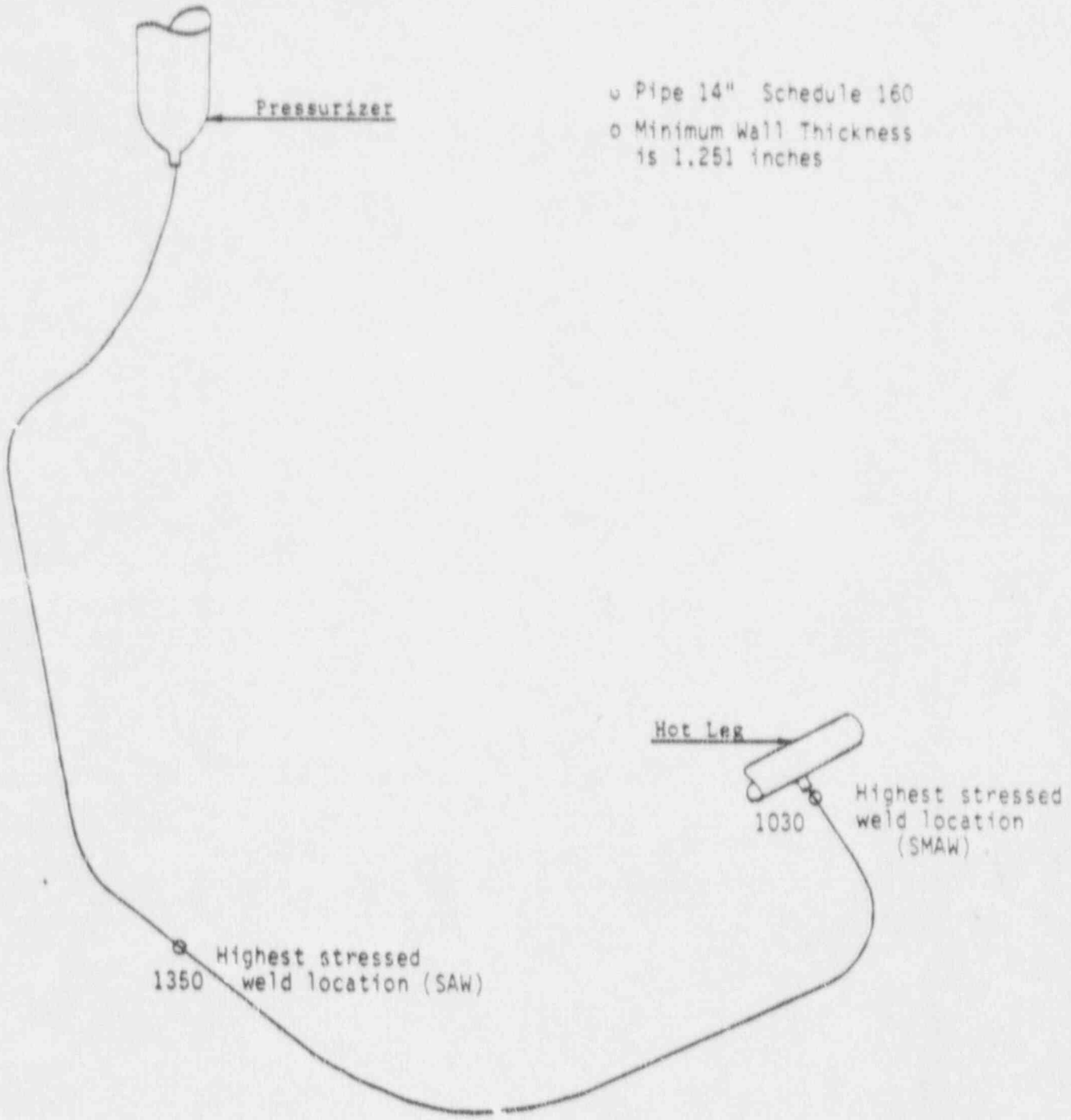

Figure 4-1 Byron Units 1 & 2 Surge Line
Showing Governing Locations

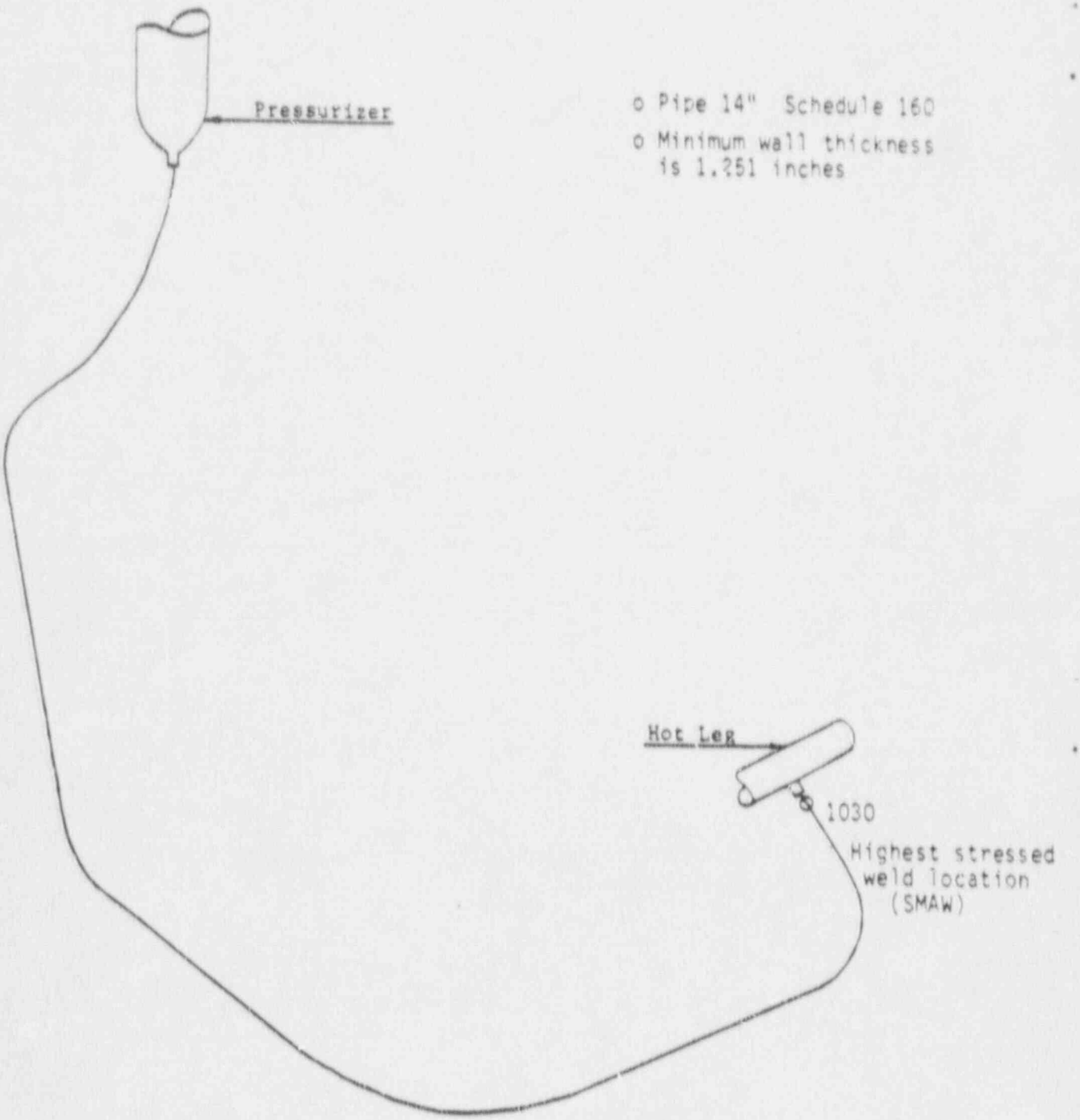

Figure 4-2 Braidwood Units 1 & 2 Surge Line Showing Governing Locations

SECTION 5.0
FRACTURE MECHANICS EVALUATION

5.1 Global Failure Mechanism

Determination of the conditions which lead to failure in stainless steel should be done with plastic fracture methodology because of the large amount of deformation accompanying fracture. One method for predicting the failure of ductile material is the [----------]^{a,c,e} method, based on traditional plastic limit load concepts, but accounting for [----------]^{a,c,e} and taking into account the presence of a flaw. The flawed component is predicted to fail when the remaining net section reaches a stress level at which a plastic hinge is formed. The stress level at which this occurs is termed as the flow stress. [----------]^{a,c,e} This methodology has been shown to be applicable to ductile piping through a large number of experiments and is used here to predict the critical flaw size in the pressurizer surge line. The failure criterion has been obtained by requiring equilibrium of the section containing the flaw (Figure 5-1) when loads are applied. The detailed development is provided in Appendix A for a through-wall circumferential flaw in a pipe section with internal pressure, axial force, and imposed bending moments. The limit moment for such a pipe is given by:

[----------]^{a,c,e} (5-1)

where:

[----------

----------]^{a,c,e}

[----------

---------- ----

---------- ----------

---------- ----------

---------- ----------

----------]^{a,c,e} (5-2)

The analytical model described above accurately accounts for the internal pressure as well as imposed axial force as they affect the limit moment. Good agreement was found between the analytical predictions and the experimental results (reference 5-1). Flaw stability evaluations, using this analytical model, are presented in section 5.3.

5.2 Leak Rate Predictions

Fracture mechanics analysis shows in general that postulated through-wall cracks in the surge line would remain stable and do not cause a gross failure of this component. However, if such a through-wall crack did exist, it would be desirable to detect the leakage such that the plant could be brought to a safe shutdown condition. The purpose of this section is to discuss the method which will be used to predict the flow through such a postulated crack and present the leak rate calculation results for through-wall circumferential cracks.

5.2.1 General Considerations

The flow of hot pressurized water through an opening to a lower back pressure (causing choking) is taken into account. For long channels where the ratio of the channel length, L, to hydraulic diameter, D_H, (L/D_H) is greater than [--]^{a,c,e}, both [----------]^{a,c,e} must be considered. In this situation the flow can be described as being single-phase through the channel until the local pressure equals the saturation pressure of the fluid.

At this point, the flow begins to flash and choking occurs. Pressure losses due to momentum changes will dominate for [----------]^{a,c,e} However, for large L/D_H values, the friction pressure drop will become important and must be considered along with the momentum losses due to flashing.

5.2.2 Calculational Method

In using the [----------

----------]^{a,c,e}.

The flow rate through a crack was calculated in the following manner. Figure 5-2 from reference 5-2 was used to estimate the critical pressure, Pc, for the primary loop enthalpy condition and an assumed flow. Once Pc was found for a given mass flow, the [----------]^{a,c,e} was found from figure 5-3 taken from reference 5-2. For all cases considered, since [----------]^{a,c,e} Therefore, this method will yield the two-phase pressure drop due to momentum effects as illustrated in figure 5-4. Now using the assumed flow rate, G, the frictional pressure drop can be calculated using

$$\Delta P_f = [f\frac{(L/D_H - 40)G^2}{\rho\, 2g_c\, (144)}]^{a,c,e} \qquad (5\text{-}3)$$

where the friction factor f is determined using the [----------]^{a,c,e} The crack relative roughness, ε, was obtained from fatigue crack data on stainless steel samples. The relative roughness value used in these calculations was [----------]^{a,c,e} RMS.

The frictional pressure drop using Equation 5-3 is then calculated for the assumed flow and added to the [----------]a,c,e to obtain the total pressure drop from the system under consideration to the atmosphere. Thus,

$$\text{Absolute Pressure} - 14.7 = [\text{----------}]^{a,c,e} \quad (5\text{-}4)$$

for a given assumed flow G. If the right-hand side of equation 5-4 does not agree with the pressure difference between the piping under consideration and the atmosphere, then the procedure is repeated until equation 5-4 is satisfied to within an acceptable tolerance and this results in the flow value through the crack.

5.2.3 Leak Rate Calculations

Leak rate calculations were performed as a function of postulated through-wall crack length for the critical locations previously identified. The crack opening area was estimated using the method of reference 5-3 and the leak rates were calculated using the calculational methods described above. The leak rates were calculated using the normal operating loads at the governing nodes identified in section 4.0. The crack lengths yielding a leak rate of 10 gpm (10 times the leak detection capability of 1.0 gpm) for critical locations at the Byron Unit 1 & 2 and Braidwood Units 1 & 2 pressurizer surge lines are shown in Tables 5-1, 5-2, 5-3 and 5-4.

5.3 Stability Evaluation

A typical segment of the nozzle under maximum loads of axial force F and bending moment M is schematically illustrated as shown in figure 5-5. In order to calculate the critical flaw size, plots of the limit moment versus crack length are generated as shown in figures 5-6 to 5-29. The critical flaw size corresponds to the intersection of this curve and the maximum load line. The critical flaw size is calculated using the lower bound base metal tensile properties established in section 3.0.

The weld at the locations of interest (i.e. the governing location) are SMAW and SAW welds. Therefore, "Z" factor corrections for SMAW and SAW welds were applied (references 5-4 and 5-5) as follows:

$$Z = 1.15\ [1 + 0.013\ (O.D. - 4)]\ \text{(for SMAW)} \qquad (5\text{-}5)$$

$$Z = 1.30\ [1 + 0.010\ (O.D. - 4)]\ \text{(for SAW)} \qquad (5\text{-}6)$$

where OD is the outer diameter in inches. Substituting OD = 14.00 inches, the Z factor was calculated to be 1.2995 for SMAW and 1.43 for SAW. The applied loads were increased by the Z factors and the plots of limit load versus crack length were generated as shown in figure 5-6 to 5-29. Tables 5-5, 5-6, 5-7 and 5-8 show the summary of critical flaw sizes for Byron, Braidwoods Units 1 & 2.

5.4 References

5-1 Kanninen, M. F. et al., "Mechanical Fracture Predictions for Sensitized Stainless Steel Piping with Circumferential Cracks" EPRI NP-192, September 1976.

5-2 [Fauske, H. K., "Critical Two-Phase, Steam Water Flows," Proceedings of the Heat Transfer and Fluid Mechanics Institute, Stanford, California, Standford University Press, 1961.][a,c,e]

5-3 Tada, H., "The Effects of Shell Corrections on Stress Intensity Factors and the Crack Opening Area of Circumferential and a Longitudinal Through-Crack in a Pipe," Section II-1, NUREG/CR-3464, September 1983.

5-4 NRC letter from M. A. Miller to Georgia Power Company, J. P. O'Reilly, dated September 9, 1987.

5-5 ASME Code Section XI, Winter 1985 Addendum, Article IWB-3640.

5-6 Standard Review Plan; Public Comment Solicited; 3.6.3 Leak-Before-Break Evaluation Procedures; Federal Register/Vol. 52, No. 167/Friday, August 28, 1987/Notices, pp. 32626-32633.

TABLE 5-1

Leak Rate Crack Length for Byron Unit 1

Node Point	Load Case	Temperature (°F)	Crack Length (in.) (for 10 gpm leakage)
			a,c,e
1030	[redacted]	[redacted]	[redacted]
			[redacted]
			[redacted]
1350			[redacted]
			[redacted]
			[redacted]

TABLE 5-2

Leak Rate Crack Length for Byron Unit 2

Node Point	Load Case	Temperature (°F)	Crack Length (in.) (for 10 gpm leakage)
			a,c,e
1030	[	[	[
		[	[
		[	[
1350		[	[
		[	[
	]	[	[

TABLE 5-3

Leak Rate Crack Length for Braidwood Unit 1

Node Point	Load Case	Temperature (°F)	Crack Length (in.) (for 10 gpm leakage)
			a,c,e
1030	[	----------	]

TABLE 5-4

Leak Rate Crack Length for Braidwood Unit 2

Node Point	Load Case	Temperature (°F)	Crack Length (in.) (for 10 gpm leakage)
			a,c,e
1030	[	----------	]

TABLE 5-5

Summary of Critical Flaw Size for Byron Unit 1

Node Point	Load Case	Temperature (°F)	Critical Flaw Size (in)
			a,c,e
1030	[		]
1350			

a

TABLE 5-6

Summary of Critical Flaw Size for Byron Unit 2

Node Point	Load Case	Temperature (°F)	Critical Flaw Size (in)
			a,c,e
1030	[	----------	]

1350		----------	

TABLE 5-7

Summary of Critical Flaw Size for Braidwood Unit 1

Node Point	Load Case	Temperature (°F)	Critical Flaw Size (in)
1030	[	----------	] a,c,e

TABLE 5-8

Summary of Critical Flaw Size for Braidwood Unit 2

Node Point	Load Case	Temperature (°F)	Critical Flaw Size (in)
			a,c,e
1030	[	----------	]

Figure 5-1 Fully Plastic Stress Distribution

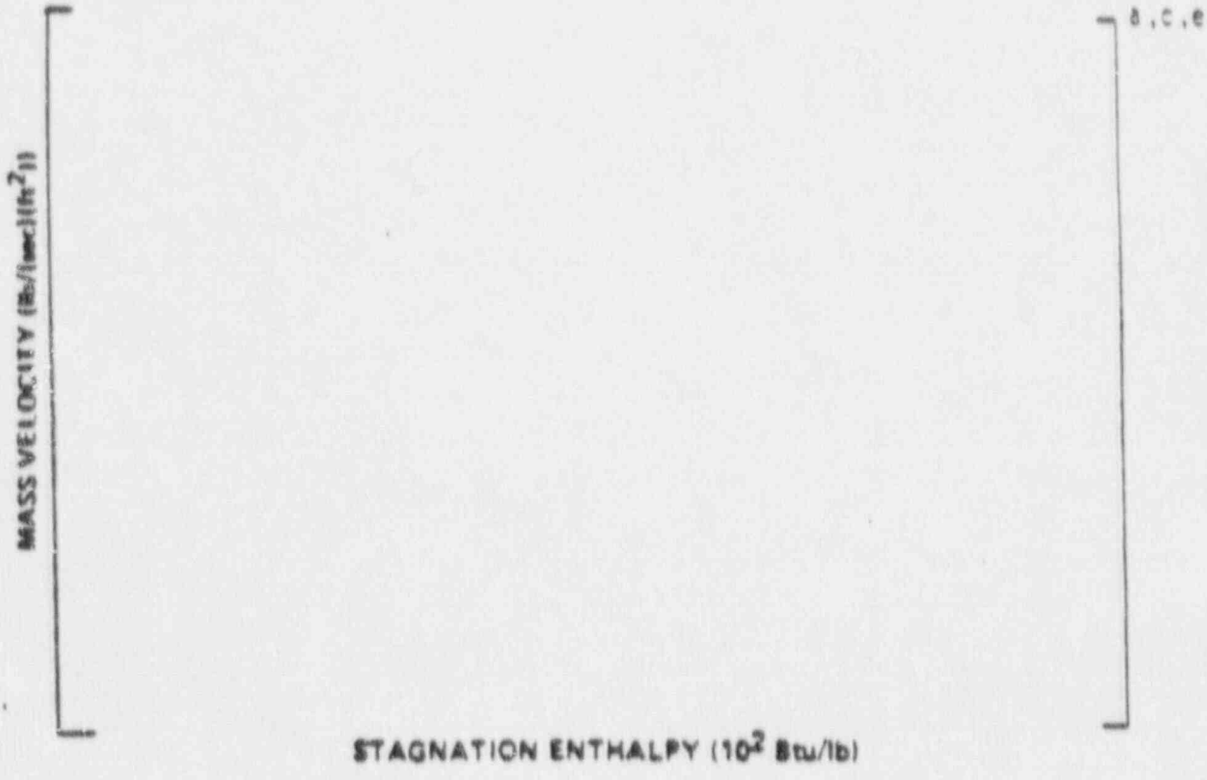

Figure 5-2 Analytical Predictions of Critical Flow Rates of Steam-Water Mixtures

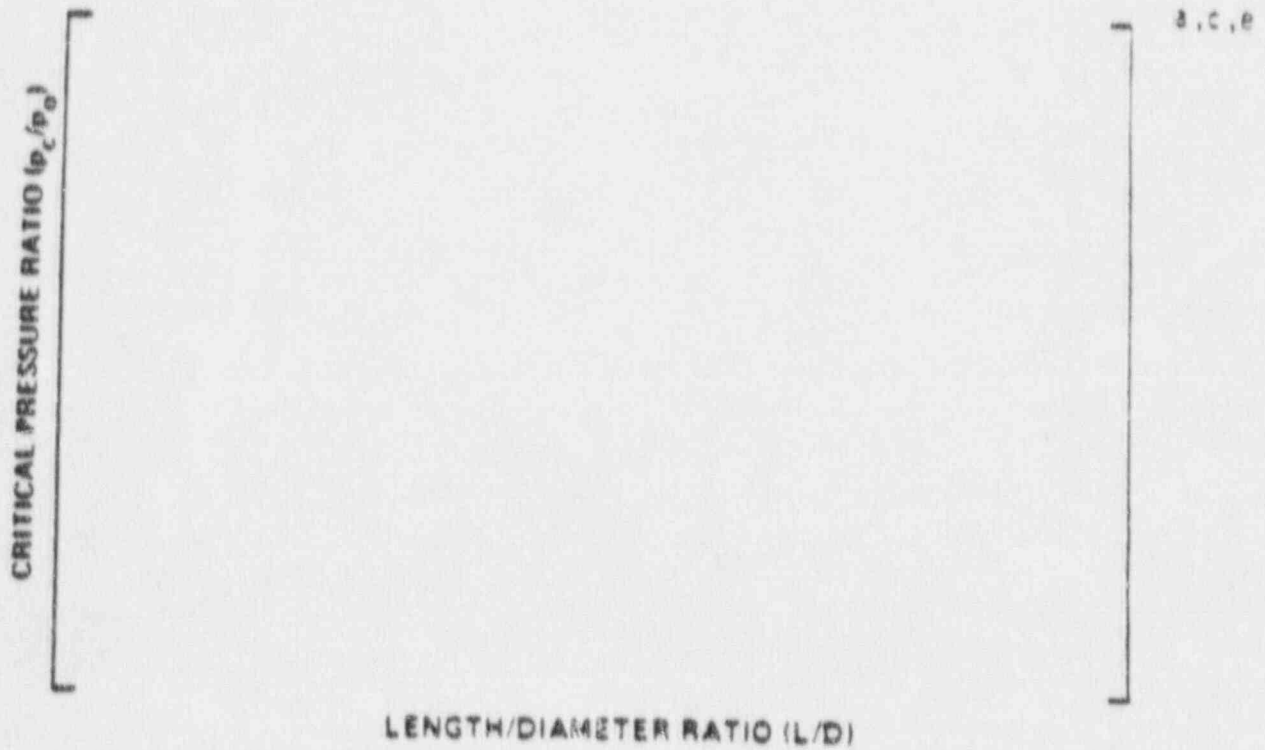

Figure 5-3 [ ]^{a,c,e} Pressure Ratio as a Function of L/D

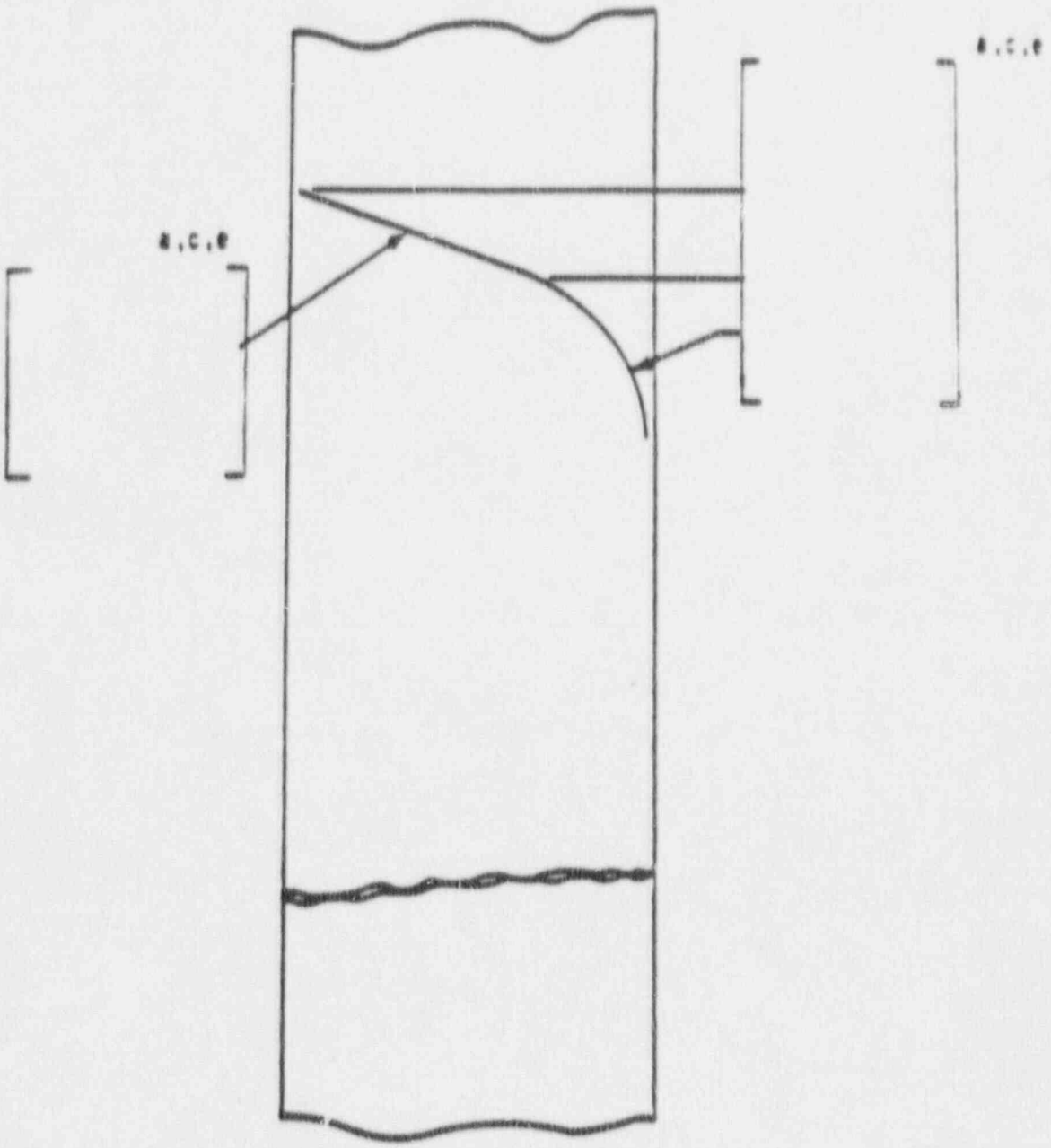

Figure 5-4. Idealized Pressure Drop Profile Through a Postulated Crack

Figure 5-5. Loads Acting on the Model at the Governing Location

Figure 5-6. Critical Flaw Size Prediction for Byron Unit 1
Node 1030 Case D

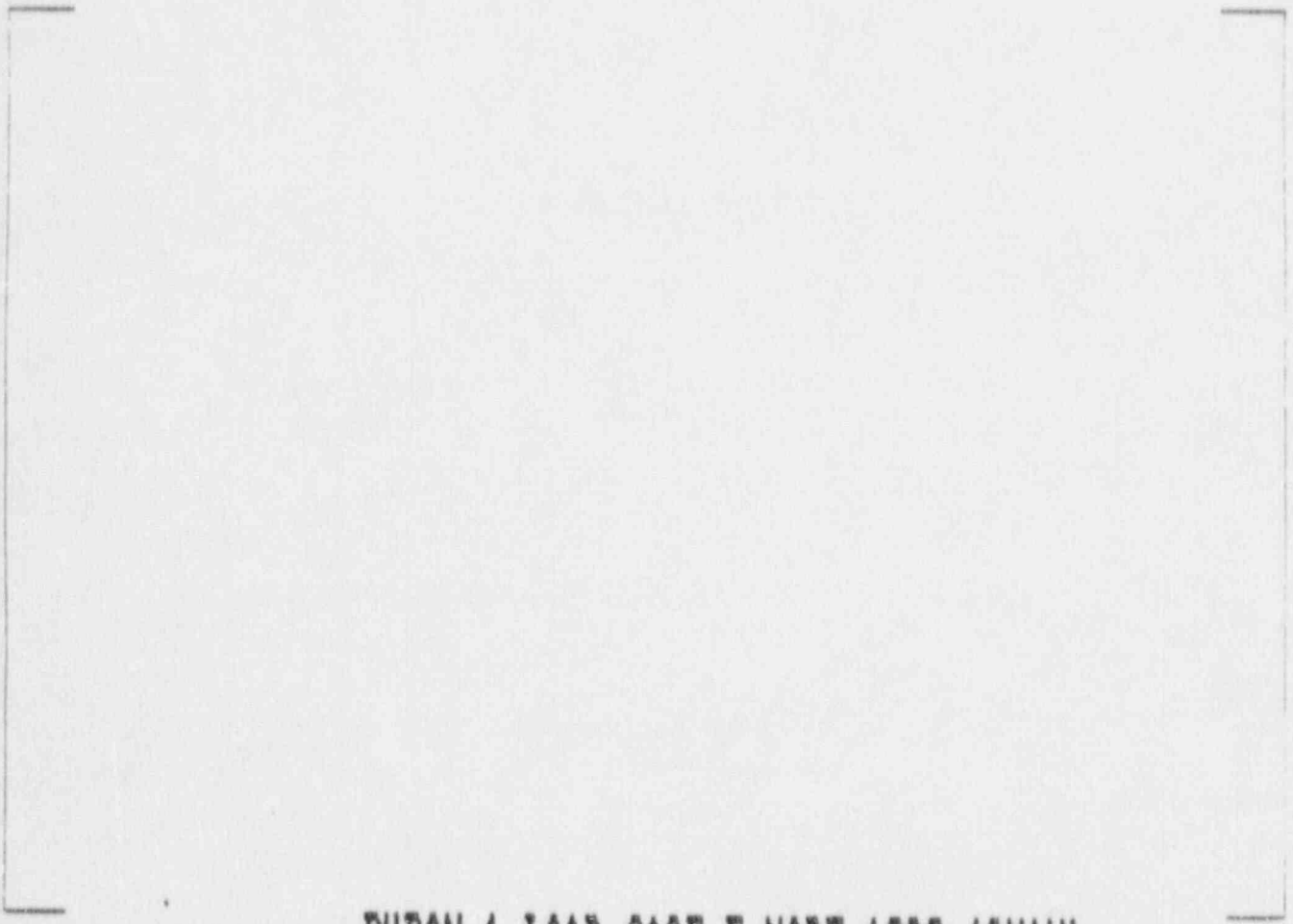

Figure 5-7. Critical Flaw Size Prediction for Byron Unit 1
Node 1030 Case E

Figure 5-8 Critical Flaw Size Prediction for Byron Unit 1
Node 1030 Case F

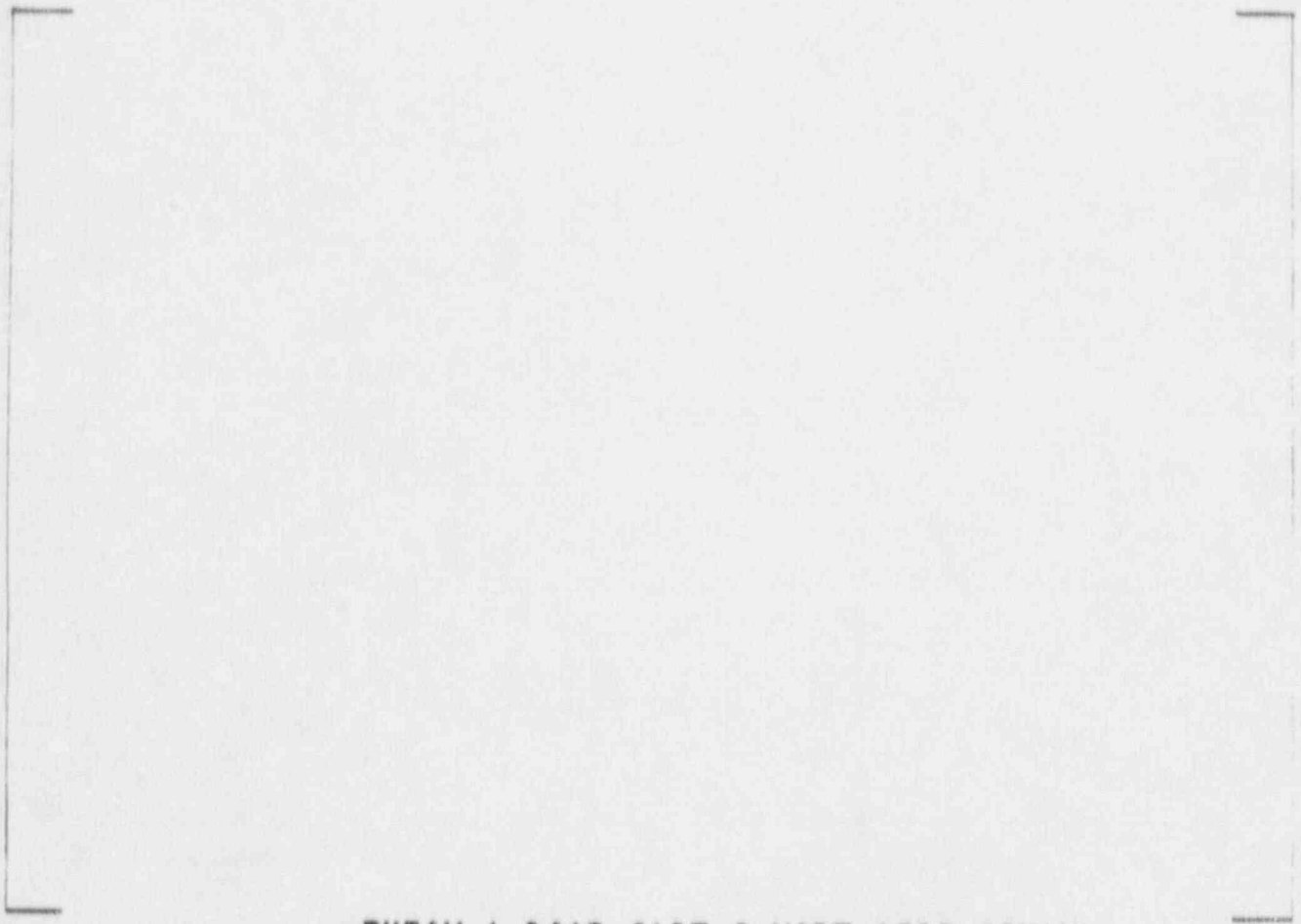

Figure 5-9 Critical Flaw Size Prediction for Byron Unit 1
Node 1030 Case G

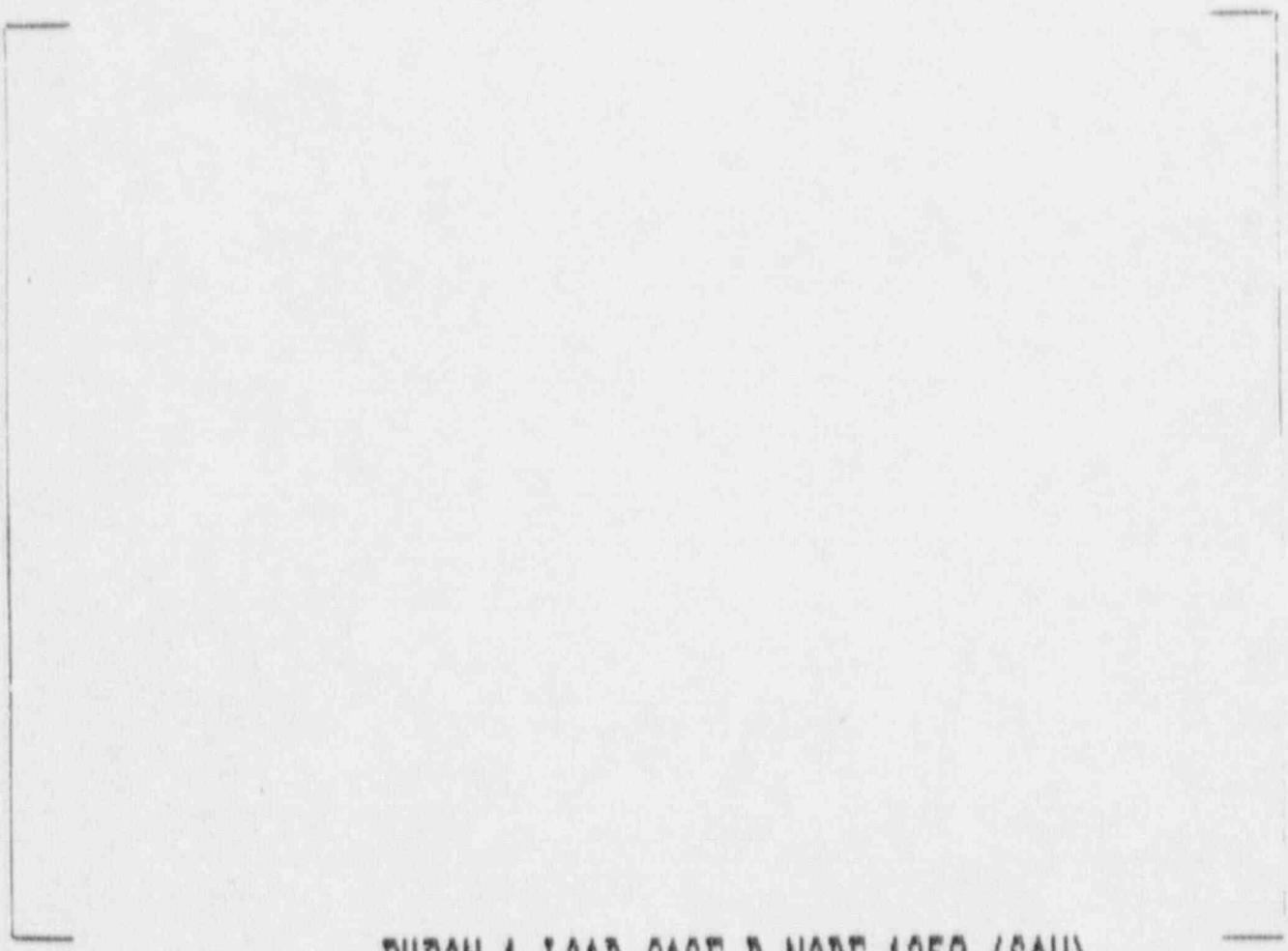

Figure 5-10 Critical Flaw Size Prediction for Byron Unit 1
Node 1350 Case D

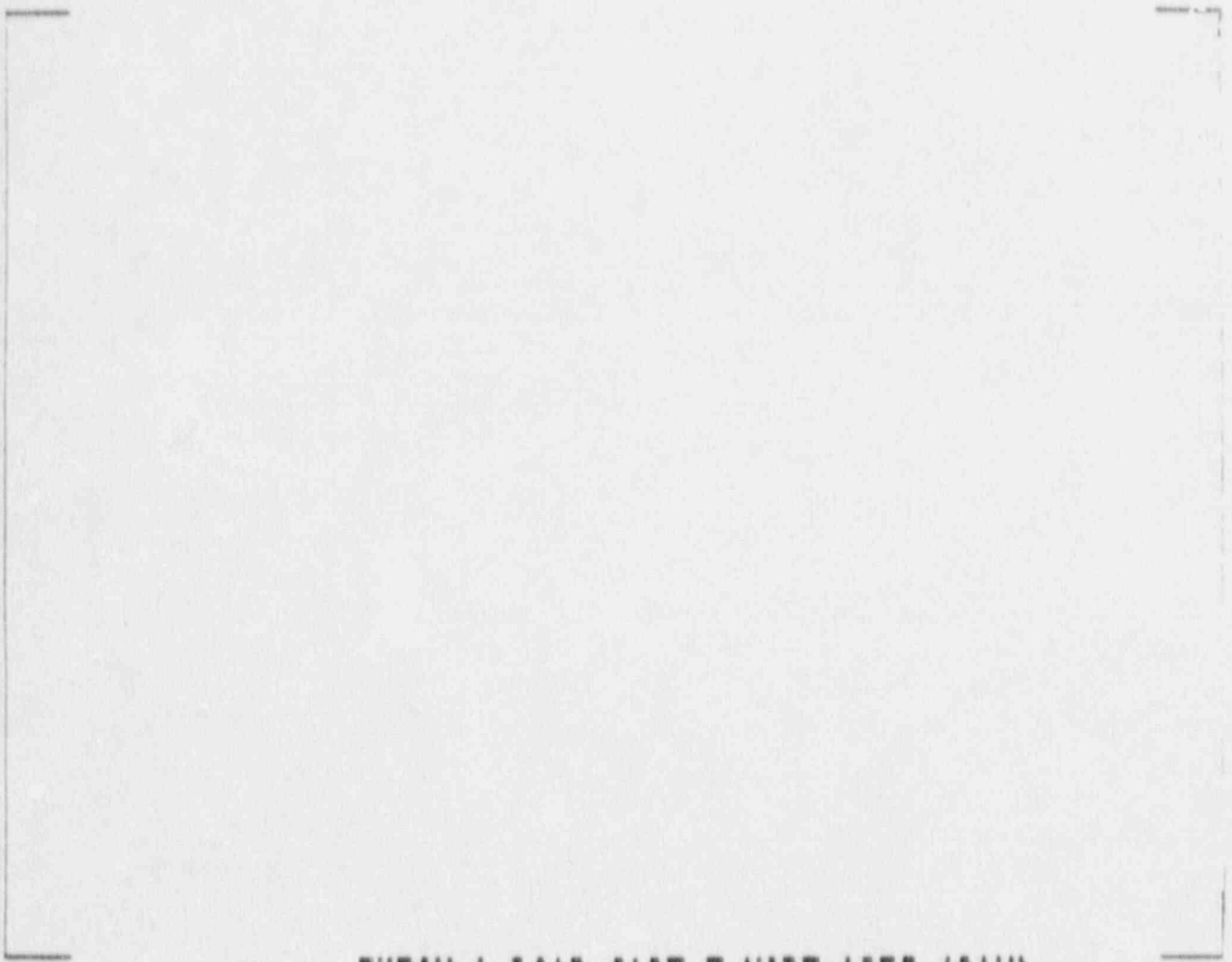

Figure 5-11 Critical Flaw Size Prediction for Byron Unit 1
Node 1350 Case E

Figure 5-12 Critical Flaw Size Prediction for Byron Unit 1
Node 1350 Case F

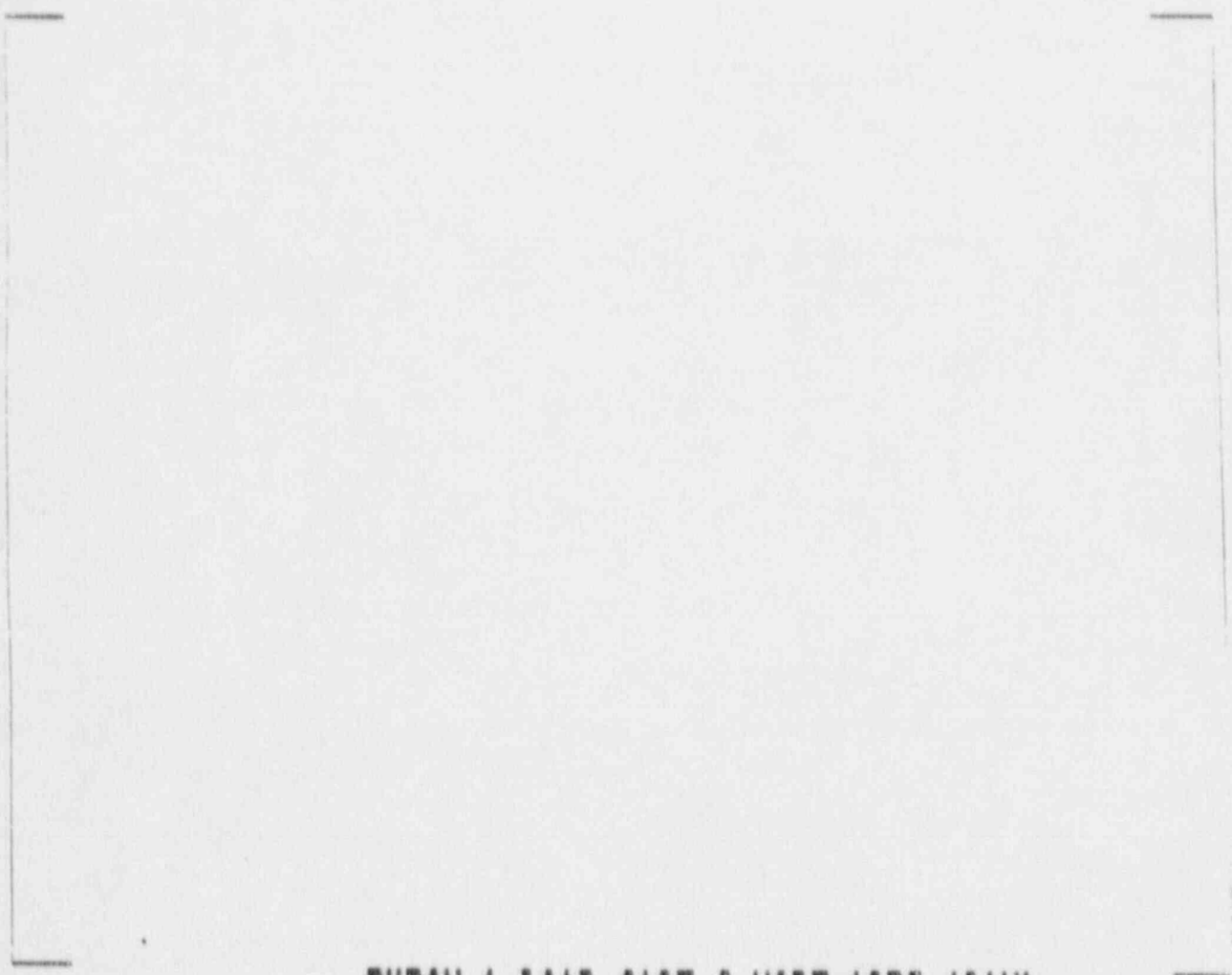

Figure 5-13 Critical Flaw Size Prediction for Byron Unit 1
Node 1350 Case G

a,c,e

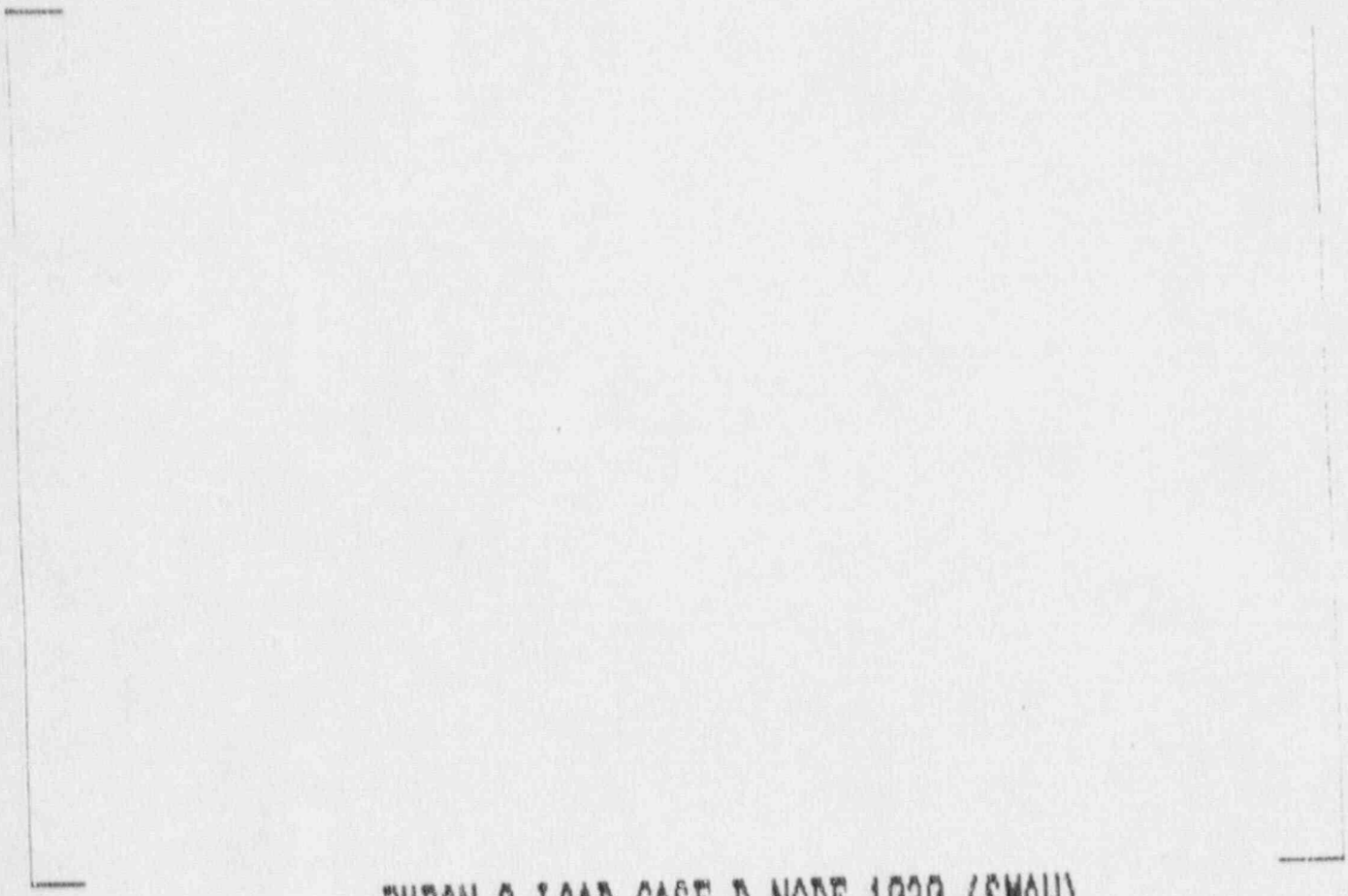

Figure 5-14 Critical Flaw Size Prediction for Byron Unit 2
Node 1030 Case D

a,c,e

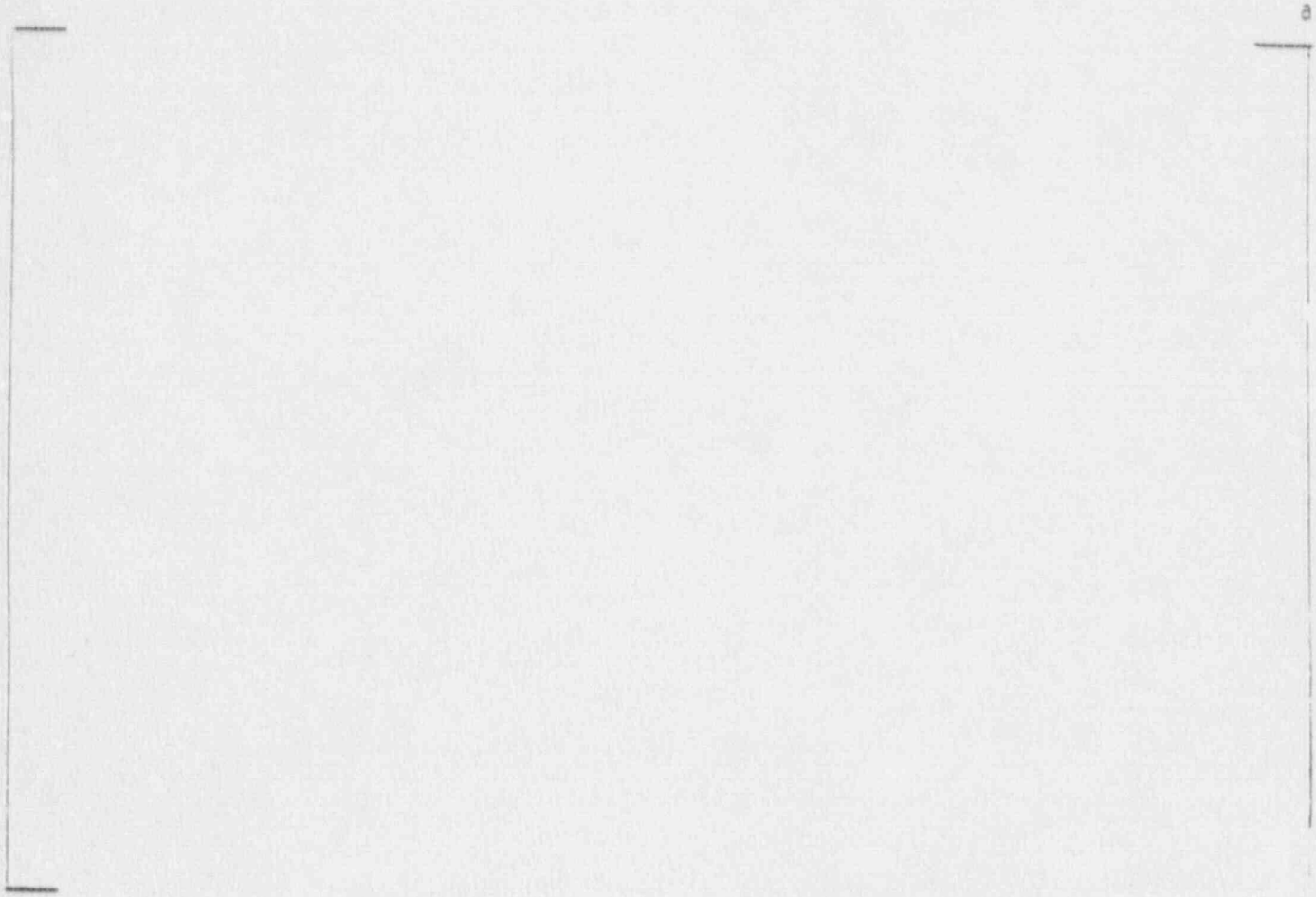

Figure 5-15 Critical Flaw Size Prediction for Byron Unit 2
Node 1030 Case E

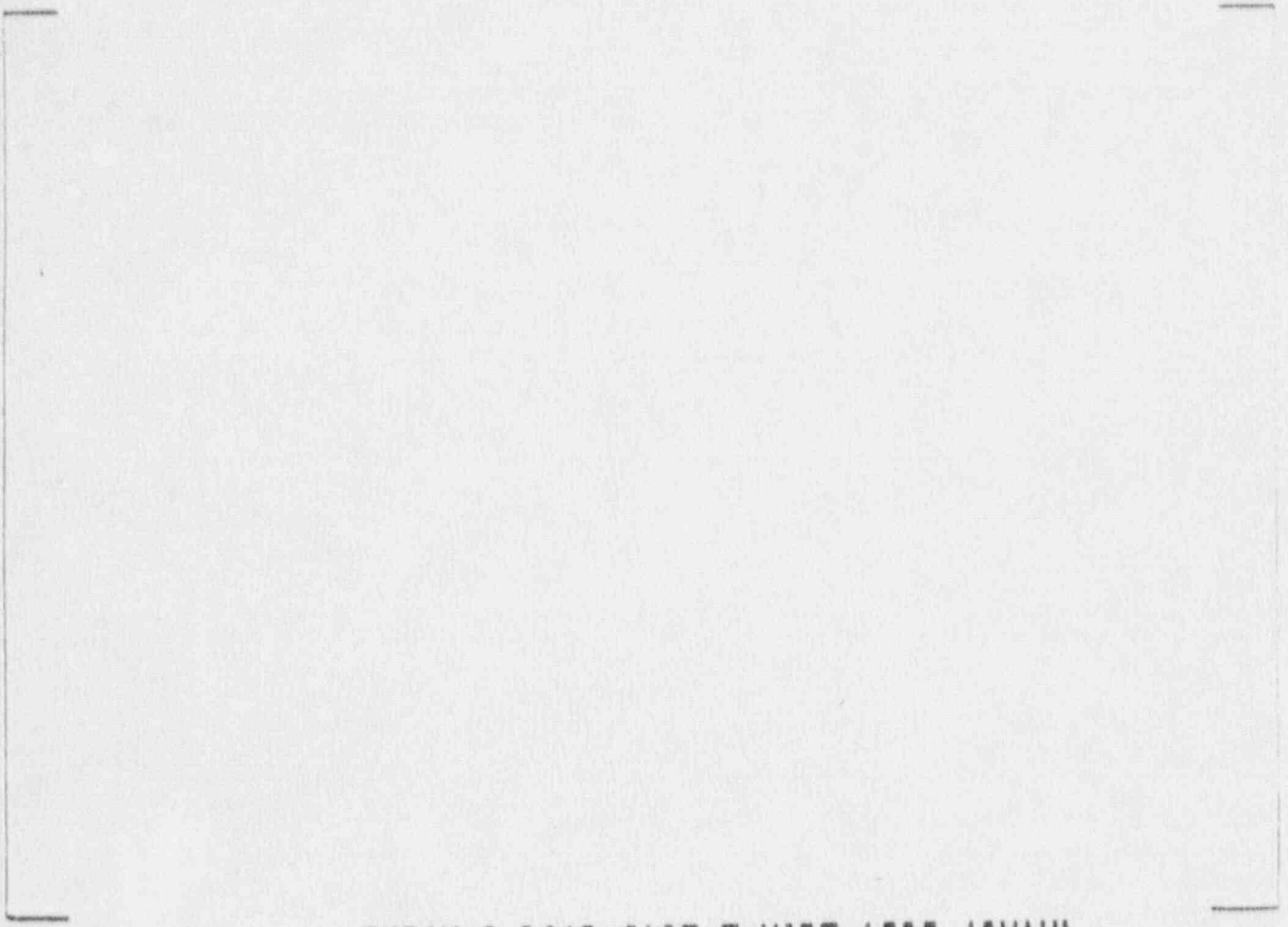

Figure 5-16 Critical Flaw Size Prediction for Byron Unit 2
Node 1030 Case F

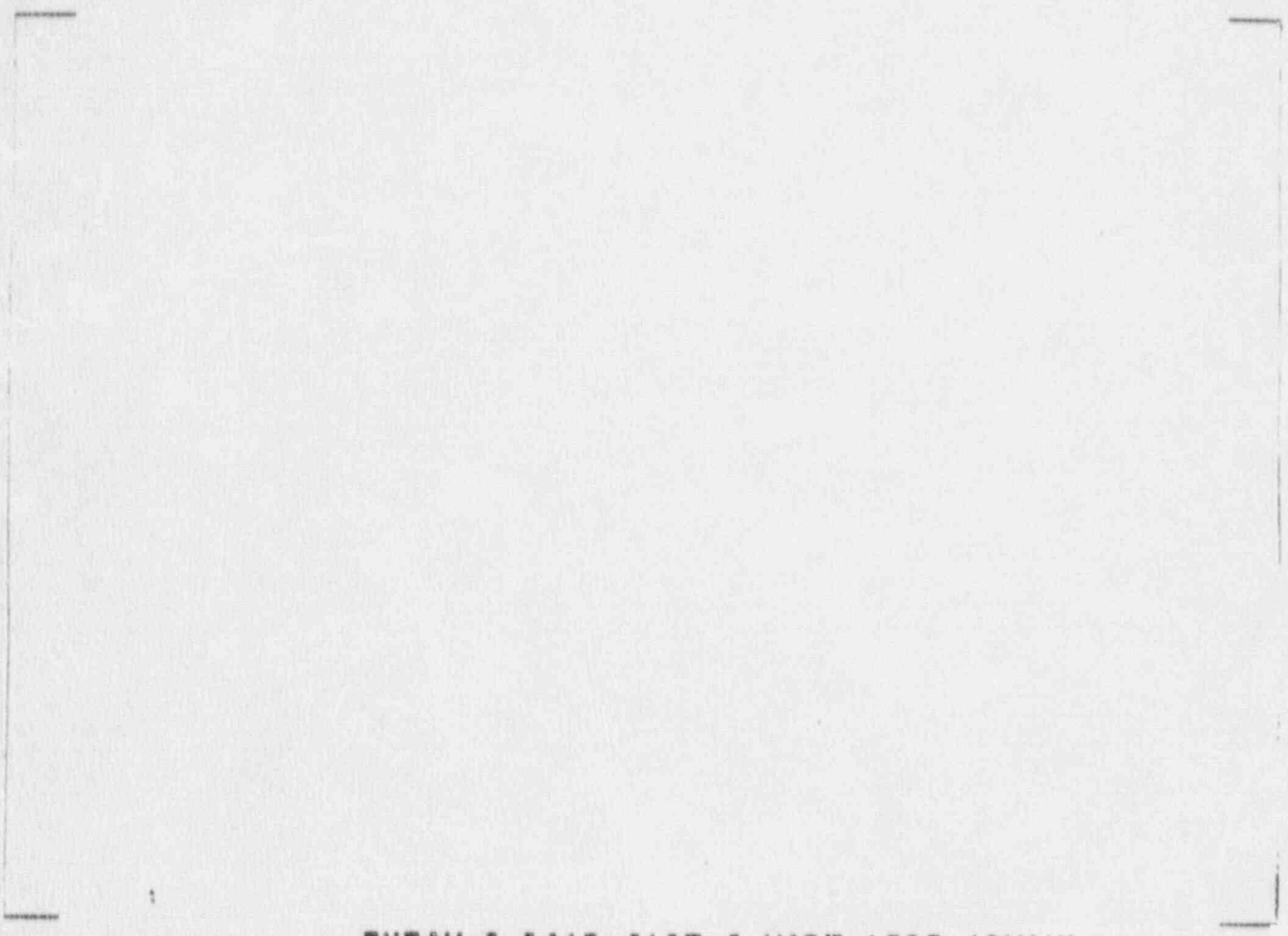

Figure 5-17 Critical Flaw Size Prediction for Byron Unit 2
Node 1030 Case G

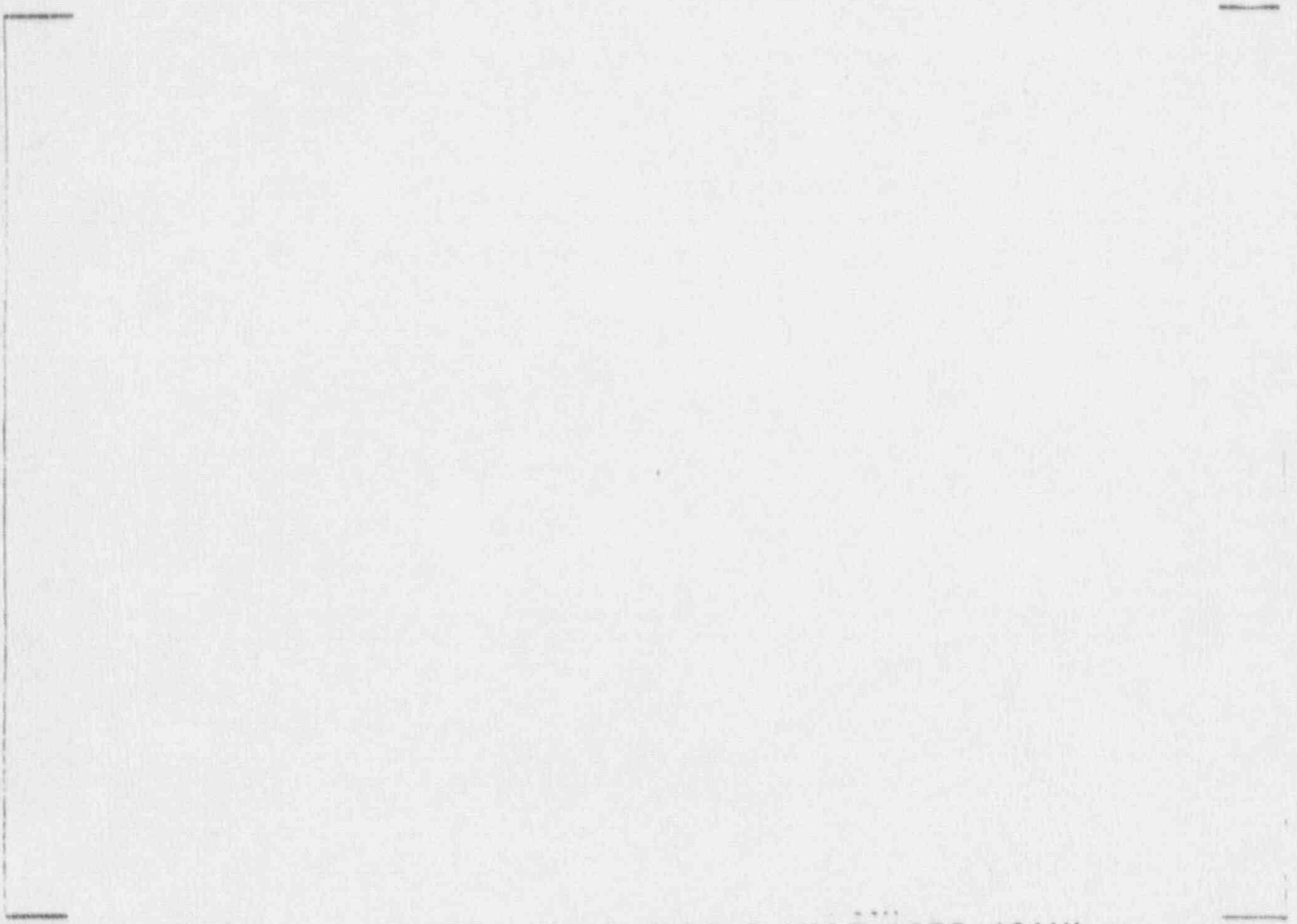

Figure 5-18 Critical Flaw Size Prediction for Byron Unit 2
Node 1350 Case D

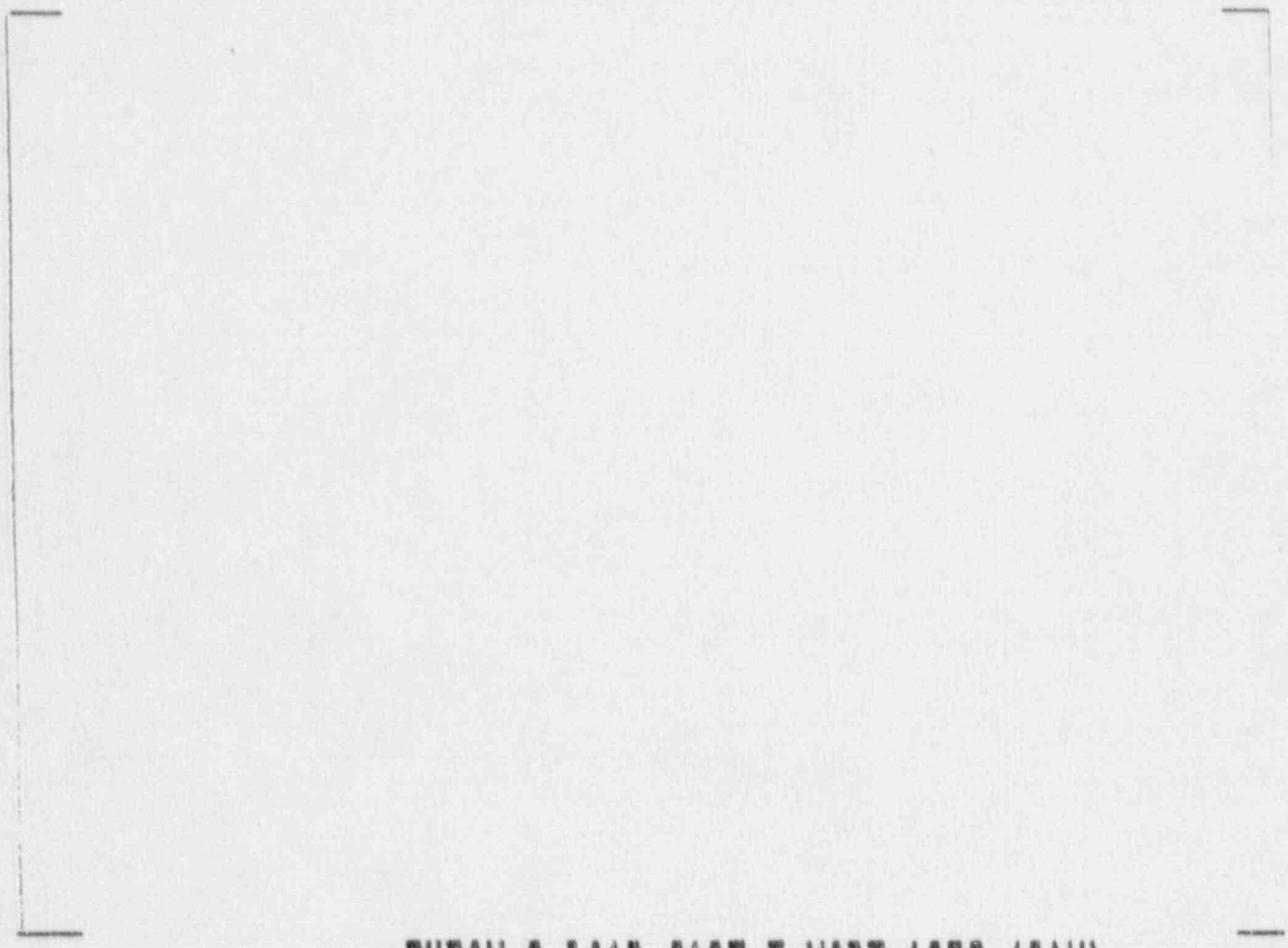

Figure 5-19 Critical Flaw Size Prediction for Byron Unit 2
Node 1350 Case E

a,c,e

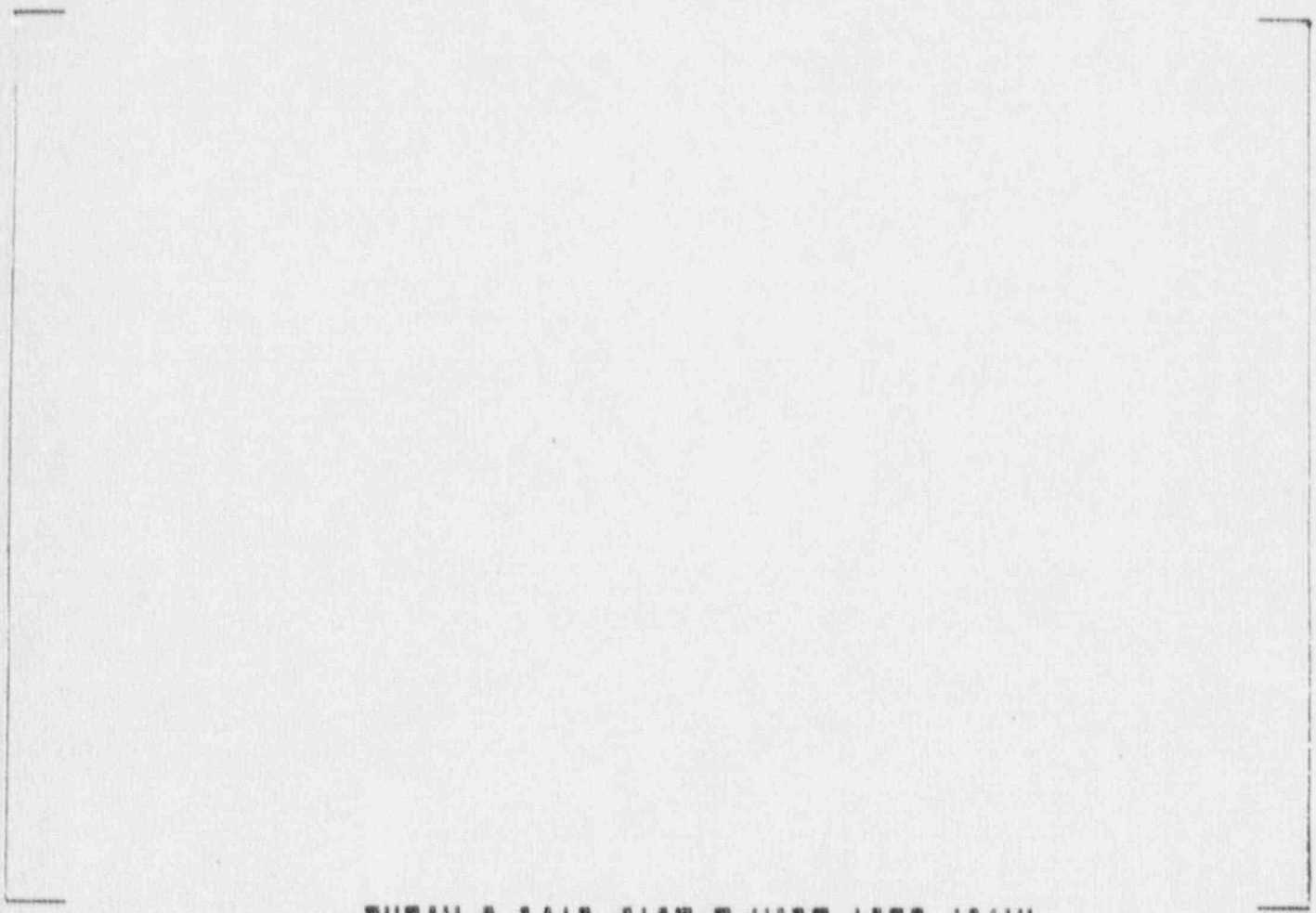

Figure 5-20 Critical Flaw Size Prediction for Byron Unit 2
Node 1350 Case F

a,c,e

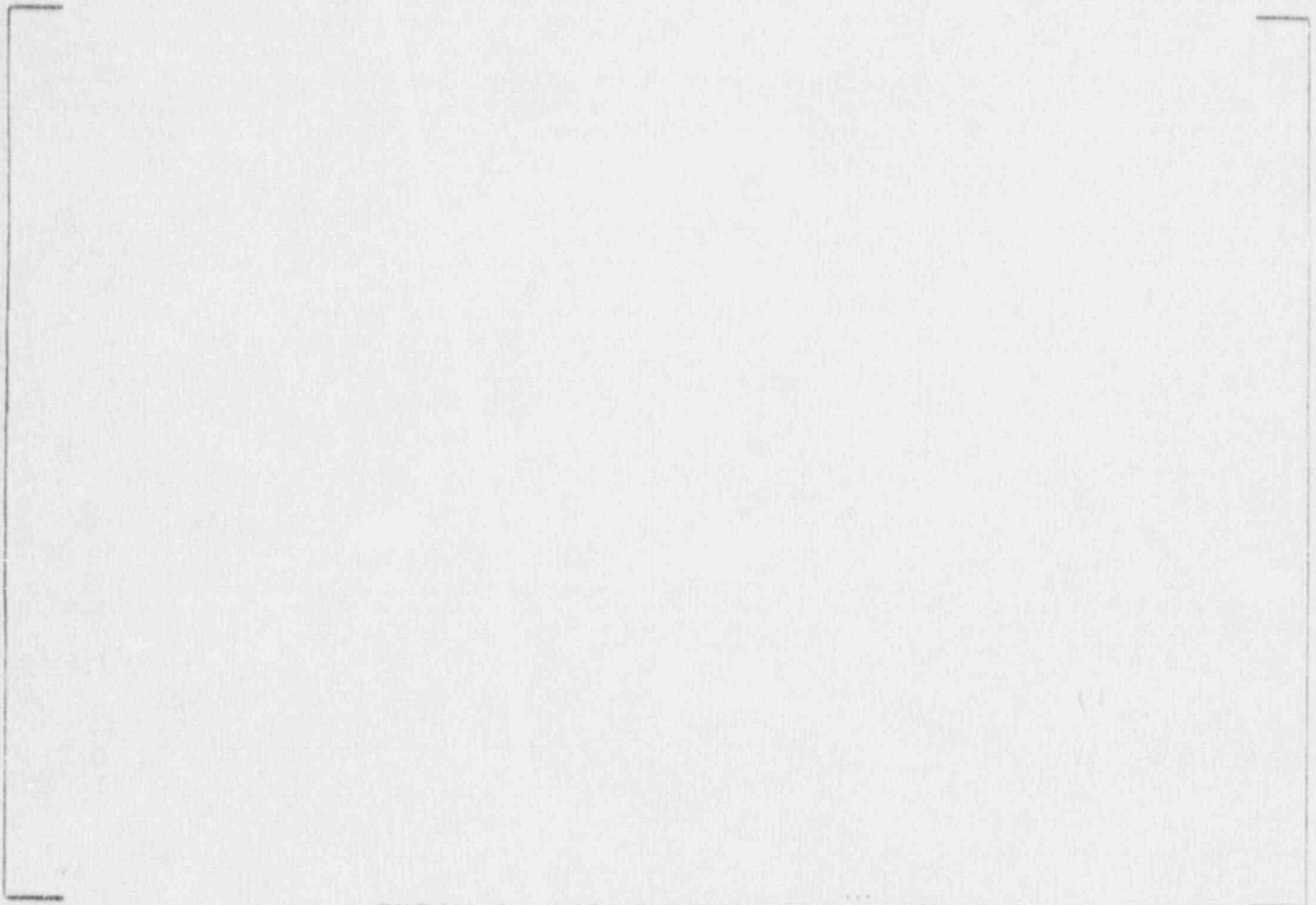

Figure 5-21 Critical Flaw Size Prediction for Byron Unit 2
Node 1350 Case G

a,c,e

Figure 5-22 Critical Flaw Size Prediction for Braidwood Unit 1
Node 1030 Case D

a,c,e

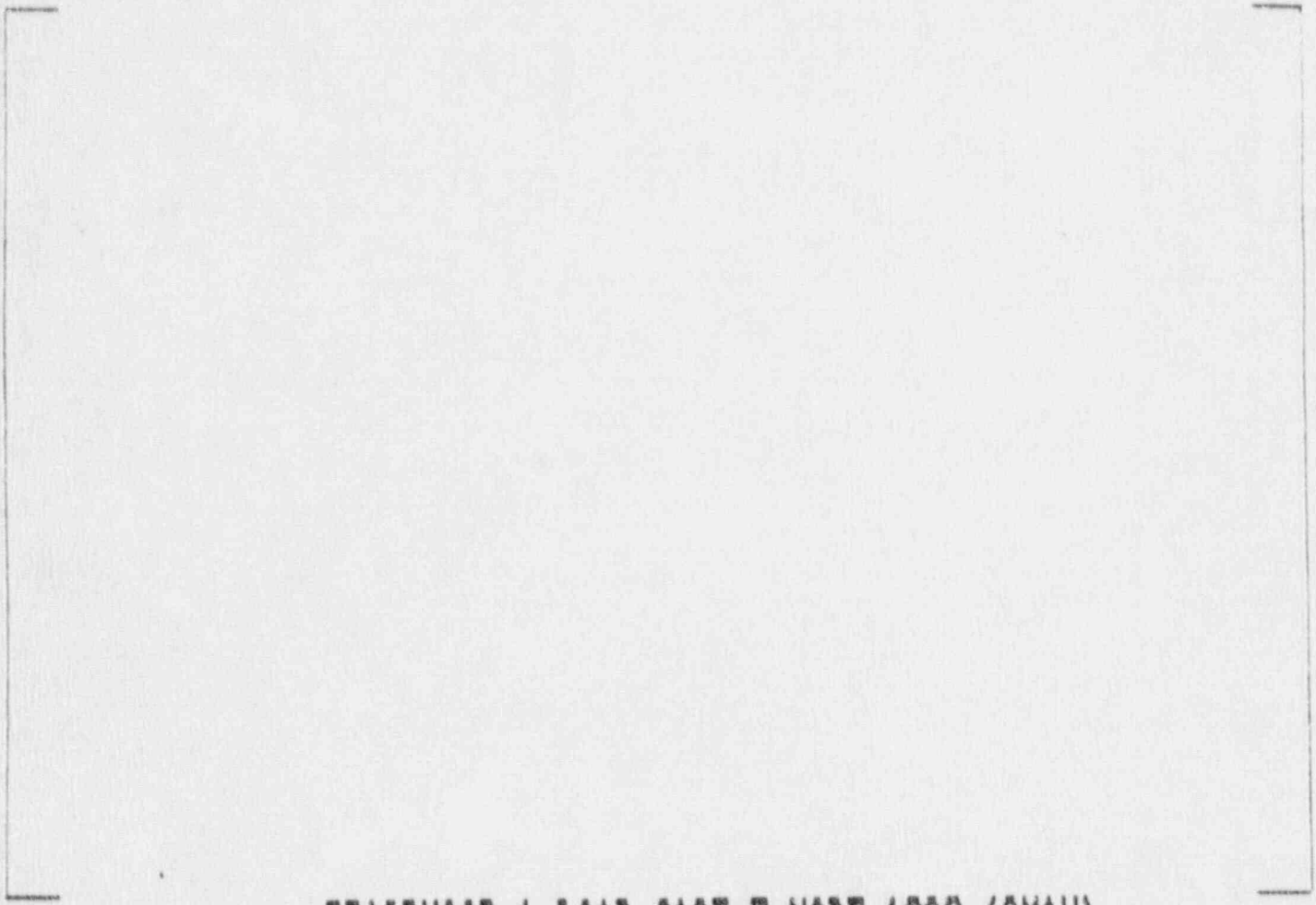

Figure 5-23 Critical Flaw Size Prediction for Braidwood Unit 1
Node 1030 Case E

a,c,e

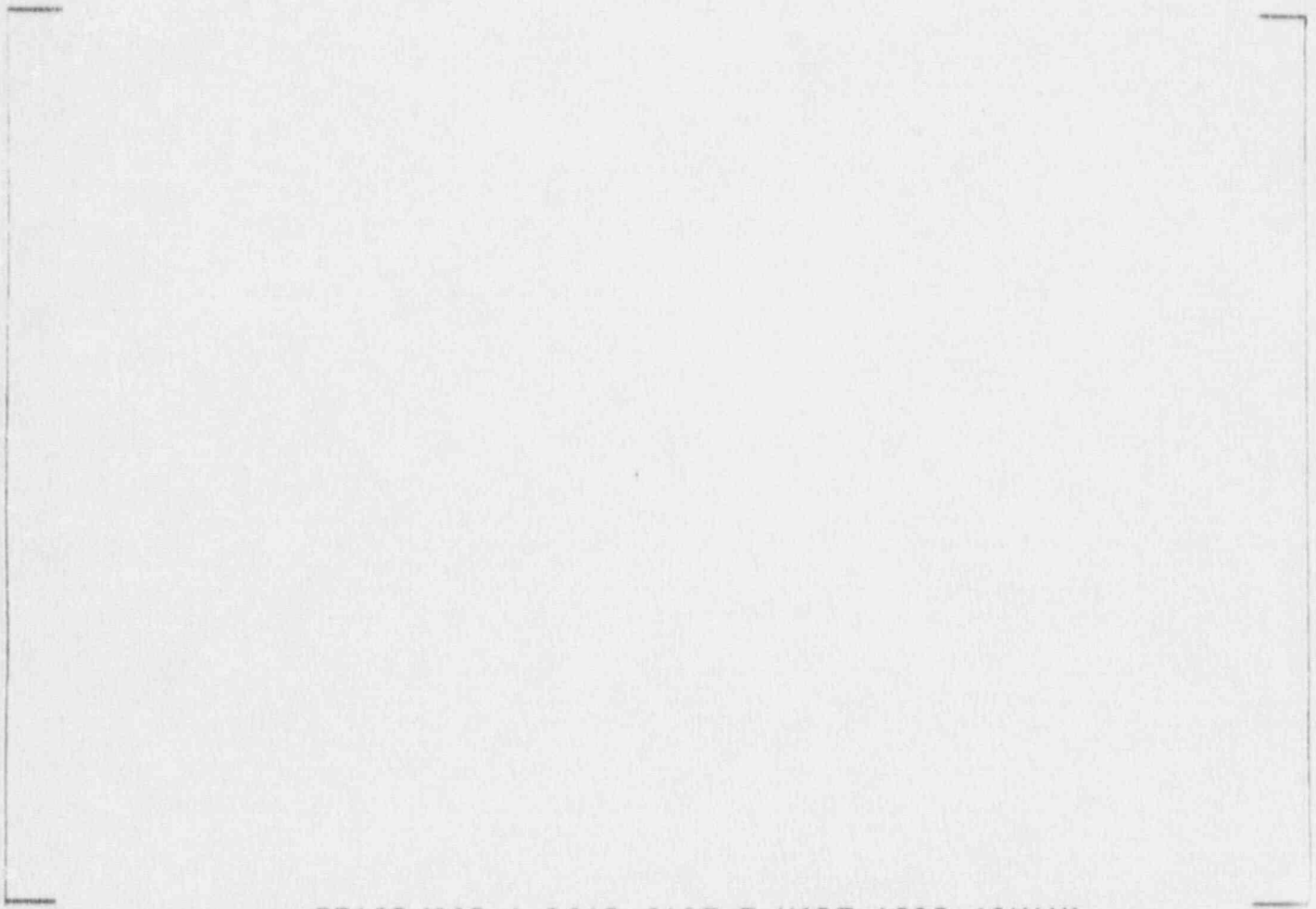

Figure 5-24 Critical Flaw Size Prediction for Braidwood Unit 1
Node 1030 Case F

a,c,e

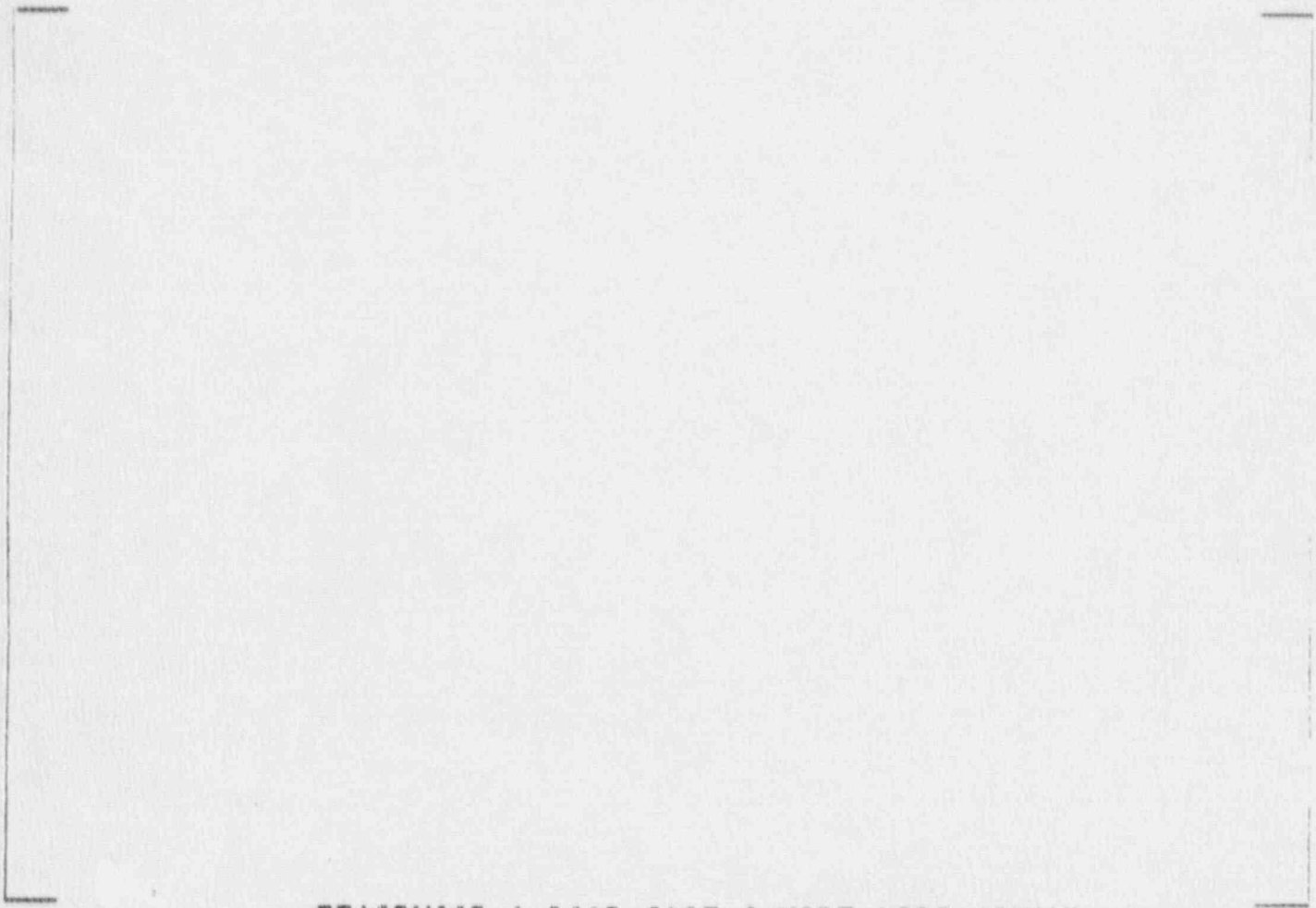

Figure 5-25 Critical Flaw Size Prediction for Braidwood Unit 1
Node 1030 Case G

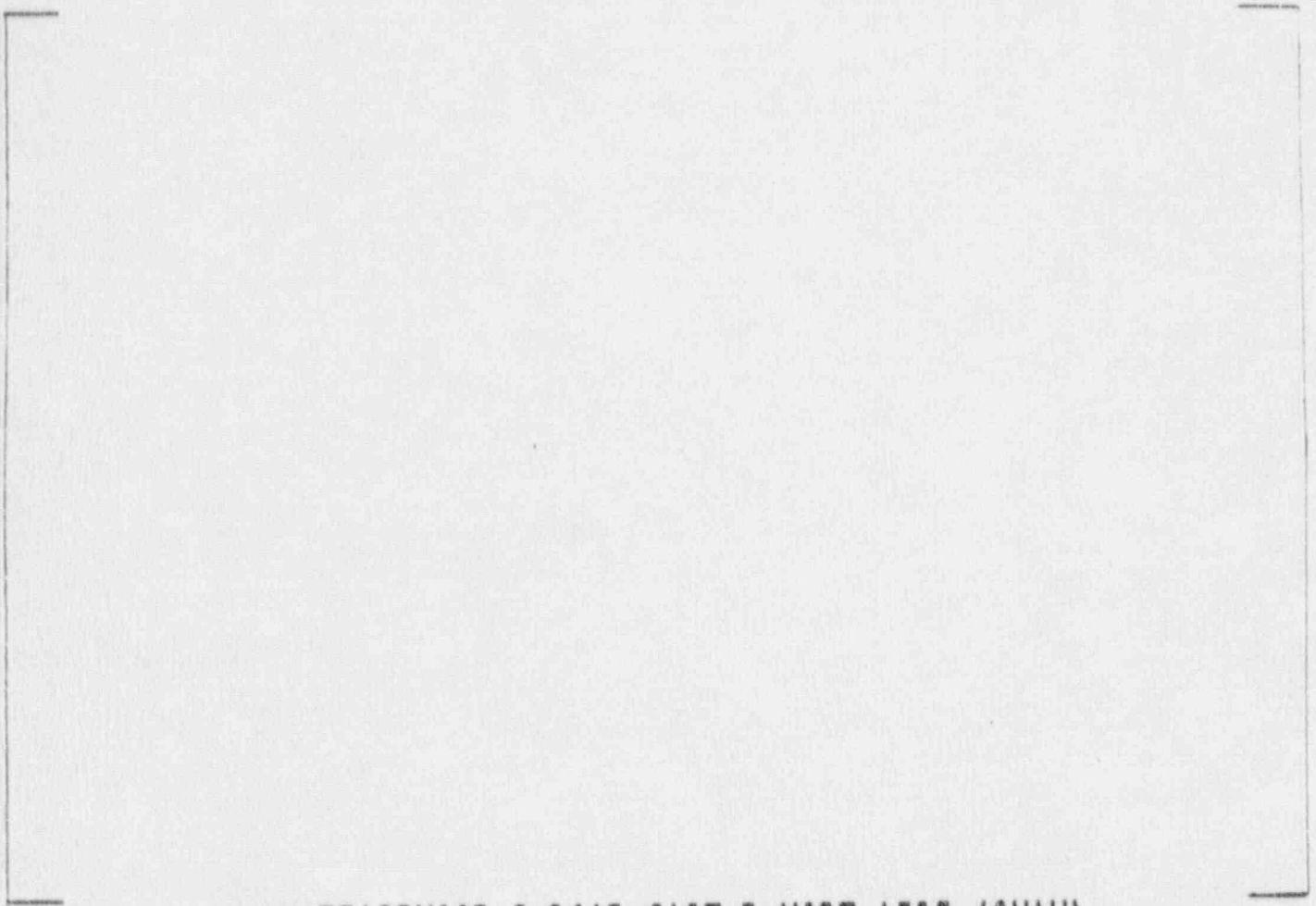

Figure 5-25 Critical Flaw Size Prediction for Braidwood Unit 2
Node 1030 Case D

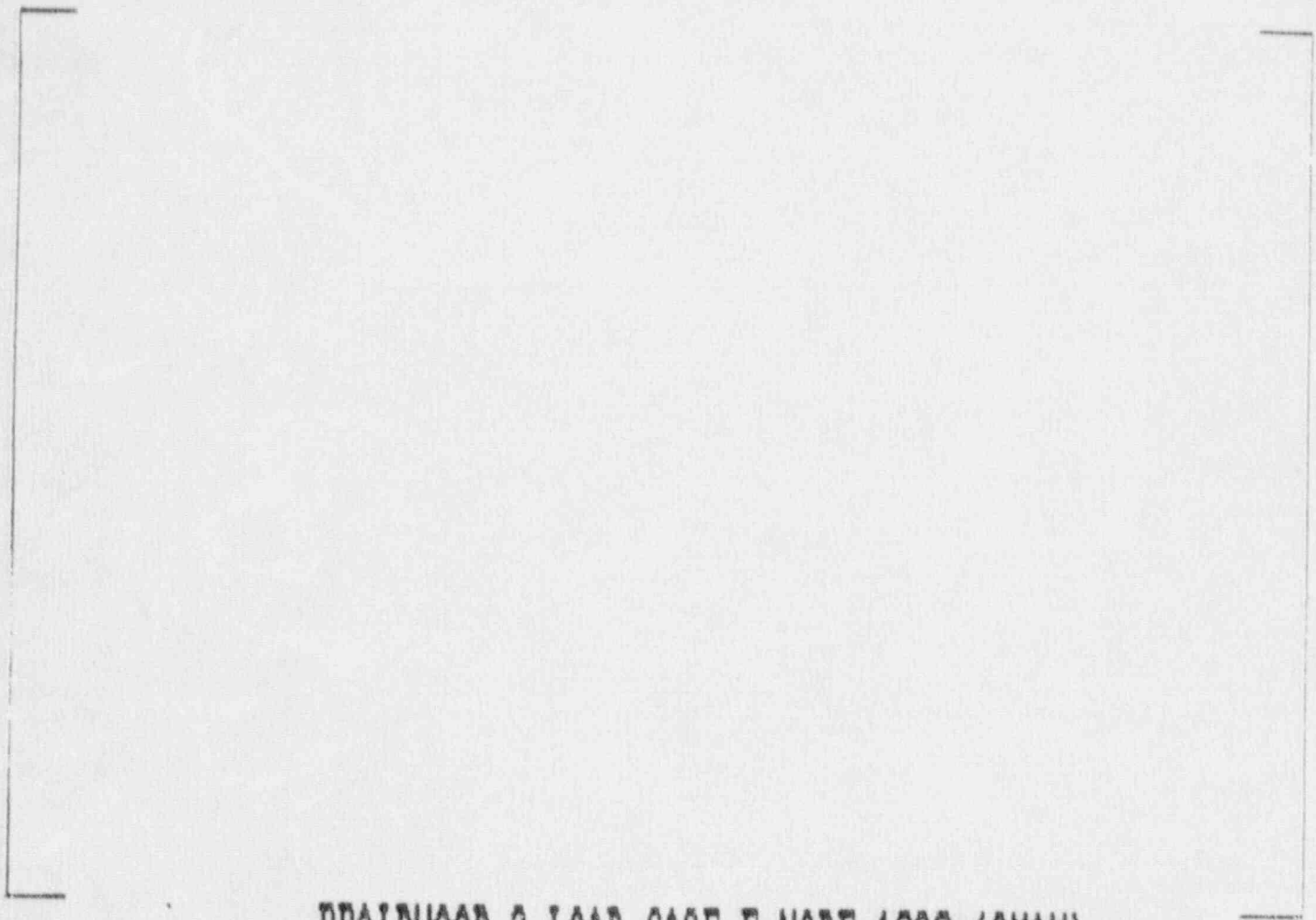

Figure 5-27 Critical Flaw Size Prediction for Braidwood Unit 2
Node 1030 Case E

a,c,e

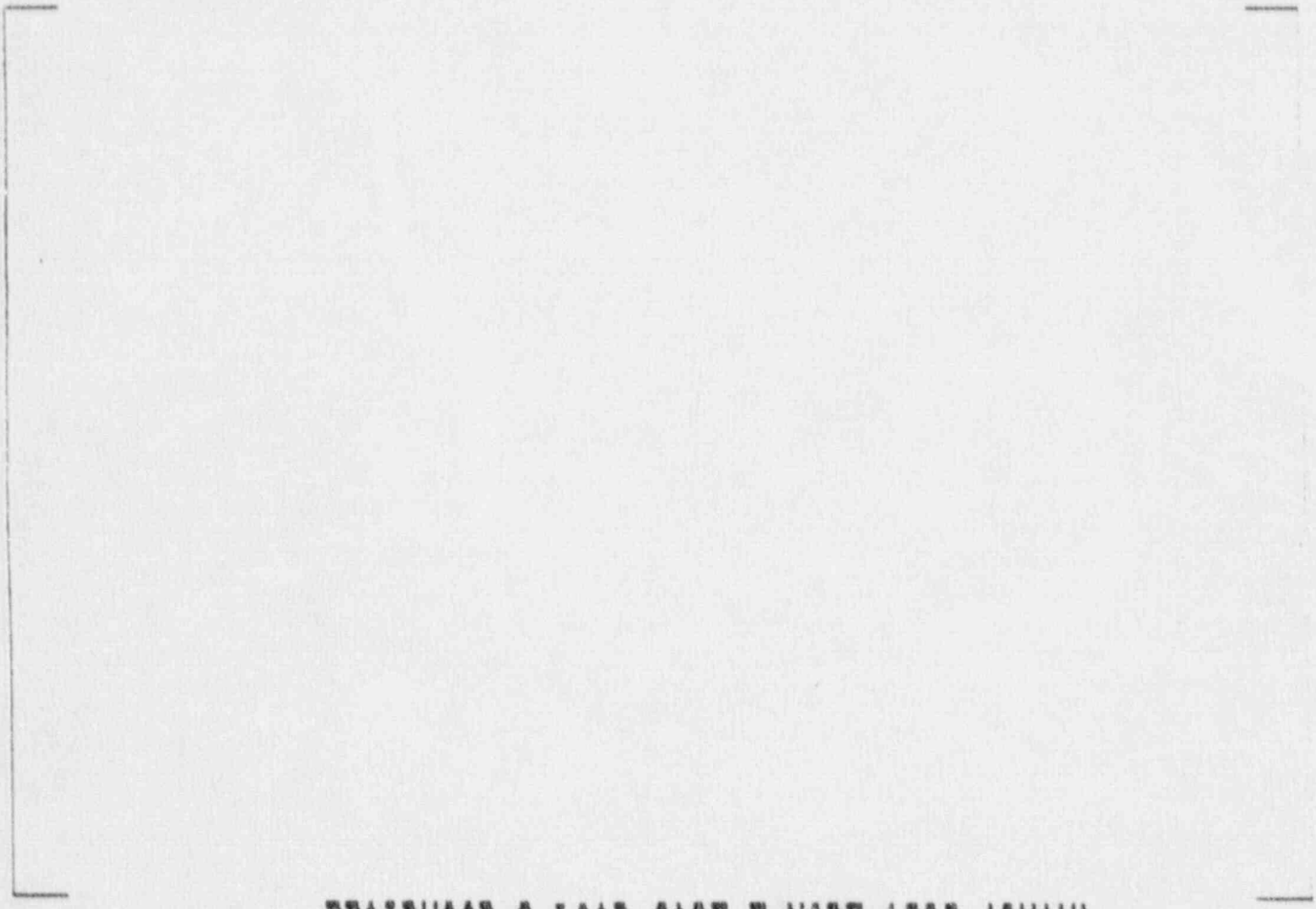

Figure 5-28 Critical Flaw Size Prediction for Braidwood Unit 2
Node 1030 Case F

a,c,e

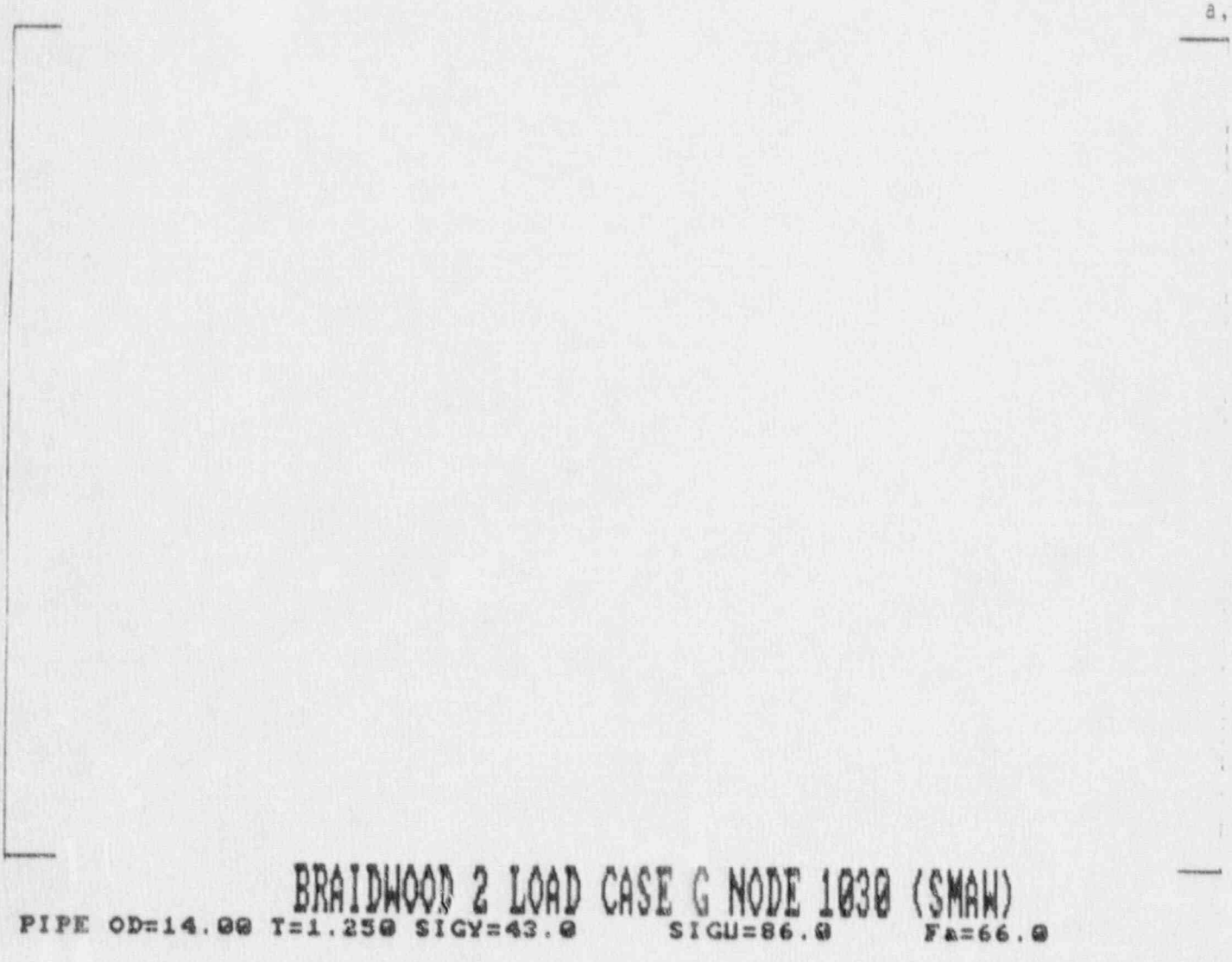

Figure 5-29 Critical Flaw Size Prediction for Braidwood Unit 2
Node 1030 Case G

SECTION 6.0
ASSESSMENT OF FATIGUE CRACK GROWTH

6.1 Introduction

To determine the sensitivity of the pressurizer surge line to the presence of small cracks when subjected to the transients discussed in WCAP-12743, fatigue crack growth analyses were performed. This section summarizes the analyses and results.

Figure 6-1 presents a general flow diagram of the overall process. The methodology consists of seven basic steps as shown in figure 6-2. Steps 1 through 4 are discussed in WCAP-12743. Steps 5 through 7 are specific to fatigue crack growth and are discussed in this section.

There is presently no fatigue crack growth rate curve in the ASME Code for austenitic stainless steels in a water environment. However, a great deal of work has been done recently which supports the development of such a curve. An extensive study was performed by the Materials Property Council Working Group on Reference Fatigue Crack Growth concerning the crack growth behavior of these steels in air environments, published in reference 6-1. A reference curve for stainless steels in air environments, based on this work, is in the 1989 Edition of Section XI of the ASME Code. This curve is shown in figure 6-3.

A compilation of data for austenitic stainless steels in a PWR water environment was made by Bamford (reference 6-2), and it was found that the effect of the environment on the crack growth rate was very small. For this reason it was estimated that the environmental factor should be set at 1.0 in the crack growth rate equation from reference 6-1. Based on these works (references 6-1 and 6-2) the fatigue crack growth law used in the analyses is as shown in figure 6-4.

6.2 Initial Flaw Size

Various initial surface flaws were assumed to exist. The flaws were assumed to be semi-elliptical with a six-to-one aspect ratio. The largest initial flaw assumed to exist was one with a depth equal to 10% of the nominal wall thickness, the maximum flaw size that could be found acceptable by Section XI of the ASME Code.

6.3 Results of FCG Analysis

Fatigue crack growth analysis were performed at the reactor coolant loop nozzle junction at location 1 (which corresponds to the highest usage factor in the surge line) and at location 2 as shown in Figure 6-5. Location 2 corresponds to the location of highest ASME Section III equation 12 stress.

Results of the fatigue crack growth analysis are presented in table 6-1 for an initial flaw of 10% nominal wall thickness.

Conservatisms existing in the fatigue crack growth analysis are listed below.

1. Plant operational transient data has shown that the conventional design transients contain significant conservatisms

[2. ----------]

3. ----------]^{a,c,e}

4. Fatigue crack growth calculations are based conservatively on elastic stresses

5. FCG neglects fatigue life prior to initiation

6.4 References

6-1. James, L. A. and Jones, D. P., "Fatigue Crack Growth Correlations for Austenitic Stainless Steel in Air," in Predictive Capabilities in Environmentally Assisted Cracking, ASME publication PVP-99, December 1985.

6-2. Bamford, W. H., "Fatigue Crack Growth of Stainless Steel Reactor Coolant Piping in a Pressurized Water Reactor Environment," ASME Trans. Journal of Pressure Vessel Technology, Feb. 1979.

TABLE 6-1

FATIGUE CRACK GROWTH RESULTS FOR 10% OF WALL INITIAL FLAW SIZE

Location	Position	Initial Size (in)	Initial (% Wall)	Final (40 yr) Size (in)	Final Flaw (% Wall)	a,c,e

a,c,e

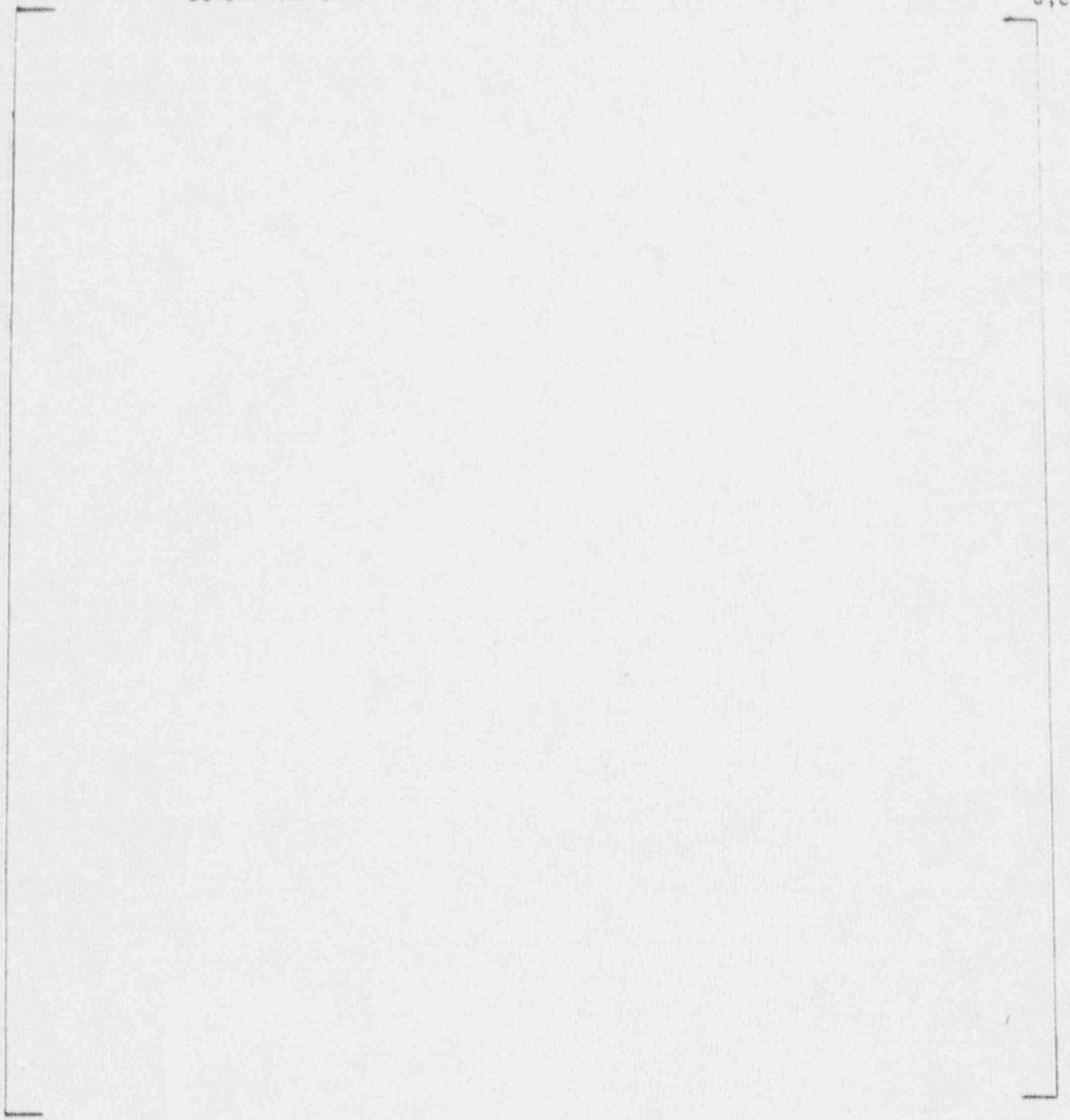

Figure 6-1 Determination of the Effects of Thermal Stratification on Fatigue Crack Growth

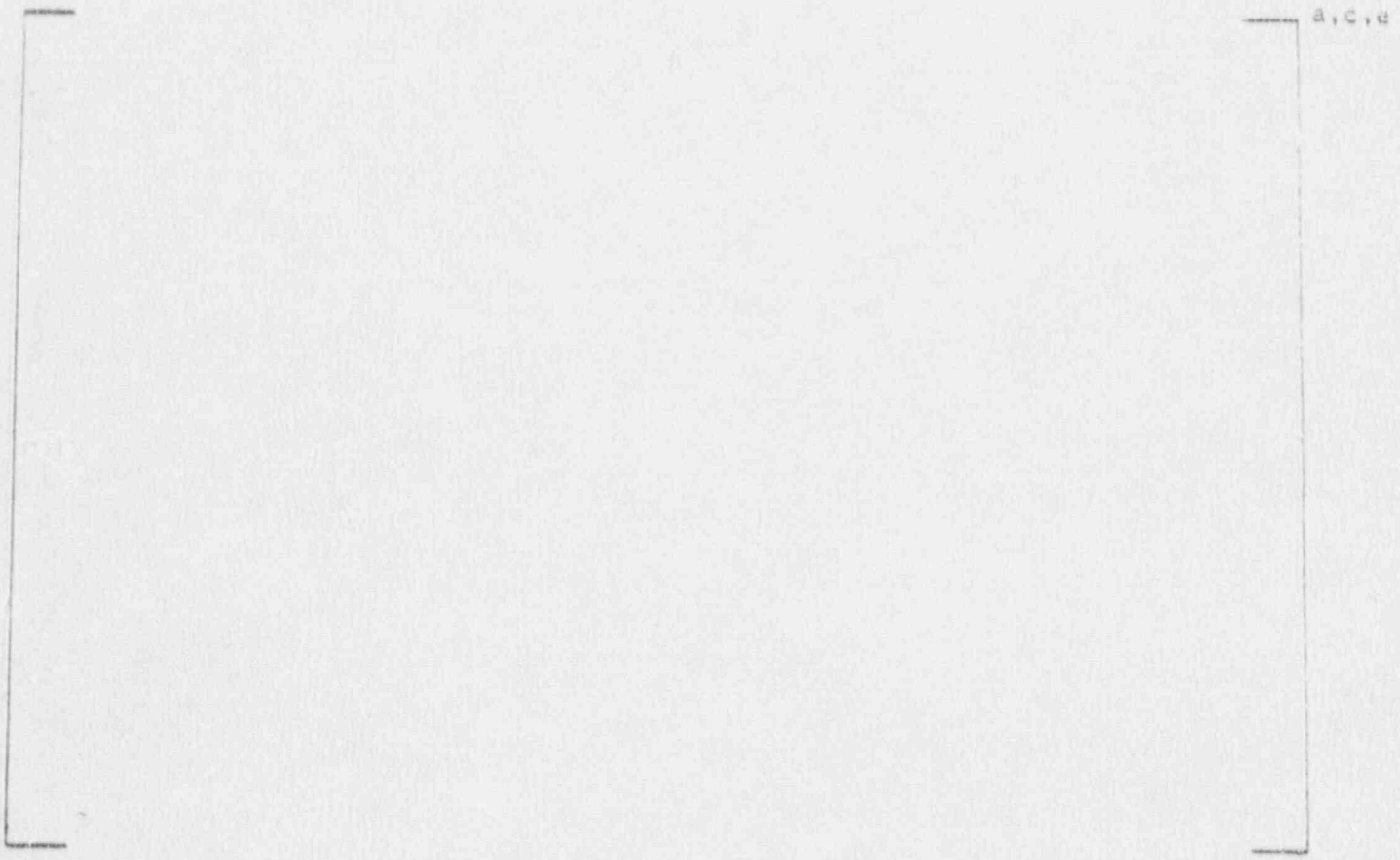

Figure 6-2 Fatigue Crack Growth Methodology

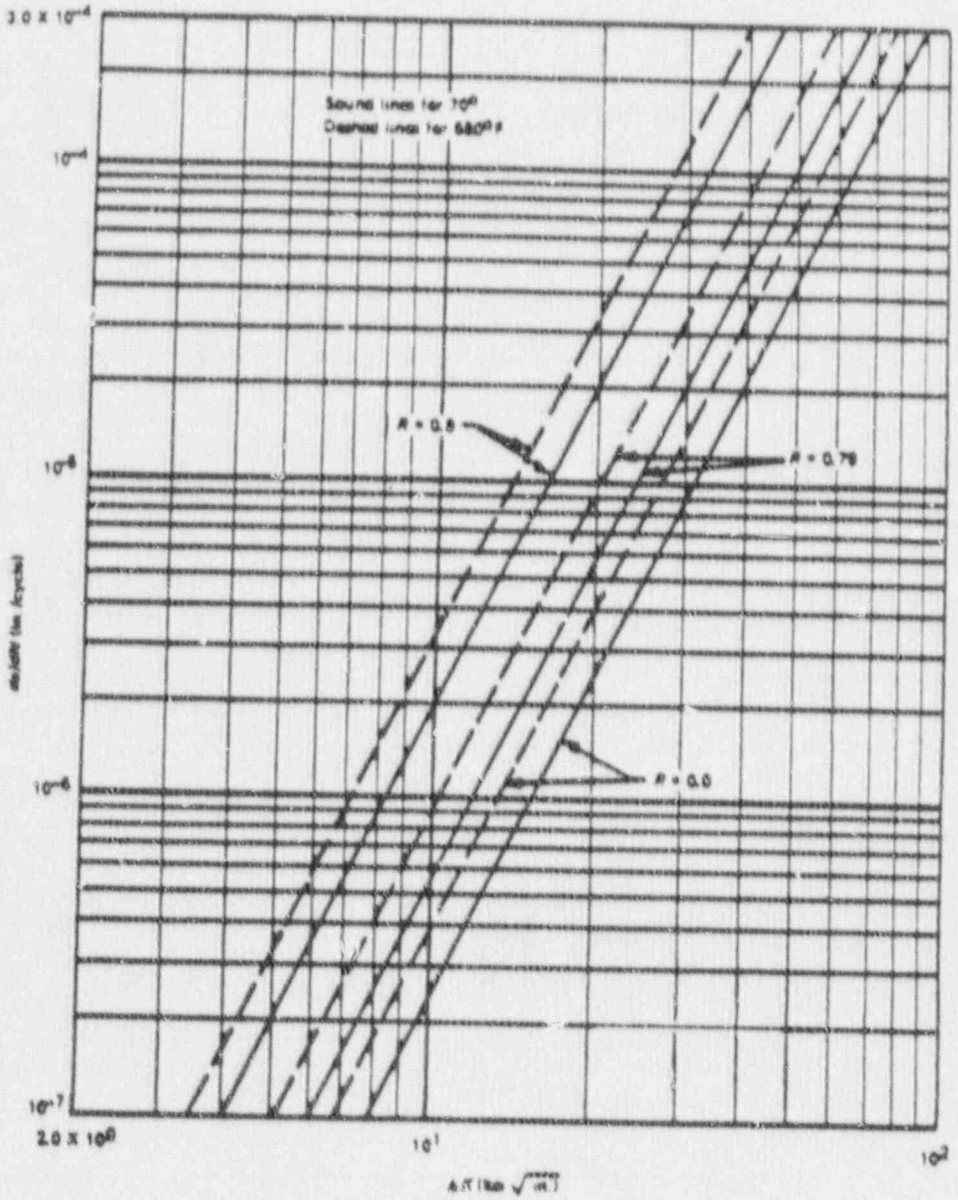

Figure 6-3 Fatigue Crack Growth Rate Curve for Austenitic Stainless Steel

$$\frac{da}{dn} = C\ F\ S\ E\ \Delta K^{3.30}$$

where

$\frac{da}{dn}$ = Crack Growth Rate in inches/cycle

C = 2.42×10^{-20}

F = Frequency factor (F = 1.0 for temperature below 800°F)

S = R ratio correction (S = 1.0 for R = 0; S = 1 + 1.8R for $0 < R < .8$; and S = -43.35 + 57.97R for $R > 0.8$)

E = Environmental Factor (E = 1.0 for PWR)

ΔK = Range of stress intensity factor, in psi $\sqrt{in}$

R = The ratio of the minimum K_I (K_{Imin}) to the maximum K_I (K_{Imax}).

Figure 6-4. Fatigue Crack Growth Equation for Austenitic Stainless Steel

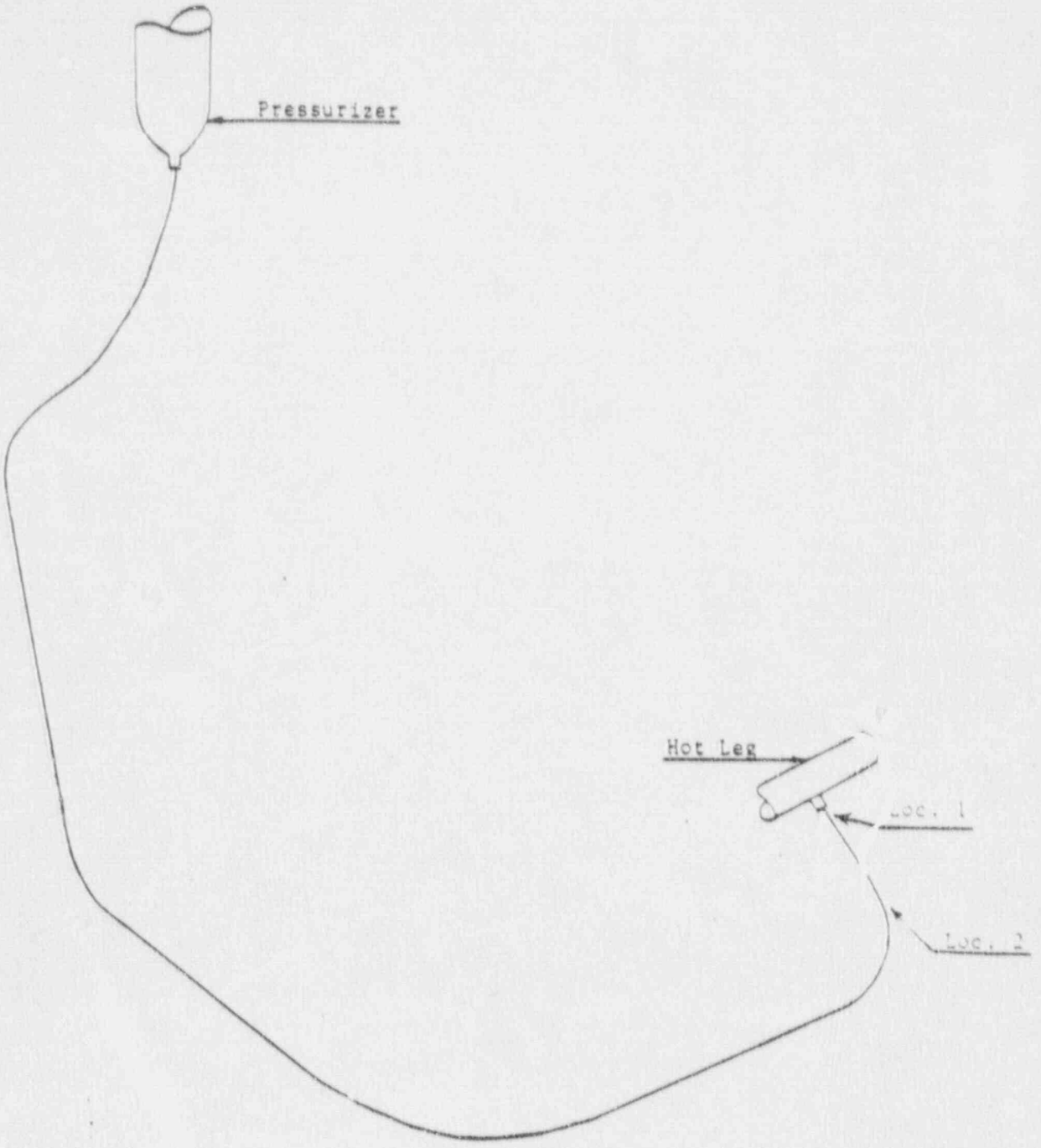

Figure 6-5. Fatigue Crack Growth Critical Locations

SECTION 7.0
ASSESSMENT OF MARGINS

In the preceding sections, the leak rate calculations, fracture mechanics analysis and fatigue crack growth assessment were performed. Margins at the critical locations are summarized below:

In Secton 5.3 using the IWB-3640 approach (i.e. "Z" factor approach), the "critical" flaw sizes at the governing locations are calculated. In Section 5.2 the crack lengths yielding a leak rate of 10 gpm (10 times the leak detection capability of 1.0 gpm) for the critical locations are calculated. The leakage size flaws, the instability flaws, and margins are given in Tables 7-1, 7-2, 7-3 and 7-4. The margins are the ratio of instability flaw to leakage flaw. The margins for analysis combination cases A/D, [----------]^{a,c,e} well exceed the factor of 2. The margin for the extremely low probability event defined by [--------]^{a,c,e} is [----------]^{a,c,e} As stated in Section 4.3, the probability of simultaneous occurrence of SSE and maximum stratification due to shutdown because of leakage is estimated to be less than 10^{-11}. Thus, the fracture mechanics calculations for case B/G demonstrate extreme conservatism. The Case A (in the instance case [---]^{a,c,e}) is of little relevance since leakage would be detected for the leakage flaw size of case [-]^{a,c,e}.

In this evaluation, the leak-before-break methodology is applied conservatively. The conservatisms used in the evaluation are summarized in Table 7-5.

TABLE 7-1

Leakage Flaw Sizes, Critical Flaw Sizes and Margins
for Byron Unit 1

Node	Load Case	Critical Flaw Size (in)	Leakage Flaw Size (in)	Margin	
1030	A/D	11.35	4.75	2.39	
	[				a,c,e
	---	-----	----	----	
	---	-----	----	----	
	---	-----	----	----	
	----	-----	----	----	
	----	-----	----	----	]
1350	A/D	15.00	5.30	2.83	
	[				a,c,e
	---	-----	----	----	
	---	-----	----	----	
	---	-----	----	----	
	---	-----	----	----	
	----	-----	----	----	]

[a] These are judged to be low probability events

TABLE 7-2

Leakage Flaw Sizes, Critical Flaw Sizes and Margins
for Byron Unit 2

Node	Load Case	Critical Flaw Size (in)	Leakage Flaw Size (in)	Margin
1030	A/D	10.99	4.75	2.31
				a,c,e
	---	-----	----	----
	---	-----	----	----
	---	-----	----	--
	---	-----	----	----
	---	-----	----	----
1350	A/D	15.09	5.30	2.85
				a,c,e
	---	-----	----	----
	---	-----	----	----
	--	-----	----	-----
	---	-----	----	-----
	---	-----	----	-----

[a] These are judged to be low probability events

TABLE 7-3

Leakage Flaw Sizes, Critical Flaw Sizes and Margins
for Braidwood Unit 1

Node	Load Case	Critical Flaw Size (in)	Leakage Flaw Size (in)	Margin	
1030	A/D	11.76	4.95	2.42	
[					a,c,e
	---	-----	----	----	
	---	-----	----	----	
	---	-----	----	----	
	---	-----	----	----	
	---	-----	----	----	]

A These are judged to be low probability events

TABLE 7-4

Leakage Flaw Sizes, Critical Flaw Sizes and Margins
for Braidwood Unit 2

Node	Load Case	Critical Flaw Size (in)	Leakage Flaw Size (in)	Margin
1030	A/D	11.95	4.85	2.46
[				] a,c,e
	---	-----	----	----
	---	-----	----	----
	---	-----	----	----
	---	-----	----	----
	---	-----	----	----

[a] These are judged to be low probability events

TABLE 7-5

LBB Conservatisms

- Factor of 10 on Leak Rate
- Factor of 2 on Leakage Flaw for all cases (except 1.66 for B/G case which is an extremely low probability event)
- Algebraic Sum of Loads for Leakage
- Absolute Sum of Loads for Stability
- Average Material Properties for Leakage
- Minimum Material Properties for Stability

SECTION 8.0
CONCLUSIONS

This report justifies the elimination of pressurizer surge line pipe breaks as the structural design basis for Byron Units 1 and 2 and Braidwood Units 1 & 2 as follows:

a. Stress corrosion cracking is precluded by use of fracture resistant materials in the piping system and controls on reactor coolant chemistry, temperature, pressure, and flow during normal operation.

b. Water hammer should not occur in the RCS piping (primary loop and the attached class 1 auxiliary lines) because of system design, testing, and operational considerations.

c. The effects of low and high cycle fatigue on the integrity of the surge line were evaluated and shown acceptable. The effects of thermal stratification were evaluated and shown acceptable.

d. Ample margin exists between the leak rate of small stable flaws and the criterion of Reg. Guide 1.45.

e. Ample margin exists between the small stable flaw sizes of item d and the critical flaw size.

f. With respect to stability of the reference flaw, ample margin exists between the maximum postulated loads and the plant specific maximum faulted loads.

The postulated reference flaw will be stable because of the ample margins in d, e and f and will leak at a detectable rate which will assure a safe plant shutdown.

Based on the above, it is concluded that pressurizer surge line breaks should not be considered in the structural design basis of Byron Units 1 & 2 and Braidwood Units 1 & 2.

APPENDIX A
LIMIT MOMENT

APPENDIX A
LIMIT MOMENT

[

]a,c,e

a,c,e

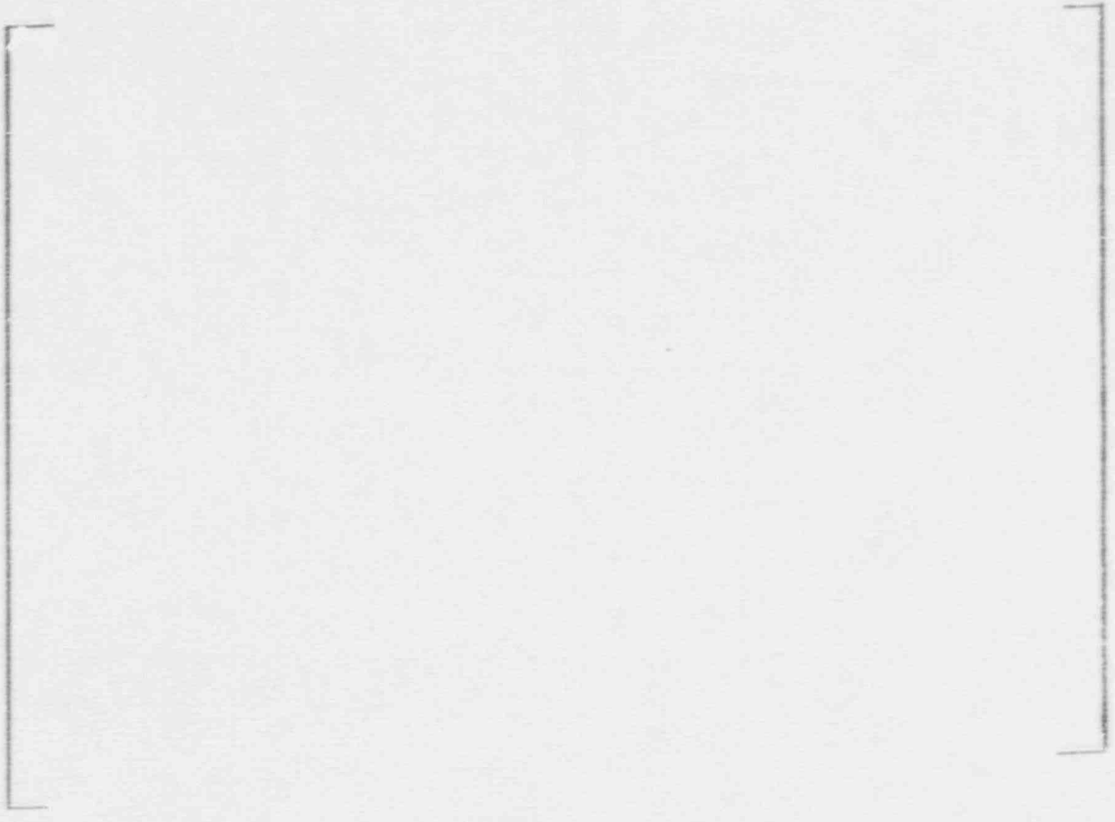

Figure A-1. Pipe With A Through-Wall Crack In Bending